

Die approbierte Originalversion dieser Dissertation ist in der Hauptbibliothek der Technischen Universität Wien aufgestellt und zugänglich.

<http://www.ub.tuwien.ac.at>



The approved original version of this thesis is available at the main library of the University of Technology.

<http://www.ub.tuwien.ac.at/eng>

Dissertation

Improvements in Modeling Gross Primary Productivity over Northern Eurasia

Ausgeführt zum Zwecke der Erlangung des akademischen Grades eines
Doktors der Naturwissenschaften

unter der Leitung von

Univ.Prof. Dipl.-Ing Dr.techn Wolfgang Wagner
Forschungsgruppen Photogrammetrie & Fernerkundung
E120

begutachtet von

Ao. Univ.Prof. Dipl.-Ing. Dr.nat.techn. Josef Eitzinger
Institut für Meteorologie
Universität für Bodenkultur Wien

eingereicht an der Technischen Universität Wien
Fakultät für Mathematik und Geoinformation

von

Ian McCallum
0527544
Schlossplatz 1, A-2361
Laxenburg, Austria

Wien, März
2014



TECHNISCHE
UNIVERSITÄT
WIEN
Vienna University of Technology

Dissertation

Improvements in Modeling Gross Primary Productivity over Northern Eurasia

submitted for the academic degree of
Doctor of Natural Science

under the supervision of

Univ.Prof. Dipl.-Ing Dr.techn Wolfgang Wagner
Research Group Photogrammetry & Remote Sensing
E120

reviewed by

Ao. Univ.Prof. Dipl.-Ing. Dr.nat.techn. Josef Eitzinger
Institute of Meteorology
University of Natural Resources and Life Sciences, Vienna

submitted to the Vienna University of Technology
Faculty of Mathematics and Geoinformation

by

Ian McCallum
0527544
Schlossplatz 1, A-2361
Laxenburg, Austria

Vienna, March
2014

Abstract

Carbon is removed from the atmosphere via photosynthesis by plants, balancing carbon gain through gross primary productivity (GPP) and carbon loss via plant respiration defined as net primary productivity (NPP). With some 16% of the atmospheric CO₂ passing through the earth's terrestrial biosphere annually, the importance of the biosphere in regulating the earth's carbon cycle cannot be overstated. Global observations of atmospheric CO₂ concentrations confirm that carbon exchange in terrestrial ecosystems is large in scale and sensitive to climate.

With anthropogenic CO₂ emissions having tripled in the last 50 years, such large fluxes occurring between carbon pools provide great potential for global change mitigation through biospheric uptake. Recent findings however, point to a potential weakening or saturation of the terrestrial uptake at the global level, with large regional variation. Weakening or saturation would have large implications for the carbon cycle and ultimately climate change. It is thus imperative to ensure that monitoring efforts are capable of accurately detecting such subtle shifts in regional and global productivity.

The overall objective of this research is to improve the modeling of ecosystem photosynthesis or gross primary productivity (GPP), specifically over Northern Eurasia (NE). A variety of methods exist to monitor terrestrial GPP, with this study focusing on production efficiency models (PEM). PEMs in particular combine the meteorological constraint of available sunlight with the ecological constraint of the amount of leaf area absorbing that solar energy, a process that lends itself to detection via satellite observation. This study has identified a number of issues with PEMs in need of improvement. These include issues pertaining to the use of alternative biophysical datasets in models, the design of diagnostic models and the consideration of unique biome level characteristics, the parameterization of diagnostic models with in-situ data and the upscaling of model results.

Initially, the general functioning of six PEMs was reviewed (along with the broader PEM literature) to determine potential improvements to the general PEM methodology, including suggestions for coordinated research. Following that, large disagreement among global land cover datasets often employed in PEMs was demonstrated, cautioning against the use of a single dataset. Furthermore, the performance of four global fraction of absorbed photosynthetically active radiation (fAPAR) datasets over NE has been analysed showing large variation with RMSE reaching upwards of 50%. The comparison also identified the most suitable fAPAR dataset for application over NE. However, dataset choice is very much land cover or biome dependent. For the time being, it is necessary to include multiple fAPAR products when performing global assessments.

Next a simultaneous calibration of four GPP models across five Russian boreal eddy covariance (EC) stations clearly demonstrated that accounting for temperature acclimation particularly at northern (temperature controlled) sites significantly improves the fit of modeled versus eddy covariance (EC) derived daily GPP values. RMSE values at a northern site in 2003 ranged from 8-24% across the models (lowest values include temperature acclimation and a non-linear light response). These results indicate that inclusion of temperature acclimation on sites experiencing cold temperatures is crucial. Developing

models that address unique biome-level properties calibrated with in-situ data may help to improve the accuracy of global PEMs.

Finally, incorporating the findings highlighted above, a technique for regional gridded GPP mapping has been developed utilizing eddy covariance estimates over Russia, a region sparsely covered with in-situ sites. The diagnostic model was previously validated over this region and utilises satellite-derived fAPAR deemed most appropriate for Russia. Results were compared against those from the Moderate Resolution Imaging Spectroradiometer (MODIS) (using a carbon accounting approach as the baseline) over Russia demonstrating that this new method yields plausible results. With RMSE values of 13% versus 23%, respectively, the new methodology achieves substantial improvements over a large region, thus more accurately estimating GPP than a model parameterized globally. Furthermore it demonstrates that an upscaling procedure, even using limited EC data, is effective. However, the most obvious difficulty with the method presented is the lack of in situ measurements, particularly over regions such as Russia.

In summary, findings from this dissertation contribute to a more accurate depiction of vegetation productivity over NE, thus reducing uncertainty in gross primary productivity estimates. Future efforts should focus on up-scaling, using statistical methods and semi-empirical models. In order to facilitate this, there is a need for a substantial expansion of the ground based observation network.

Kurzfassung

Kohlenstoff wird über Photosynthese durch Pflanzen der Atmosphäre entzogen, ein Vorgang der Kohlenstoffaufbau durch Bruttoprimärproduktion (BPP) und Kohlenstoffabbau durch Pflanzenatmung - definiert als Nettoprimärproduktion (NPP) - im Gleichgewicht hält. Mit etwa 16% des atmosphärischen CO₂, das jährlich in diesem Prozess die terrestrische Biosphäre durchläuft, kann die Bedeutung dieser in der Regulierung des Kohlenstoffkreislaufes der Erde nicht genug betont werden. Globale Beobachtungen von atmosphärischen CO₂ Konzentrationen bestätigen, dass der Kohlenstoffaustausch in terrestrischen Ökosystemen in großem Rahmen stattfindet und klimasensitiv ist.

Im Hinblick auf die Verdreifachung der anthropogenen CO₂ Emissionen in den letzten 50 Jahren bietet dieser große Austausch zwischen den Kohlenstoffspeichern und damit Aufnahme durch die Biosphäre ein großes Potenzial für die Minderung globaler Veränderungen. Neue Erkenntnisse weisen jedoch auf eine potentielle Abschwächung oder Sättigung des terrestrischen Aufnahmevermögens auf globaler Ebene hin, allerdings mit regionalen Unterschieden. Eine Abschwächung oder Sättigung hätte weitreichende Folgen für den Kohlenstoffkreislauf und letztlich den Klimawandel. Daher gilt es sicherzustellen, dass Monitoring-Ansätze in der Lage sind subtile Verschiebungen in regionaler und globaler Produktivität genau zu erfassen.

Das übergreifende Ziel dieser Forschungsarbeit ist die Verbesserung in der Modellierung von ökosystemarer Photosynthese bzw. Bruttoprimärproduktion (BPP), insbesondere für Nord Eurasien (NE). Aus der Vielzahl von Methoden zum Monitoring von terrestrischer BPP fokussiert diese Arbeit auf Produktionseffizienzmodelle (PEM). PEMs stellen die meteorologische Bedingung von verfügbarem Sonnenlicht in Kombination mit der ökologischen hinsichtlich der Blattflächenmenge zur Absorption dieser solaren Energie dar; ein Prozess, zu dessen Erfassung sich Satellitenbeobachtung anbietet. Eine Reihe von verbesserungsbedürftigen Aspekten für PEMs wurde in dieser Forschungsarbeit identifiziert. Diese inkludieren die Anwendung von alternativen biophysikalischen Datensätzen in Modellen, das Design von diagnostischen Modellen und die Berücksichtigung von eindeutigen Biom Merkmalen, die Parametrisierung von diagnostischen Modellen mit in-situ Daten und das Up-Scaling von Modellergebnissen.

Zunächst wurde die grundsätzliche Funktionalität von sechs PEMs untersucht (zusammen mit einer breiteren Literaturanalyse zu PEM), um mögliche Verbesserungen zur generellen PEM Methodik festzulegen sowie auch Empfehlungen für koordinierte Forschung auszusprechen. Eine darauf aufbauende zweite Untersuchung konnte erhebliche Unterschiede zwischen Datensätzen zu globaler Landbedeckung aufzeigen, die typischerweise in PEMs eingesetzt werden, und daher vor der Anwendung von nur einem Datensatz warnen. Vertiefend wurde im Folgenden die Performance von vier globalen Datensätzen zu dem Anteil an absorbiertes photosynthetisch wirksamer Strahlung (Fraction of absorbed Photosynthetic Active Radiation; fAPAR) über NE analysiert mit dem Ergebnis großer Abweichungen von einem RMSE bis zu 50%. Der Vergleich identifizierte auch den am besten geeigneten fAPAR Datensatz für die Anwendung über NE. Generell hängt die Wahl des Datensatzes jedoch

wesentlich von der Landbedeckung und vom Biom ab. Für globale Bewertungen ist es daher derzeit notwendig mehrere fAPAR Produkte anzuwenden.

Als nächster Schritt zeigte eine simultane Kalibrierung von vier BPP Modellen für fünf boreale Eddy Kovarianz (EC) Stationen in Russland eindeutig, dass die Einbeziehung von Temperatur Akklimatisierung speziell an nördlichen (Temperatur kontrollierten) Standorten wesentlich die Eignung von modellierten versus Eddy Kovarianz (EC) ermittelten täglichen BPP Werten verbessert. Der RMSE an einem nördlichen Standort in 2003 bewegte sich von 8-24% zwischen den Modellen (geringste Werte umfassen Temperatur Akklimatisierung und ein nicht-lineares Lichtverhalten). Diese Resultate weisen auf die Notwendigkeit hin, Temperatur Akklimatisierung an Kältestandorten mit zu berücksichtigen. Die Entwicklung von Modellen, die eindeutige Biom Eigenschaften adressieren kalibriert mit in-situ Daten könnte demnach die Genauigkeit von globalen PEMs verbessern.

Unter Einbeziehung der oben angeführten Ergebnisse, wurde letztlich eine Technik entwickelt für eine regional gerasterte BPP Erfassung unter Anwendung von Eddy Kovarianz Abschätzungen für Russland, einer Region, die nur spärlich mit in-situ Stationen ausgestattet ist. Das diagnostische Modell wurde zuvor schon für diese Region validiert und verwendet satellitengestützte fAPAR, die für Russland am geeignetsten erachtet werden. Die Resultate wurden verglichen mit jenen eines Moderate Resolution Imaging Spectroradiometer (MODIS) für Russland (unter Verwendung eines Kohlenstoffbilanzierungsansatzes als Baseline) um darzulegen, dass die neue Methode plausible Resultate liefert. Mit RMSE Werten von 13% versus 23% erreicht die neue Methode substantielle Verbesserungen für eine große Region und liefert damit genauere Ergebnisse für BPP als parametrisierte globale Modelle. Weiters zeigt die Methode, dass ein Up-Scaling Verfahren sich sogar mit eingeschränkter EC Datenverfügbarkeit als effektiv erweist. Trotzdem liegt die offensichtlichste Schwierigkeit mit der präsentierten Methode an einem Mangel von in-situ Messungen, speziell über Regionen wie Russland.

Zusammenfassend tragen die Ergebnisse dieser Forschungsarbeit zu einer genaueren Darstellung von Vegetationsproduktivität über NE bei und damit zu einer Verringerung der Unsicherheiten in den Abschätzungen zur Bruttopräprimärproduktion. Zukünftige Anstrengungen sollten auf Up-Scaling fokussieren unter der Verwendung von statistischen Methoden und halbempirischen Modellen. Um diese Entwicklung zu unterstützen ist eine substantielle Ausweitung des Bodenüberwachungsnetzwerkes notwendig.

Contents

Abstract.....	i
Kurzfassung.....	iii
List of Publications.....	vii
Abbreviations.....	viii
Acknowledgements.....	ix
1 Introduction.....	1
1.1 The Carbon Cycle.....	1
1.2 Biospheric CO ₂ Uptake.....	1
1.3 Measuring & Modeling Methodologies.....	2
1.4 Production Efficiency Model.....	3
1.5 Model uncertainties.....	4
2 Objectives.....	6
3 Materials and Methods.....	7
3.1 Study Area.....	7
3.2 Data.....	8
3.2.1 fAPAR.....	9
3.2.2 Meteorological Data.....	9
3.2.3 Land Cover.....	9
3.2.4 Eddy Covariance.....	10
3.3 Methods.....	12
3.3.1 Satellite-based terrestrial production efficiency modeling (Paper I).....	12
3.3.2 Spatial comparison of global land cover datasets (Paper II).....	12
3.3.3 Comparison of four global fAPAR datasets (Paper III).....	12
3.3.4 Improved light and temperature responses for GPP models (Paper IV).....	13
3.3.5 Continental GPP mapping: use of a diagnostic model (Paper V).....	15
4 Results.....	17
4.1 Satellite-based terrestrial production efficiency modeling (Paper I).....	17
4.2 Spatial comparison of global land cover datasets (Paper II).....	18
4.3 Comparison of four global fAPAR datasets (Paper III).....	20
4.4 Improved light and temperature responses for GPP models (Paper IV).....	22

4.5	Continental GPP mapping: use of a diagnostic model (Paper V).....	25
5	Discussion.....	29
5.1	Conclusions	32
5.2	Way Forward.....	33
6	References	35
	Appendices.....	41
	Paper I: Satellite-based terrestrial production efficiency modeling.....	
	Paper II: Spatial comparison of global land cover datasets	
	Paper III: Comparison of four global fAPAR datasets	
	Paper IV: Improved light and temperature responses for GPP models	
	Paper V: Continental GPP mapping: use of a diagnostic model	
	Curriculum Vitae	

List of Publications

This dissertation is based upon findings from the following publications found in the appendices and referred to in the text with Roman numerals:

- I. McCallum, I., Wagner, W., Schmulius, C., Shvidenko, A., Obersteiner, M., Fritz, S., and Nilsson, S., 2009. Satellite-based terrestrial production efficiency modeling, *Carbon Balance Manag.*, 4, 8, doi:10.1186/1750-0680-4-8.
- II. McCallum I, Obersteiner M, Nilsson S, Shvidenko A., 2006. A spatial comparison of four satellite derived 1 km global land cover datasets. *International Journal of Applied Earth Observation and Geoinformation*, 8(4):246-255.
- III. McCallum, I, Wagner, W, Schmulius, C, Shvidenko, A, Obersteiner, M, Fritz, S, Nilsson, S., 2010. Comparison of four global fAPAR datasets over Northern Eurasia for the year 2000. *Remote Sensing of Environment*, 114(5), 941-949.
- IV. McCallum, I., Franklin, O., Moltchanova, E., Merbold, L., Schmulius, C., Shvidenko, A., Schepaschenko, D., and Fritz, S., 2013. Improved light and temperature responses for light-use-efficiency-based GPP models, *Biogeosciences*, 10, 6577-6590, doi:10.5194/bg-10-6577-2013.
- V. McCallum, I., Franklin, O., Moltchanova, E., Shvidenko, A., and Schepaschenko, D. Continental GPP mapping: use of a diagnostic model parameterized with FLUXNET data (Manuscript).

Abbreviations

BL	Big Leaf Model
CO ₂	Carbon Dioxide
DGVM	Dynamic Global Vegetation Models
EC	Eddy Covariance
fAPAR	Fraction of Absorbed Photosynthetically Active Radiation
FLUXNET	Flux Network
GIS	Geographic Information System
GLC2000	Global Land Cover 2000
GPP	Gross Primary Productivity
IGBP	International Geosphere Biosphere Project
LAI	Leaf Area Index
LEA	Landscape Ecosystem Approach
LPJ-DGVM	Lund-Potsdam-Jena Dynamic Global Vegetation Model
LUE	Light Use Efficiency
LUE-TA	LUE-Temperature Acclimation
LUE-TAL	LUE-Temperature Acclimation Light
MODIS	Moderate Resolution Imaging Spectroradiometer
MSE	Mean Square Error
NE	Northern Eurasia
NPP	Net Primary Productivity
PAR	Photosynthetically Active Radiation
PEM	Production Efficiency Model
RMSE	Root Mean Square Error
RSS	Residual Sum of Squares
UMD	University of Maryland
VPD	Vapor Pressure Deficit

Acknowledgements

Firstly, I would like to thank Prof. Wolfgang Wagner for his supervision and guidance of my dissertation as it evolved over time. His advice, many years ago, to write this as a series of published papers proved invaluable. Special thanks also to Prof. Josef Eitzinger for reviewing this dissertation. I also thank Prof. Christiane Schmullius for inspiring me and many others to perform research in Russia.

I thank Prof. Sten Nilsson, who encouraged me to pursue doctoral studies while working at IIASA and a special thanks to Michael Obersteiner and Florian Kraxner who likewise continued to support these efforts. I am indebted to Prof. Anatoly Shvidenko for sharing with me his extensive knowledge of Russia and in particular its forest ecosystems. Thanks to my colleagues Steffen Fritz, Linda See and Dmitry Schepaschenko who patiently supported me to complete my dissertation and all my colleagues in the ESM Program at IIASA who provide a truly exceptional environment in which to work and who helped me complete this endeavor. I also thank Prof. Peter Duinker for his longstanding support. Furthermore, I thank Vladimir Stolbovoi for strongly encouraging me to start these efforts many years ago and Walter Foith for strongly encouraging me to finish! I also thank the IIASA library team who provided invaluable research assistance.

A heartfelt thanks to all coauthors who collaborated with me on the publications that form the basis of this dissertation. In particular thanks to Elena Moltchanova and Oskar Franklin who provided me with invaluable discussions and guidance and above all the motivation to finish. I also thank Lutz Merbold who provided his flux tower knowledge and Michiel van der Molen who likewise provided data and expertise.

Thanks to all friends who supported me along the way and thanks to Felix Ortag for help over the final administrative hurdles.

Final gratitude is reserved for my wife Sabine and our family, who along with our parents and my sister provided encouragement, support and patience to the end!

Ian McCallum

1 Introduction

1.1 The Carbon Cycle

Carbon is removed from the atmosphere via photosynthesis by plants, and in doing so constitutes almost half of the organic matter on Earth. Upon entering the terrestrial ecosystem it is termed gross primary productivity (GPP), with the difference between carbon gain via GPP and carbon loss through plant respiration defined as net primary productivity (NPP) ([Chapin, Matson et al. 2002](#)). The carbon balance of vegetation and ecosystems governs the productivity of the biosphere and the impact of ecosystems on the Earth system ([Chapin, Matson et al. 2002](#)).

With some 16% of the atmospheric CO₂ passing through the earth's terrestrial biosphere annually ([Prentice 2001](#)), the importance of the biosphere in regulating the earth's carbon cycle cannot be overstated. Furthermore, global patterns of variation in the atmospheric CO₂ concentration provide convincing evidence that carbon exchange by terrestrial ecosystems is large in scale and sensitive to climate. With such large fluxes occurring between carbon pools, great potential for global change mitigation lies within these processes. Even minor shifts in the fluxes at such a magnitude have large consequences in terms of net ecosystem carbon balance. This assumes however that the processes that govern the carbon cycle can be reasonably understood both in space and time and that the uncertainties can be controlled.

1.2 Biospheric CO₂ Uptake

It is extremely likely that more than half of the observed increase in global average surface temperature from 1951 to 2010 was caused by the anthropogenic increase in greenhouse gas concentrations and other anthropogenic forcing's together ([IPCC 2013](#)). Increases in the earth's mean surface temperature are assumed to benefit vegetation productivity over many areas of the globe and thus increase the carbon stored in vegetation. In fact, anthropogenic CO₂ emissions have tripled in the last 50 years, with a proportional biospheric uptake, thus significantly mitigating the effects of rising CO₂ ([Baker 2007](#)). Previous studies have shown that climate constraints were relaxing with increasing temperature allowing an upward trend in NPP from 1982 – 1999 ([Nemani, Keeling et al. 2003](#)). Others however caution against a possible overestimation by remote sensing methods ([Lapenis, Shvidenko et al. 2005](#)).

Recent findings point to a possible weakening or saturation of the terrestrial carbon uptake at both the global ([Le Quere, Raupach et al. 2009](#); [Zhao and Running 2010](#)) and continental levels ([Nabuurs, Lindner](#)

[et al. 2013](#)). Weakening or saturation could have large implications for future atmospheric CO₂ levels and ultimately climate change. It is thus imperative to ensure that monitoring and modeling efforts are capable of accurately detecting such subtle shifts in vegetation productivity. Our limited understanding of terrestrial carbon cycling translates into a major source of uncertainty for predictions of future climate change. Continuous global monitoring of NPP will be essential in determining whether the reduced NPP over the past 10 years is a decadal variation or a turning point to a declining terrestrial carbon sequestration under changing climate ([Zhao and Running 2010](#)). Hence we turn to a variety of methodologies to estimate carbon fluxes, with the ultimate goal to establish a global carbon observation system ([Ciais, Dolman et al. 2013](#)).

1.3 Measuring & Modeling Methodologies

At the regional or global scale, carbon fluxes (i.e. GPP, NPP) cannot be directly observed ([Cramer, Kicklighter et al. 1999](#)). NPP is difficult to measure (in-situ) over large areas owing to spatial variability of environmental conditions and limitations in the accuracy of allometric equations ([Goetz and Prince 1999](#)). Therefore, a variety of methods have been developed to estimate carbon fluxes. These include among others in-situ flux towers ([e.g., Friend, Arneeth et al. 2007](#)), carbon accounting techniques ([e.g., Shvidenko and Nilsson 2003](#)), process-based vegetation models ([e.g., Sitch, Smith et al. 2003](#)), inverse modelling ([e.g., Stephens, Gurney et al. 2007](#)) and diagnostic satellite-based techniques ([e.g., Running, Nemani et al. 2004](#)), with each methodology having advantages and shortcomings, as described below.

The eddy covariance (EC) method, a micrometeorological technique, provides a direct measure of the net exchange of carbon and water between vegetated canopies and the atmosphere ([Baldocchi, Falge et al. 2001](#)). Although flux tower data represent point measurements with a maximum footprint of 1km² (dependent upon if sensor height was selected to observe such a dimension) they can be used to validate models and to spatialize biospheric fluxes at regional and continental scales ([Papale and Valentini 2003](#)). In reality however, the footprint is highly dynamic in space and time depending on friction velocity, sensible heat flux, temperature, and wind direction. Globally some 500 towers exist, however large gaps exist in the network ([Ciais, Dolman et al. 2013](#)).

Carbon accounting ([Shvidenko and Nilsson 2003](#)) is founded on three major components: a multilayer Geographic Information System (GIS); satellite-derived data; and a range of semi empirical regional models for forest growth and yield, biomass fractions, heterotrophic respiration, etc. ([Quegan, Beer et al. 2011](#)). These are integrated in a multilayer GIS. This amalgamates comprehensive data on vegetation, soils, hydrology and landforms with regression-based estimates of how greenhouse gas fluxes depend

on these factors and on climate ([Quegan, Beer et al. 2011](#)). Results are generally based on long-term data and hence reflect an average value. The process is labor intensive.

Dynamic Global Vegetation Models (DGVMs) are generally designed to calculate carbon fluxes and pool dynamics in the biosphere at the global scale, especially their variations under changing climate and atmospheric CO₂. DGVMs generally incorporate modules to estimate photosynthesis, autotrophic and heterotrophic respiration, mortality, disturbances due to fire, allocation of carbon to plant compartments, soil carbon storage, evapotranspiration and hydrology ([Quegan, Beer et al. 2011](#)). If unconstrained, such models have difficulty matching in-situ measurements.

Atmospheric inversion uses model-based estimates of atmospheric transport to calculate the spatial distribution of surface CO₂ fluxes that best matches a set of atmospheric CO₂ concentration measurements, within their errors ([Enting and Mansbridge 1989](#)). Its accuracy is limited by the sparseness of the atmospheric network and by unknown biases in the transport models ([Gurney, Law et al. 2002](#)). The spatial resolution for which fluxes can be safely estimated, typically around 1000–5000 km, is much coarser than for the bottom-up methods ([Quegan, Beer et al. 2011](#)).

A variety of satellite-based methods have been developed including direct methods (e.g. photochemical reflectance index), model linkages (e.g. SiBCASA) and Production Efficiency Models (PEM) (e.g. MODIS MOD17A2/A3). In particular, diagnostic or PEMs, have been developed to monitor primary production, taking advantage of available satellite data. PEMs combine the meteorological constraint of available sunlight reaching a site with the ecological constraint of the amount of leaf-area absorbing that solar energy, avoiding many complexities of carbon balance theory ([Running, Nemani et al. 1999](#)). These models are generally based on the theory of light use efficiency (LUE), which states that a relatively constant relationship exists between photosynthetic carbon uptake (GPP) and absorbed photosynthetically active radiation (APAR) at the canopy level ([Anderson, Norman et al. 2000](#); [Sjoestrom, Ardoe et al. 2011](#)). In addition to LUE, PEMs typically require inputs of meteorological data (i.e. radiation, temperature and others) and the satellite-derived fraction of absorbed photosynthetically available radiation (fAPAR). Uncertainty in any of these input variables can strongly bias the results.

1.4 Production Efficiency Model

Of all the existing methodologies described above, only the PEM approach is designed to harnesses satellite observations which provide globally consistent, spatially highly resolved observations over time

of numerous surface variables that affect carbon exchanges ([Cihlar, Denning et al. 2002](#)). Furthermore, this approach lends itself to calibration against flux tower data. PEMs complement the many ecophysiological process models that simulate carbon exchange ([Goetz, Prince et al. 1999](#)). In particular, the MODIS MOD17A2/A3 C5.1 product has been providing globally consistent estimates over the globe for more than a decade ([Zhao and Running 2010](#)). The basic PEM approach is as follows,

$$GPP = PAR f_{APAR} LUE \varepsilon \quad (1)$$

where GPP represents daily gross primary productivity (g C m^{-2}), PAR is photosynthetic active radiation (MJ m^{-2}), f_{APAR} is the fraction of absorbed PAR and LUE is the potential LUE in terms of GPP (g C MJ^{-1}). Potential LUE is the maximum LUE attainable on a site without environmental constraints. Potential LUE is reduced to actual LUE via environmental scalars ε (e.g. temperature, vapour pressure deficit).

1.5 Model uncertainties

A variety of problems have been noted with the PEM approach, particularly when applying global parameterizations to local applications ([Pan, Birdsey et al. 2006](#); [Turner, Ritts et al. 2006](#); [McCallum, Wagner et al. 2009](#); [Shvidenko, Schepaschenko et al. 2010](#)). This is not surprising as temperature, radiation, and water interact to impose complex and varying limitations on vegetation activity and LUE in different parts of the world ([Churkina and Running 1998](#)). A landmark inter-comparison of NPP models at the turn of the century found general agreement globally among results (with PEMs fitting well within the range) ([Cramer, Kicklighter et al. 1999](#)). However, a recent model-data comparison of GPP from 26 models (including LUE models) noted that none of the models matched estimated GPP within observed uncertainty ([Schaefer, Schwalm et al. 2012](#)). On average, models over-predicted GPP under dry conditions and for temperatures below 0°C . This is occurring for many reasons, including: (1) the majority of models have not been calibrated with in-situ data and hence cannot replicate the detailed in-situ estimates; (2) models generally operate at much coarser spatial resolution than in-situ measurements; and (3) models are designed to be generally applicable at the continental or global level, thus often do not include certain biome-level specificities which may be captured with in-situ estimates ([McCallum, Franklin et al. 2013](#)).

While it appears that between model variability is often relatively low, within model variability is likely much higher (more so at a regional scale). Models that agree on the value of certain outputs (e.g. annual NPP) may disagree on the underlying processes (e.g. differences in rates of photosynthesis vs. plant respiration) ([Ruimy, Kergoat et al. 1999](#)). A comparison of MODIS NPP and NPP derived from carbon

accounting over Russia closely agreed in terms of annual mean, while detecting substantial bias in MODIS NPP for low and high productive forests ([Shvidenko A. 2011](#)).

In particular, determination of LUE ([Ahl, Gower et al. 2004](#); [Still, Randerson et al. 2004](#)) and autotrophic respiration ([Turner, Ritts et al. 2005](#)) remain highly uncertain. Additional uncertainties have been identified in the meteorological data ([Heinsch, Zhao et al. 2006](#)) and in the biophysical data ([Seixas, Carvalhais et al. 2007](#)), both key components in PEMs. Biases in meteorological analyses can introduce substantial error into GPP and NPP estimations, and emphasize the need to minimize these biases to improve the quality of GPP and NPP products ([Zhao, Running et al. 2006](#)). Considerable disagreements among global land cover datasets and classification legends not primarily suited for specific applications such as carbon cycle model parameterizations pose significant challenges and uncertainties in the use of such data sets ([Jung, Henkel et al. 2006](#); [McCallum, Obersteiner et al. 2006](#)). The choice of a specific fAPAR dataset may also significantly affect model results ([Beer, Reichstein et al. 2010](#); [McCallum, Wagner et al. 2010](#)). Furthermore the construction of a PEM and in particular the choice of which variables to include has a large impact on the resulting estimations ([McCallum, Franklin et al. 2013](#)). It appears imperative that unique biome specific properties are included in any PEM model. If we wish to increase our confidence in our ability to monitor GPP and predict potential saturation of the terrestrial carbon sink, it is crucial that we minimize the uncertainties described above.

2 Objectives

The overall objective of this research is to improve the modeling of vegetation productivity, specifically over Northern Eurasia. A number of issues in need of improvement have been identified in the literature. These include issues pertaining to the design of diagnostic models and the consideration of unique biome level characteristics, the use of alternative biophysical datasets in models, the parameterization of summary-type diagnostic models with in-situ data and the upscaling of model results. The specific objectives of the individual papers are listed here:

- I. To describe the general functioning of six PEMs identified in the literature; to review each model to determine potential improvements to the general PEM methodology; to review the related literature on satellite-based GPP and NPP modeling for additional possibilities for improvement; and based on this review, propose items for coordinated research.
- II. To highlight for the user community the discrepancies between existing global land cover datasets and decreasing agreement as these products are used for regional applications. The aim is to increase awareness of model uncertainty introduced by land cover datasets.
- III. To provide an indication of the performance of four global fAPAR datasets over Northern Eurasia in the year 2000 through quantitative comparison and analysis. The aim is to highlight the discrepancy among available datasets (which would translate into model uncertainty) and to select the most suitable dataset for application over NE.
- IV. To calibrate four GPP models (of increasing complexity) simultaneously across five Russian boreal EC stations and evaluate their performance with cross validation. We aim to demonstrate that accounting for temperature acclimation and to a lesser extent non-linear light response of daily GPP will largely improve model performance.
- V. To develop a GPP PEM for Russia that incorporates the findings from papers (I-IV). The aim is to demonstrate that this approach is better able to estimate GPP than a model parameterized globally. Furthermore it demonstrates an upscaling procedure using limited EC data.

3 Materials and Methods

3.1 Study Area

Northern Eurasia is the largest extra-tropical landmass and contains the largest terrestrial reservoir of carbon ([Tarnocai, Canadell et al. 2009](#)). It is also one of the regions with the largest climatic variations and is consistently predicted by climate models to respond strongly to climate warming ([Joos, Colin Prentice et al. 2001](#)). In addition, it hosts a range of processes that interact with climate through complex and poorly understood feedback loops ([McGuire, Chapin III. et al. 2006](#)). These include: changes in surface albedo due to variations in snow cover and vegetation; thawing of permafrost, with potential strong effects on hydrology and vegetation through the impact on the water table; changes in the forest fire regime from different temporal dynamics of temperature and precipitation, with associated effects on, for example, land cover; and changes in hydrology, leading to drying and oxidation of bogs and a shifting balance between methane and carbon dioxide emissions ([Quegan, Beer et al. 2011](#)).

Russia comprises almost one fourth of the world's forest cover, making these boreal forests a unique natural phenomenon at the global scale. In addition vast areas are characterized by tundra ecosystems, dominated by shrubs, grasses and sedges, mostly above permafrost (Figure 1). Furthermore, significant agricultural and grassland areas occur outside of permafrost regions. This large land area undergoes great annual changes in albedo and productivity as seasonal temperatures swing well above and below 0° C. Large regions lie in various stages of permafrost and the area is prone to catastrophic disturbance in the form of fire ([Goldammer 1996](#); [Kajii, Kato et al. 2002](#); [Balzter, Gerard et al. 2005](#); [Shvidenko and Schepaschenko 2013](#)). The climate of both the boreal forests and the tundra ecosystems in Eastern Siberia can resemble that of a boreal/arctic desert during long periods of the growing season ([Vygodskaya, Milyukova et al. 1997](#)).

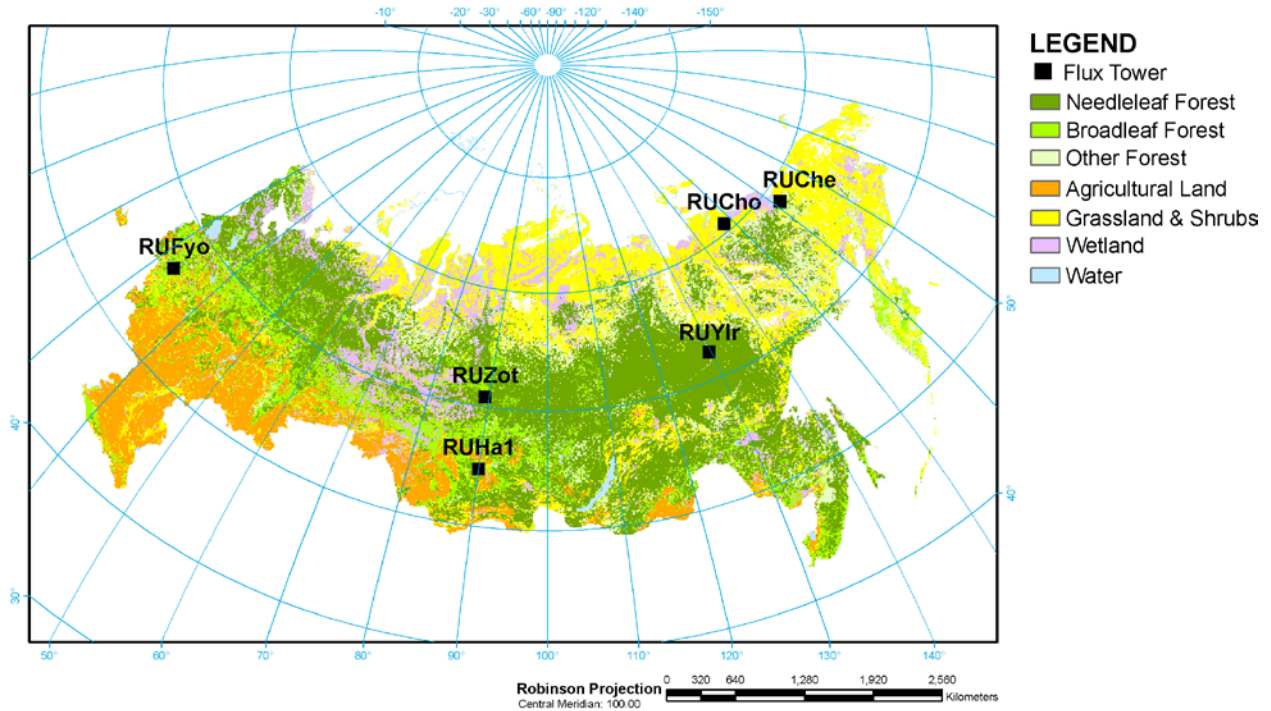


Figure 1. Map of Russian land cover, including locations of flux towers used in this study ([Schepaschenko, McCallum et al. 2011](#)).

3.2 Data

The various spatial datasets required for this study appear in Table 1. The datasets represent a mixture of meteorological reanalysis data and satellite-based biophysical datasets. All datasets were resampled to 0.25° (with the exception of the land cover products). fAPAR was resampled to daily temporal resolution.

Table 1. Spatial datasets used over the course of this study.

Description	Time	Orig. Size	Units	Source
Photosynthetically Active Radiation (PAR)	2002-2005	1.5°	$W\ m^{-2}s^{-1}$	ecmwf.int (ERA-Interim)
Temperature	2002-2005	1.5°	K	ecmwf.int (ERA-Interim)
Dew Point Temperature	2002-2005	1.5°	K	ecmwf.int (ERA-Interim)
Fraction of Absorbed PAR	2002-2005	0.25°	%	fAPAR.jrc.ec.europa.eu
Mean Temperature (May to September)	1975-2000	1.0°	K	http://mars.jrc.ec.europa.eu/

International Geosphere- Biosphere Project	1992-1993	1km ²	-	http://www.usgs.gov/;
University of Maryland	1992-1993	1km ²	-	http://www.geog.umd.edu/
GLC2000	1999-2000	1km ²	-	http://bioval.jrc.ec.europa.eu/ products/glc2000
MODIS	2000-2001	1km ²	-	http://modis.gsfc.nasa.gov/

3.2.1 fAPAR

fAPAR is defined as the fraction of Photosynthetically Active Radiation (PAR) absorbed by vegetation, where PAR is the solar radiation reaching the vegetation in the wavelength region 0.4 – 0.7 micrometers. Various fAPAR datasets were compared over Northern Eurasia ([McCallum, Wagner et al. 2010](#)). Results suggested that the JRC fAPAR ([Gobron, Pinty et al. 2006](#)) performed well for this region, and hence that dataset was used in this study.

3.2.2 Meteorological Data

This study employs reanalysis data from the European Centre for Medium Range Weather Forecast (ECMWF) – specifically the ERA-Interim datasets. ERA-Interim makes use of data from the increasing number of new instruments on satellites from 2003 onwards. A major problem with the use of observations for climate analysis is the presence of biases ([Dee, Uppala et al. 2011](#)). In spite of best efforts to remove all systematic errors at the source, some residual biases inevitably remain. It is, however, assumed that the coarse resolution meteorological data represent ground conditions and are homogeneous within each cell. *VPD* was estimated from dew point temperature T_d (°K) and air temperature T_a (°K) according to ([Monteith and Unsworth 1990](#)). In a comparison against two other meteorological reanalysis datasets, ECMWF had the highest accuracy ([Zhao, Running et al. 2006](#)).

3.2.3 Land Cover

Four global land cover datasets were analyzed in a global comparison study ([McCallum, Obersteiner et al. 2006](#)), namely the IGBP, UMD, GLC2000 and MODIS land cover datasets. Three of the four datasets utilized the IGBP land cover classification (UMD utilised a simplified IGBP approach), which includes 11 categories of natural vegetation covers distinguished by life form, 3 classes of urban and cropland mosaic lands and 3 classes of non-vegetated lands for a total of 17 classes ([Strahler, Muchoney et al. 1999](#)). The legend aimed to be exhaustive, so that every part of the earth's surface was assigned to a class; exclusive so that classes would not overlap; and structured so classes are equally interpretable

with 1-km data, higher resolution satellite imagery or ground observation ([Loveland, Reed et al. 2000](#)). Alternatively, the GLC2000 classification utilises the Land Cover Classification System (LCCS) ([Di Gregorio and Jansen 2000](#)) producing a total of 23 land cover classes, which were mapped onto the IGBP legend.

3.2.4 Eddy Covariance

Data for model calibration was obtained from www.fluxdata.org for six sites with EC flux measurements in Russia: Cherskii, Chokurdakh, Fyodorovskoe, Hakasia, Zotino, and Yakutia (Table 2). The eddy covariance method, a micrometeorological technique, provides a direct measure of the net exchange of carbon and water between vegetated canopies and the atmosphere ([Baldocchi, Falge et al. 2001](#)). For all sites, gap-filled and flux-partitioned daily data was obtained, having been treated according to standard procedures ([Reichstein, Falge et al. 2005](#); [Papale, Reichstein et al. 2006](#)). In particular, the partitioning of net ecosystem exchange into GPP and terrestrial ecosystem respiration was done according to ([Reichstein, Falge et al. 2005](#)). See individual tower references for a description of the methodology applied at each tower (Table 2). In addition to the data used in ([McCallum, Franklin et al. 2013](#)), we used the Yakutia Larch site ([Dolman, Maximov et al. 2004](#)). This data was partitioned into GPP using an online flux partitioning tool (<http://www.bgc-jena.mpg.de/~MDIwork/eddyproc/>). Figure 2 demonstrates the correlation between the daily GPP, biophysical variable fAPAR and meteorological data (temperature, VPD and radiation) at the tower sites.

Table 2. Description of FLUXNET tower sites used in this study.

Site Name	Location (°)	Tower Height (m)	Data Years Used	Dominant Land Cover	Mean Annual Temp. (°C)	Mean Annual Precip. (mm)	Tower References
Cherskii (RU-Che)	68.61N 161.34 E	5.3	2002 - 2004	Tundra - Grass	-12.5	200 - 215	(Corradi, Kolle et al. 2005 ; Merbold, Kutsch et al. 2009)
Chokurdakh (RU-Cho)	70.61N 147.89E	4.7	2003 - 2004	Tundra - Grass	-10.5	212	(van der Molen, van Huissteden et al. 2007)
Fyodorovskoe (RU-Fyo)	56.46 N 32.92 E	31.0	2003 - 2004	Evergreen Needleleaf Spruce Forest	3.7	584.3	(Milyukova, Kolle et al. 2002)
Hakasia	54.72 N	4.5	2002	Steppe	0.4	304	(Marchesini, Papale)

(RU-Ha1)	90.00 E		–					et al. 2007
			2004					
Zotino (RU-Zot)	60.80 N 89.35 E	27.0	2002 - 2004	Evergreen Needleleaf Pine Forest	-1.5	593		(Arneeth, Kurbatova et al. 2002; Tchebakova, Kolle et al. 2002)
Yakutia (RU-Ylr)	62.255N 129.619E	34	2002- 2005	Larch Forest	- 10.4	213		(Dolman, Maximov et al. 2004)

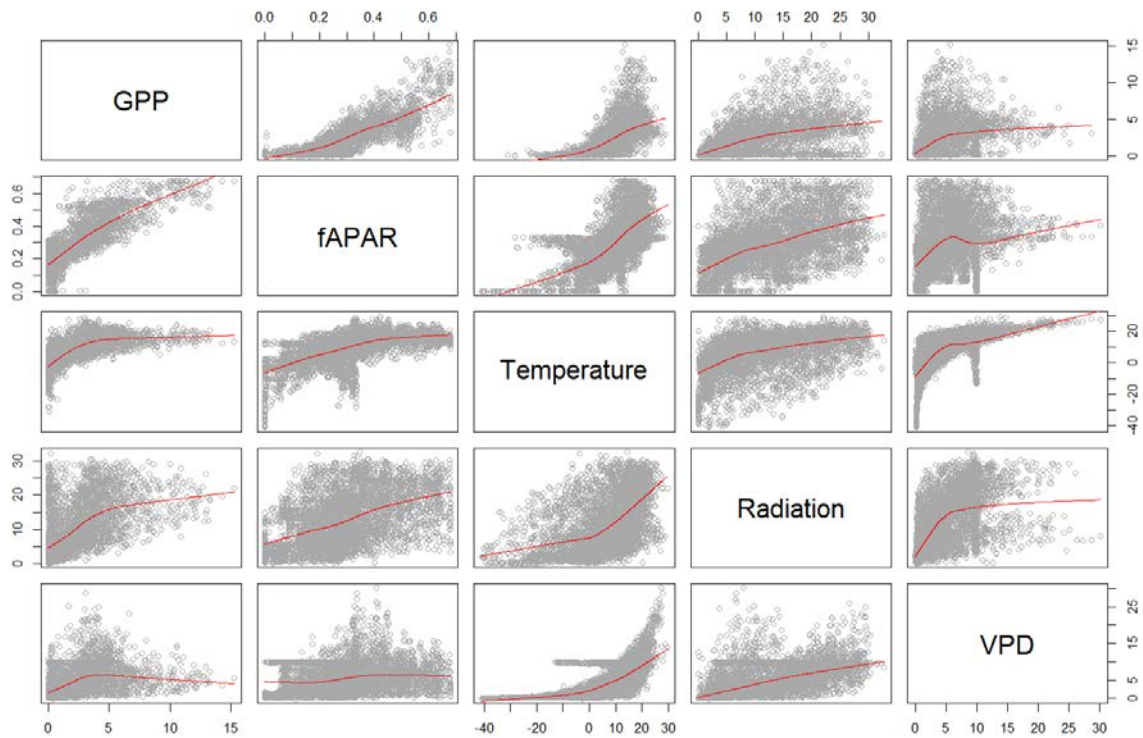


Figure 2. Scatterplots of GPP ($\text{g C m}^{-2} \text{ day}^{-1}$) against fAPAR, Temperature ($^{\circ}\text{C}$), Radiation ($\text{MJ m}^{-2} \text{ day}^{-1}$) and VPD (hPA) at the flux tower sites for the years 2002-2005. Red line shows locally weighted regression.

3.3 Methods

The following briefly describes the methods employed in each of the studies in this dissertation. For further details please refer to the papers in the Appendix.

3.3.1 Satellite-based terrestrial production efficiency modeling (Paper I)

Paper I is comprised of a literature review on the topic of satellite-based terrestrial production efficiency modeling. The first step was a review of the key attributes and results of six published PEMs (i.e. CASA, GLO-PEM; TURC, C-Fix, MOD17 and BEAMS). This was then expanded to a general review of available publications with a total of 109 references being included in the final review. The general review began with the history of PEMs, followed by a description of the common approach taken, an assessment of the error sources and variability in PEMs and finally a synthesis of key research items identified in the published literature.

3.3.2 Spatial comparison of global land cover datasets (Paper II)

Paper II consisted of spatially comparing four global land cover products (i.e. IGBP, UMD, GLC2000 and MODIS). Initially all datasets were geometrically aligned. Once all datasets were assigned to the common IGBP classification, the four datasets were merged. A comparison was performed to identify the level of agreement between each 1 km² pixel in the four datasets using the IGBP classification. Four levels of agreement were distinguished: no agreement—pixels containing a unique IGBP class in each dataset; partial agreement—pixels where two of the four datasets are in agreement (it is possible that the other two pixels are identical to each other—no distinction was made); high agreement—where three of the datasets agree for the same pixel; and full agreement—where all four datasets within a pixel were in agreement.

In addition to the global comparison, seven test sites were selected (5 by 5 degree areas) across the globe representing the continents. These sites allow for a regional comparison of the datasets. In addition, the heterogeneity of the landscape was measured in order to further explain some of the differences between the datasets. Using an eight neighbor rule, patches (contiguous areas of similar land cover class) were delineated and counted for each land cover dataset based on the standard IGBP classification.

3.3.3 Comparison of four global fAPAR datasets (Paper III)

Paper III consisted of an analysis of four global fAPAR datasets (i.e. MODIS, CYCLOPES, JRC, and GLOBCARBON). After reviewing all available products, the year 2000 with a monthly time-step and 0.25°

resolution was chosen for comparison. Some products have a resolution as fine as 1-km and an 8-day frequency, however owing to both the size of the region and the lack of finer information from some datasets, the 0.25° and monthly time-step was deemed appropriate for this analysis. Datasets with resolution finer than 0.25° were aggregated to 0.25°, based on the mean value of all cells falling within the resultant 0.25° cell. Datasets with a time-step more frequent than monthly were aggregated into monthly values by taking the mean of all values recorded within the month. In the case of GLOBCARBON, a quality flag was used to assign the monthly mean.

Additionally, to aid in comparison of the various products and to better identify where differences related to land cover are occurring, we made use of the Global Land Cover 2000 product (GLC2000) ([Bartalev, Belward et al. 2003](#)). This product was specifically created for Russia by regional experts and should, therefore, adequately represent the distribution of vegetation types. We aggregated the 23 GLC2000 classes into the following six classes to obtain the basic land cover types and simplify the analysis (percent vegetated area represented by each aggregated class): deciduous broadleaf forest (3%); evergreen needleleaf forest (14%); deciduous needleleaf forest (33%); mixed forest (14%); shrubs/grasses (26%); and cropland (10%). This distribution is similar to the areal statistics in the land and forest account of Russia. Owing to the lack of in-situ data, we focus in this study on indirect evaluation in order to examine the various global products and their applicability to Northern Eurasia. Techniques applied include measures of temporal and spatial consistency, including spatial correlation and root mean square error (RMSE) among the datasets.

3.3.4 Improved light and temperature responses for GPP models (Paper IV)

Four diagnostic models (LUE, LUE-TA, LUE-TAL and BL) were chosen for parameterization in this study ([McCallum, Franklin et al. 2013](#)), namely:

- 1) LUE, the LUE approach parameterized according to ([Running 2000](#)),

$$GPP = PAR f_{APAR} LUE f_1(T) f_2(VPD) \quad (2)$$

where GPP represents daily gross primary productivity (g C m^{-2}), PAR is photosynthetic active radiation (MJ m^{-2}), f_{APAR} is the fraction of absorbed PAR and LUE is the potential LUE in terms of GPP (g C MJ^{-1}). Potential LUE is the maximum LUE attainable on a site without environmental constraints. Potential LUE is reduced to actual LUE via the environmental scalars for daily minimum temperature $f_1(T)$ and daily vapour pressure deficit $f_2(VPD)$, both of which are defined as linear ramp functions [0,1] as per ([Running 2000](#)).

- 2) LUE-TA, the LUE approach parameterized according to ([Mäkelä, Pulkkinen et al. 2008](#)) but without a light modifier. The basic LUE approach (Eqn. 2) was again employed, however both $f_1(T)$ and $f_2(VPD)$ were parameterized differently. The modifying function $f_1(T)$ is defined here as ([Mäkelä, Pulkkinen et al. 2008](#))

$$f_1(T) = \min \left\{ \frac{S_k}{S_{max}}, 1 \right\}, \quad (3)$$

where the empirical parameter S_{max} (°C) determines the value of S_k (°C) at which the temperature modifier attains its saturating level. The effect of VPD $f_2(VPD)$ was estimated according to ([Landsberg and Waring 1997](#))

$$f_2(VPD) = e^{KD} \quad (4)$$

where K is an empirical parameter assuming typically negative values and D (kPa) is vapor pressure deficit.

- 3) LUE-TAL, the LUE approach parameterized according to ([Mäkelä, Pulkkinen et al. 2008](#)) with a light modifier. Again the basic LUE approach (Eqn. 2) was used, parameterized according to (LUE-TA). In addition, to account for non-linearity in the photosynthetic response to APAR, a light modifier $f_3(L)$ was defined to yield the rectangular hyperbola light response function when multiplied with the linear response included in the LUE-TA model ([Mäkelä, Pulkkinen et al. 2008](#))

$$f_3(L) = \frac{1}{\gamma_{APAR} + 1} \quad (5)$$

where γ ($m^2 \text{ mol}^{-1}$) is an empirical parameter defined according to ([Mäkelä, Pulkkinen et al. 2008](#)).

- 4) BL, a non-rectangular hyperbola (big leaf) model (e.g., [Hirose and Werger 1987](#); [Hirose, Ackerly et al. 1997](#)). Daily gross primary production GPP is thus defined here according to

$$GPP = \frac{h}{2\theta} \left[\phi I_a + E_a A_{max} - \sqrt{(\phi I_a + E_a A_{max})^2 - 4\phi I_a E_a A_{max} \theta} \right] \quad (6a)$$

where

$$E_a = f_1(T) f_2(VPD) \quad (6b)$$

where h is day length; θ convexity of leaf photosynthesis; ϕ quantum efficiency; I_a absorbed photosynthetically active radiation; E_a environmental modifier for temperature $f_1(T)$ and VPD

$f_2(VPD)$; and A_{max} light saturated canopy-photosynthesis. The effect of temperature $f_1(T)$ on daily A_{max} was modelled using the concept of state of acclimation ([Mäkelä, Pulkkinen et al. 2008](#)), i.e. it acclimates dynamically to temperature with a time delay. The effect of VPD $f_2(D)$ on A_{max} was estimated according to ([Landsberg and Waring 1997](#)).

The LUE models (i.e. LUE, LUE-TA and LUE-TAL) follow the standard approach, each including two environmental modifiers for temperature and vapor pressure deficit (VPD), and in the third instance a non-linear light modifier. The big leaf (BL) model also includes two environmental modifiers for temperature and VPD, and is inherently non-linear in its light response. Initially, all models are calibrated against five EC sites within Russia for the years 2002-2005.

Each model was estimated separately for each site and year. Parameters were optimized by means of a search on a coarse grid. Model diagnostics were based on the regression of EC tower based GPP against modeled GPP. The minimum residual sum of squares (RSS) has been used as the calibration criteria. Fit was further appraised using both the coefficient of determination (r^2) and root mean square error (RMSE). Evaluation of the performance of the models used in this study utilized 10-out cross-validation. For each site, measured GPP values were dropped (consecutively) ten at a time while the remaining values were used to estimate the parameters. The estimated parameter values were then used to predict GPP of the dropped data points (i.e. those not used in the parameter estimation). The differences between these predictions (of the dropped data points) and the measured data were used to calculate the mean square error (MSE), which were used to evaluate the model's ability to predict GPP, averaged for all data. The leave-10-out cross-validation was performed a similar amount of times for each model for every site-year.

3.3.5 Continental GPP mapping: use of a diagnostic model (Paper V)

This study presents a method of continental GPP mapping using a diagnostic model parameterized with limited FLUXNET data over Russia ([McCallum, Franklin et al. 2013](#)). It employs an fAPAR dataset that was deemed applicable over this region ([McCallum, Wagner et al. 2010](#)). Additionally it accounts for temperature acclimation, a phenomenon known to affect photosynthesis in boreal regions ([Mäkelä, Pulkkinen et al. 2008](#)). In particular, the relationship between model parameters for temperature, Vapor Pressure Deficit (VPD) and A_{max} with long-term mean values of temperature was used to spatially assign parameters. Evaluation of the methodology presented here was made by comparison against results obtained from carbon accounting ([Shvidenko and Nilsson 2003](#)) and a diagnostic satellite-based model ([Running, Nemani et al. 2004](#)). Previous results obtained from carbon accounting over Siberia ([Quegan,](#)

[Beer et al. 2011](#)), demonstrate that the carbon accounting method acts as a good benchmark for primary productivity.

The model applied in this study was parameterized for northern Eurasia ([McCallum, Franklin et al. 2013](#)). Leaf photosynthesis is described with the non-rectangular hyperbola big leaf (BL) model ([Hirose and Werger 1987](#); [Hirose, Ackerly et al. 1997](#)). Leaf level photosynthesis is up-scaled to daily canopy photosynthesis by integration over the canopy ([Franklin 2007](#)) and using daily canopy f_{APAR} to determine the amount of absorbed incoming radiation. All parameters are described in ([McCallum, Franklin et al. 2013](#)).

4 Results

The results obtained from the papers presented in this dissertation are briefly described below. For further details please refer to the papers in the Appendix.

4.1 Satellite-based terrestrial production efficiency modeling (Paper I)

Paper I noted a number of possibilities for improvement to the general PEM architecture – ranging from LUE to meteorological and satellite-based inputs. Current PEMs tend to treat the globe similarly in terms of physiological and meteorological factors, often ignoring unique regional aspects. Each of the six PEMs reviewed has developed unique methods to estimate NPP and the combination of the most successful of these could lead to improvements. It may be beneficial to develop regional PEMs that can be combined under a global framework. The results of this review suggest the creation of a hybrid PEM could bring about a significant enhancement to the PEM methodology and thus terrestrial carbon flux modeling.

Based upon this review, key research items were identified that appear crucial to improve the PEM methodology, including:

- LUE should not be assumed constant, but should vary by PFTs e.g. ([Heinsch, Zhao et al. 2006](#)), photosynthetic pathway e.g. ([Cao, Prince et al. 2004](#)), or other means.
- Continue to pursue relationships between satellite-derived variables and LUE or GPP e.g. ([Grace, Nichol et al. 2007](#); [Sims, Rahman et al. 2008](#)).
- Evidence is mounting that PEMs should consider incorporating diffuse radiation, especially at daily resolution e.g. ([Gu, Baldocchi et al. 2002](#); [Turner, Urbanski et al. 2003](#); [Turner, Ritts et al. 2006](#); [Jenkins, Richardson et al. 2007](#)), however caution should be applied e.g. ([Alton 2008](#)).
- Exercise caution if utilizing land cover products or LAI in PEMs ([Heinsch, Zhao et al. 2006](#); [Jung, Henkel et al. 2006](#); [McCallum, Obersteiner et al. 2006](#); [Garrigues, Lacaze et al. 2008](#)).
- Investigate incorporating scatterometer data to account for spring thaw and the freeze/thaw cycle duration e.g. ([Bartsch, Kidd et al. 2007](#)).
- Soil moisture available from satellite measurements e.g. ([Wagner, Blöschl et al. 2007](#)), should be considered for inclusion in PEMs e.g. ([Verstraeten, Veroustraete et al. 2007](#)).
- PEMs should also consider the need to account for GPP saturation when radiation is high e.g. ([Ibrom, Oltchev et al. 2008](#)).
- Consider some form of frost stress, perhaps via air temperature e.g. ([Lafont, Kergoat et al.](#)

[2002](#)), if not already included.

These research items listed above are crucial if we wish to address the error sources and variability that surround the present estimates of GPP and NPP. Results from this review show a range of variability around all of the key PEM input variables, suggesting that potential error is large.

4.2 Spatial comparison of global land cover datasets (Paper II)

Paper II resulted in a spatial comparison of four global land cover datasets (i.e. IGBP, UMD, GLC2000 and MODIS). Initially, a total percent area comparison of the four global land cover datasets assigned to each of the original IGBP land cover classes was performed. The results indicate reasonable agreement across the datasets for evergreen forest classes, open shrub lands, grasslands, croplands, urban classes and snow/ice/barren classes. However, disagreement occurs across the datasets between the deciduous and mixed forest classes, closed shrub lands, savannas, woody savannas and the cropland/vegetation mosaic. A different picture emerges when a spatial comparison is made on the level of agreement between the global datasets (Figure 3). According to Figure 3, the only major regions classified similarly in all four datasets were the snow/ice regions over Greenland, the barren/ sparsely vegetated regions over Africa and the tropical evergreen broadleaf forests of Brazil, amounting to a total of 26% of the globe.

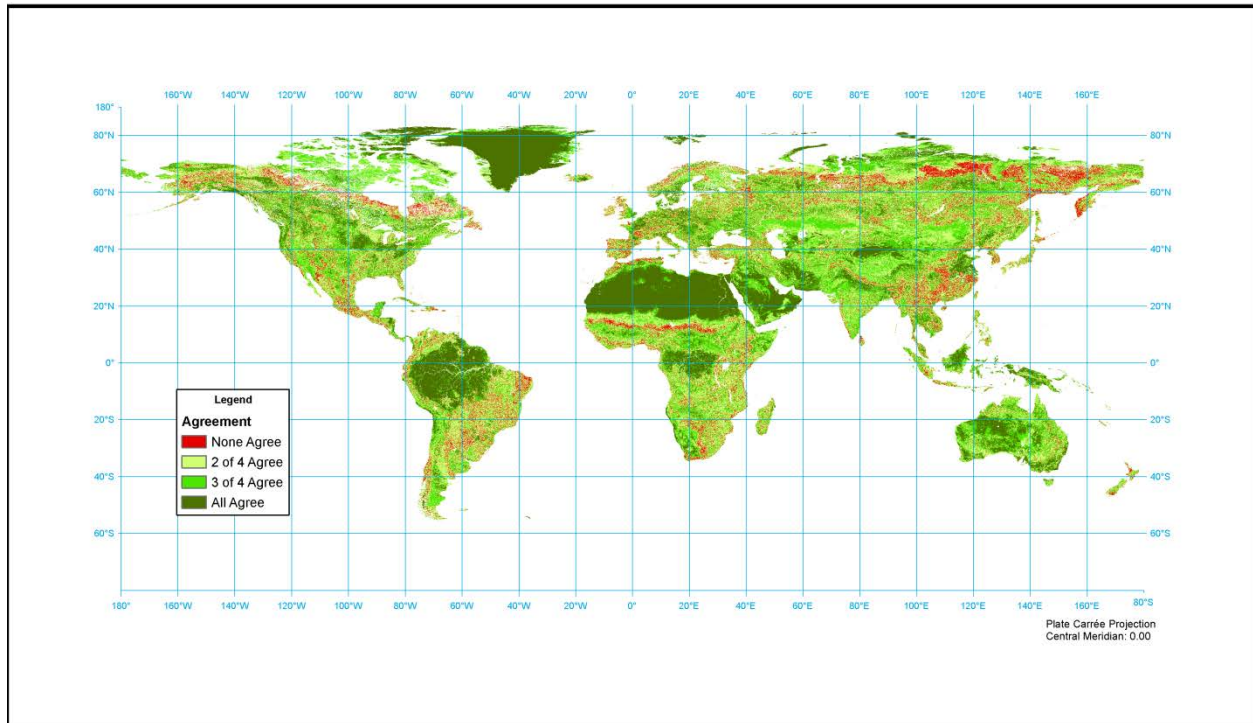


Figure 3. Global levels of agreement among the IGBP, UMD, GLC2000 and MODIS land cover datasets, compared according to the IGBP classification.

In addition to global studies, global land cover datasets are often used for analyses at the continental, country and regional levels regardless of whether or not they were intended for this purpose. Therefore, it is important to have an awareness of the possible differences between the datasets at these scales, as differences will arise between regions based on many factors. In an effort to better describe and understand the levels of agreement between the datasets, seven test sites were identified across the globe for comparison (Table 3). In the case of Russia, all four land cover datasets agree on only 9% of the pixels in the test site. Furthermore, on more than half of the pixels in the Russian test site, only two of the four products agree at best. This implies that the use of a particular land cover dataset over this area is likely to introduce additional uncertainty to any modeling exercise that relies upon it.

Table 3. Percent agreement of the four global land cover datasets (IGBP, UMD, GLC2000 and MODIS) across the seven (5 x 5 degree) test sites in decreasing order of full agreement.

Test Sites	None Agree	2 of 4 Agree	3 of 4 Agree	All Agree	Longitude (center)	Latitude (center)
S. America	0	2	16	82	-62.5	-2.5
N. America	4	37	34	25	-107.5	52.5

Europe	19	42	24	15	7.5	47.5
Africa	10	49	30	11	22.5	-7.5
Australia	8	49	33	10	147.5	-27.5
Russia	5	49	37	9	97.5	57.5
Asia	26	55	15	4	102.5	27.5

4.3 Comparison of four global fAPAR datasets (Paper III)

Results from Paper III demonstrate the seasonal trend of the four global fAPAR datasets monthly mean values over the entire study region by land cover type in the year 2000 (Figure 4). For deciduous broadleaf, evergreen needle leaf and mixed forests, MODIS begins to absorb fAPAR a full 1-2 months ahead of other products. The peak in mean fAPAR values across Northern Eurasia for all datasets and land cover types occurs in July. However, the MODIS (as in previous studies) and CYCLOPES datasets have substantially higher growing season mean values compared to the JRC and GLOBCARBON datasets. Highest agreement occurs during green-up (May) and senescence (October), however the rates of change are also largest in these two periods. Large variation occurs during the winter months, with values ranging from 0.0 to 0.4. Winter values in evergreen forests generally remain higher than deciduous values, grassland/shrublands and croplands, as expected. CYCLOPES tends to record the highest values in winter, while MODIS and GLOBCARBON the lowest.

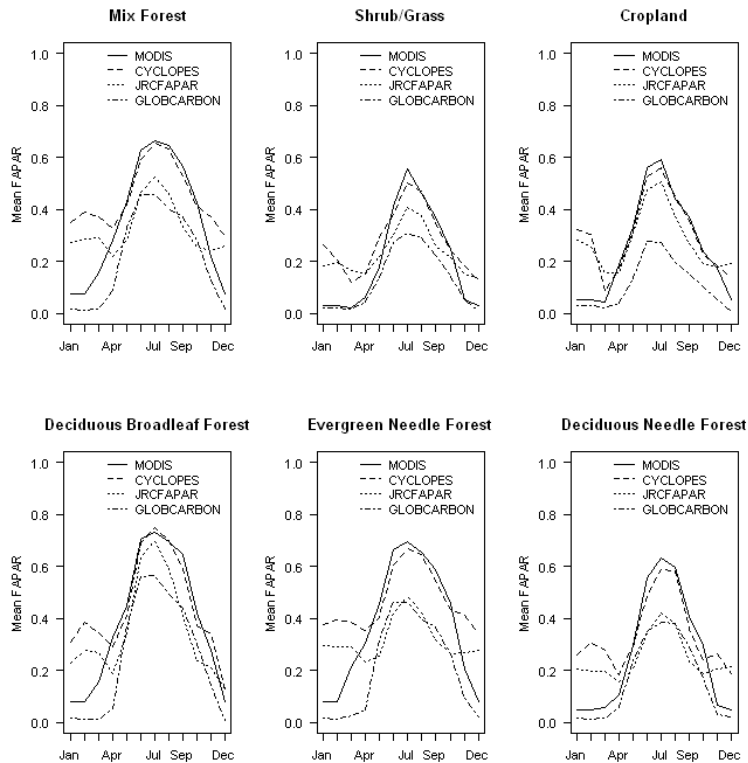


Figure 4. Comparison of monthly mean values from four global fAPAR datasets over northern Eurasia for the year 2000, by land cover type. Datasets from MODIS for January and February are not available, thus values for December were applied.

Across all six land cover classes, fAPAR mean values are highest in the forest classes, with the highest values occurring in the deciduous broadleaf class. This is particularly significant as the level of agreement among three of the datasets is also high (GLOBCARBON is significantly lower), although the deciduous broadleaf forest class represents only 3% of the vegetative area. Additionally, three of the datasets agree in croplands, again pointing to potential difficulties in the remaining dataset (GLOBCARBON) to record fAPAR in croplands. This implies that the datasets are in fact utilising a similar definition of fAPAR, and that disagreement among the remaining classes is due to algorithm and or sensor related differences. In the remaining classes the gap between the datasets is often large. In needleleaved and mixed forests, MODIS and CYCLOPES are in close agreement, but consistently higher than JRC and GLOBCARBON (also in close agreement).

An RMSE map of the four global fAPAR datasets was made for July, 2000 over northern Eurasia, highlighting agreement/disagreement, particularly noticeable in the far north (Figure 5). Below 60°N,

agreement among the datasets generally improves. An anomaly from the GLOBCARBON dataset is strongly visible in the far north (appearing in red). Agreement appears highest over the deciduous broadleaf and mixed forests, and lowest over the deciduous needle leaf forests (mean RMSE 0.16). Maximum RMSE reached upwards of 0.5.

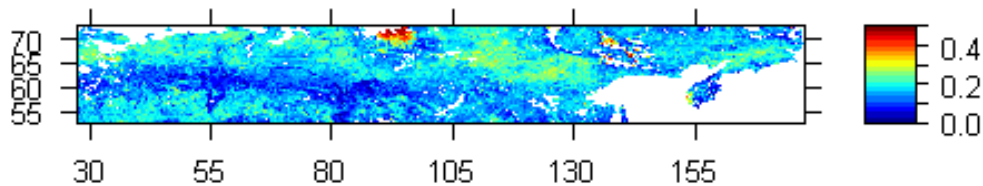


Figure 5. RMSE map of four global fAPAR datasets (MODIS, CYCLOPES, JRC and GLOBCARBON) for July, 2000 over northern Eurasia. X-axis depicts longitude (°), y-axis depicts latitude (°).

4.4 Improved light and temperature responses for GPP models (Paper IV)

Results presented in Paper IV describe improved light and temperature responses for GPP models over NE. Scatterplots, annual flux and environmental scalars are presented for the tundra (Cherskii) site for the year 2003 (Figure 6). For the Cherskii site, the LUE model performs poorly, in comparison with the LUE-TA, LUE-TAL and BL models. Both the scatterplot and annual flux indicates that the LUE approach is not able to capture the daily measurements, while the LUE-TA, LUE-TAL and BL approaches are more successful. The environmental scalars used in the four approaches are notably different, with the LUE model scalars for temperature and VPD showing large variation over the year. In contrast, the scalars for the LUE-TA and in particular the BL approaches are smoother, with VPD showing negligible effect and temperature having a very strong effect. In the case of the LUE-TAL model, the light scalar allows the temperature scalar to increase, while the VPD scalar remains largely non-limiting. Furthermore, the scatterplots in Figure 6 (top row) imply that the LUE and BL models are the least biased. The LUE-TA and LUE-TAL models seem to have a clear problem with overestimation of low values of GPP.

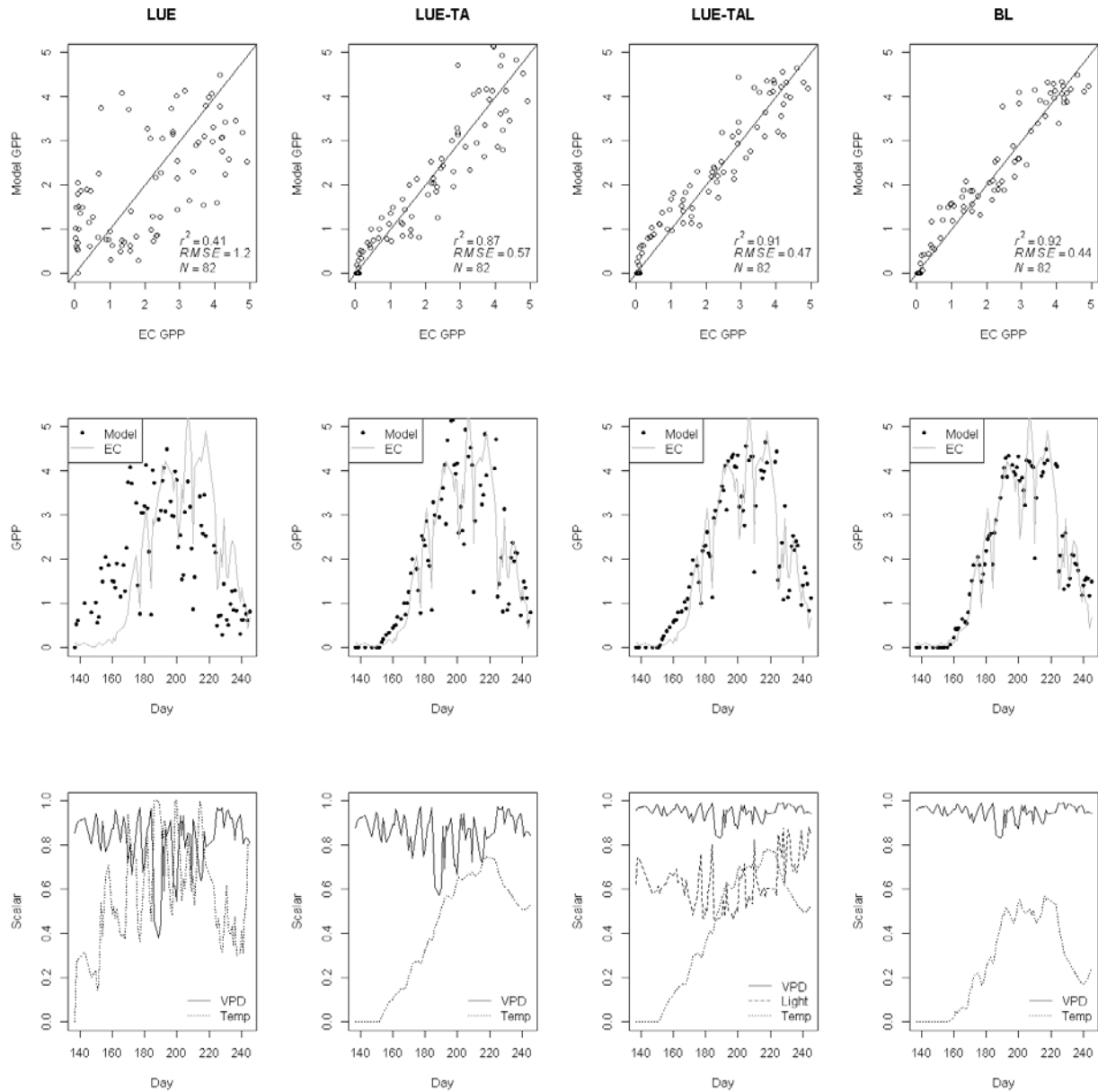


Figure 6. Results for Cherskii, 2003 from the LUE (1st column), LUE-TA (2nd column), LUE-TAL (3rd column) and BL (4th column) models where the top row depicts scatterplots of eddy covariance (EC) GPP vs. model GPP, the middle row depicts the daily course of GPP (EC and model) and the bottom row depicts the environmental scalars for temperature and VPD.

Mean square error was used as an indicator of performance resulting from cross-validation where the smaller of the MSE values is preferred (Table 4). For the majority of site-year combinations (with the

exception of RU-Che 2004/2005 and RU-Fyo 2002), the MSE values for the LUE and LUE-TA models are larger than those of the LUE-TAL and BL models. Hence, based on the 10-out cross validation performed here, the LUE-TAL and BL models, accounting for temperature acclimation and a non-linear light response, generally outperform the LUE and LUE-TA approaches. In particular, the LUE-TAL records a lower MSE in 8 of the 17 site-year combinations, along with the lowest overall mean MSE. The BL model records the lowest MSE in 6 of the 17 site-year combinations. Based on this assessment, the LUE-TAL model appears to perform better in less environmentally stressful sites, while the BL model generally outperforms in more climate controlled sites. On two occasions at the Cherskii site, the LUE-TA model outperforms the models with a non-linear light response, underscoring the effect of temperature at these locations.

Table 4. Cross validation results (MSE) from the LUE, LUE-TA, LUE-TAL and BL models for all site years, and mean results for each model. Bold indicates lowest recorded MSE values per site-year and model.

Site	Year	LUE	LUE-TA	LUE-TAL	BL
RU-Che	2002	0.451	0.43	0.24	0.309
	2003	2.152	0.377	0.269	0.211
	2004	1.269	0.43	0.452	0.672
	2005	1.646	1.62	1.806	1.804
RU-Cho	2003	1.873	0.743	0.573	0.493
	2004	0.907	0.844	0.381	0.295
	2005	3.522	1.86	1.069	0.903
RU-Fyo	2002	5.393	5.544	6.944	5.869
	2003	4.013	4.506	3.116	3.827
	2004	2.87	2.44	1.543	1.796
	2005	3.207	2.491	1.534	1.886
RU-Ha1	2002	0.505	0.458	0.223	0.289
	2003	0.732	0.557	0.313	0.492
	2004	0.589	0.477	0.462	0.576
RU-Zot	2002	1.783	0.879	0.785	0.782
	2003	1.591	1.431	0.96	0.836
	2004	1.422	1.281	0.802	1.03

Mean	1.996	1.551	1.263	1.298
-------------	-------	-------	--------------	-------

4.5 Continental GPP mapping: use of a diagnostic model (Paper V)

Paper V presents the results of continental GPP mapping using the BL model described in Paper IV. The methodology (as described above) has resulted in a spatial database mapping GPP across boreal Russia for the years 2002 - 2005. Figure 7 demonstrates a snapshot of the variables PAR, fAPAR, the environmental modifiers (temperature and VPD) and A_{\max} for day 200 in 2004. PAR shows large variation across the region resulting from cloud cover. fAPAR demonstrates generally moderate values correlated with vegetation productivity. The environmental modifiers for temperature and VPD both demonstrate favorable environmental growth conditions, with temperature still inhibiting in the far north and northeast and several pockets of limiting VPD in the warmer southeast. A_{\max} is a relatively constant value across the region with lower values in the cooler regions of the far north and montane areas.

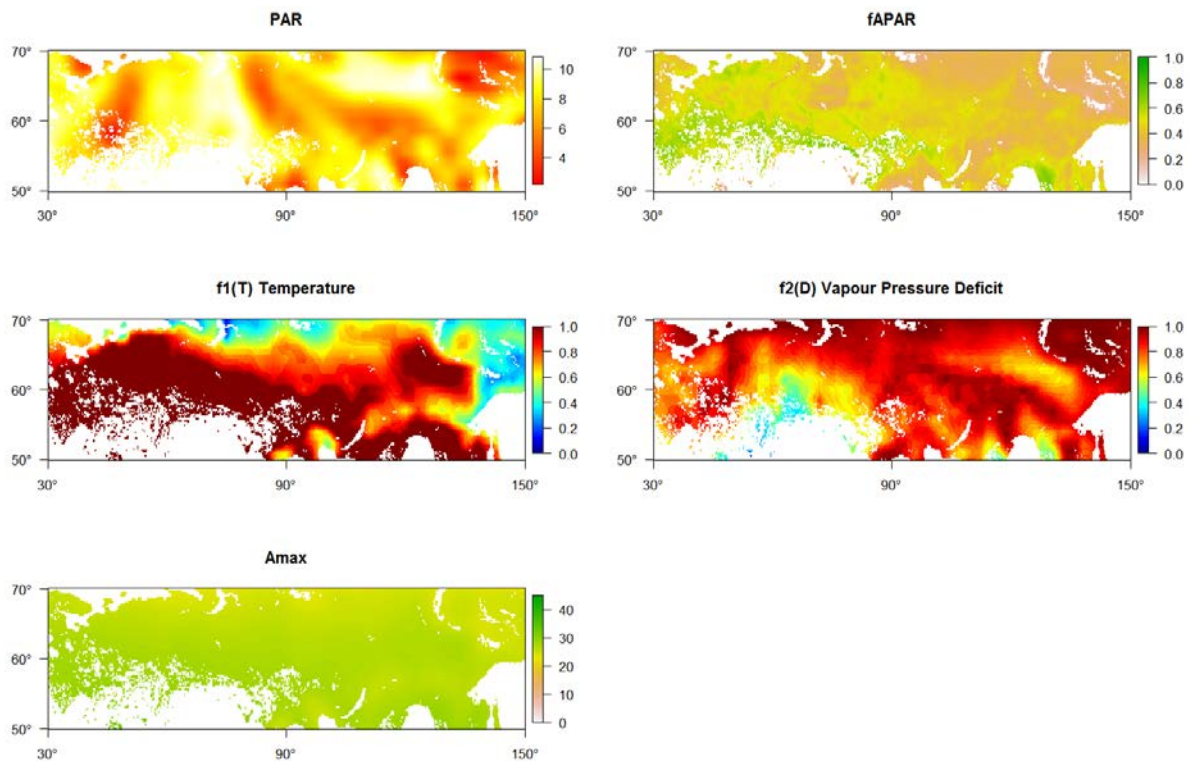


Figure 7. Maps of PAR ($W m^{-2} s^{-1}$), fAPAR, the environmental modifiers (temperature and VPD) and A_{\max} ($\mu mol CO_2 m^{-2} s^{-1}$) for day 200, year 2004.

Figure 8 shows the three gridded GPP products for 2004, namely the BL approach (this study), IIASA and MODIS products. Both of the diagnostic approaches (i.e. the BL and MODIS datasets) appear smoother and more homogeneous in comparison to the IIASA (carbon accounting) dataset. The IIASA product is very heterogeneous as it contains the most detail in terms of its underlying land cover map and the hybrid approach taken to create it. Nonetheless, general patterns of GPP agree across the datasets, although absolute values differ. The associated histograms provide further insight into the distribution of GPP across the study area. The IIASA dataset appears unimodal, with a peak at 600 g C m^{-2} although there is a hint of a second peak at 350 g C m^{-2} . Both the BL and MODIS show bimodality. The BL model obtains two peak distributions, one at 250 g C m^{-2} and a second at 550 g C m^{-2} . The MODIS dataset in particular appears bimodal, with the first peak at 250 g C m^{-2} and the second peak at 650 g C m^{-2} . The mixture of land classes across the region (i.e. forest, grasses, tundra) leads to these distributions.

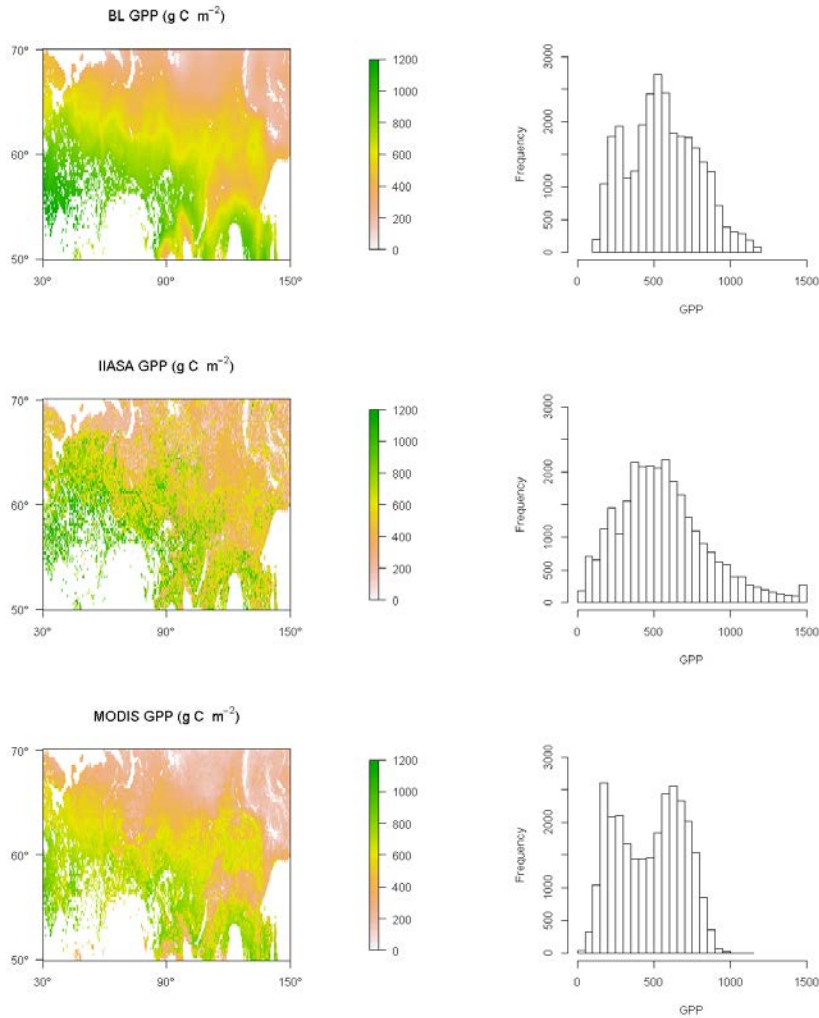


Figure 8. Annual summary for 2004 of GPP over entire study area from BL, MODIS and IIASA approaches. Scale bar set to limit of 1200 g C m^{-2} for comparison. Histograms show respective distribution of GPP for each map.

Comparing the three datasets in broad 0.25° mean longitudinal bands provides further insight into observed patterns (Figure 9). Generally, disagreement among the three products is least, east of the Ural Mountains (denoted by the dashed vertical line at 60° E). However, to the west of the Urals, the diagnostic approach of MODIS records significantly lower values than the IIASA approach in all years except 2005. Both the BL and MODIS approaches record the worst agreement in year 2002. Agreement is highest among all three products in 2005, owing in part to a higher mean temperature.

The largest differences between the BL, MODIS and IIASA results were observed in the longitudes 30° - 70° E . Both the BL and MODIS results underestimated the IIASA estimates, with MODIS recording the

greatest underestimation of 250 g C m^{-2} . This large underestimation over the most productive region of Russia (namely west of the Ural Mountains) demonstrates the potential inaccuracy of the MODIS measurements over this region. This has large implications in terms of accurately depicting the carbon flux with this method over this region. These underestimations are somewhat balanced out by weaker overestimations to the east of the Urals in some years. Overestimations to the east of the Urals are however less critical as the vegetation here is less productive, although the area is much larger.

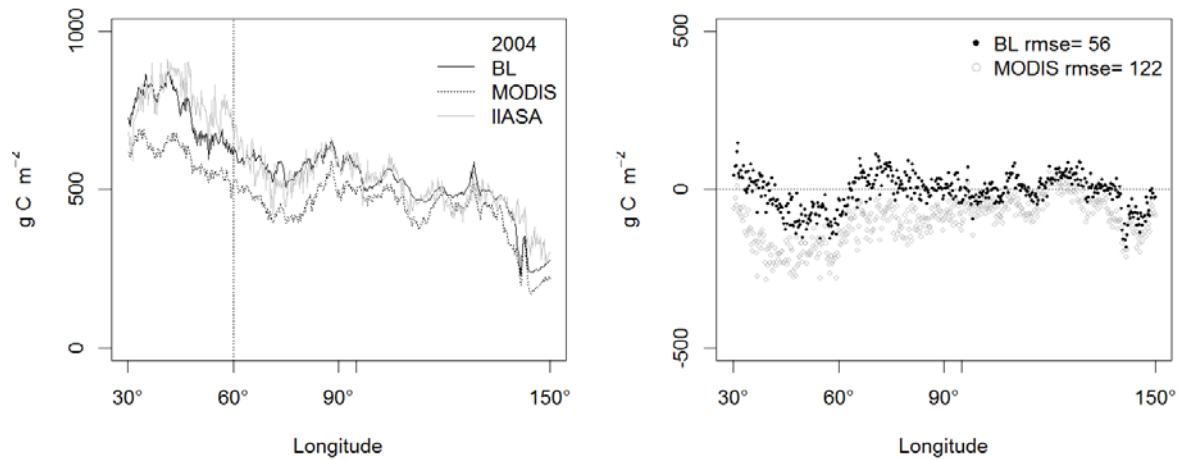


Figure 9. Mean annual longitudinal GPP in 2004 for the BL, MODIS and IIASA datasets across the study region (0.25° bands) (left column) and difference plots where IIASA results were subtracted from the BL and MODIS results (right column). Vertical bar marks the approximate location of the Ural Mountain range at 60° E. Mean RMSE values are shown for the BL and MODIS approaches (where the IIASA approach is considered the baseline).

5 Discussion

As outlined in the introduction, this dissertation has attempted to improve our understanding in regards to modelling vegetation productivity, in particular over northern Eurasia. With high levels of uncertainty in the terrestrial biospheric carbon cycle well documented, and the potential weakening or saturation of the net terrestrial carbon sink, it is becoming increasingly important to reduce these uncertainties in order to be able to better predict the future earth system response.

Hence this study began with a thorough review of the existing literature (Paper I), with the intent to design a research agenda that would help bring about a reduction in the uncertainties around some of the components of modelling vegetation productivity. Several of the items on this research agenda have been addressed in this dissertation, namely *A_{max}* was not assumed constant but allowed to vary based on a relationship with long-term average temperature, we avoided using a land cover dataset in our model owing to the large uncertainties that we identified in these datasets, and we included a non-linear light response function and incorporated temperature acclimation. Furthermore we identified discrepancies in the available global fAPAR datasets and selected one deemed most suitable for the study region. Other items were deemed beyond the scope of this dissertation but nonetheless are highlighted for future research. While some progress has been made to address some of the issues raised in this study, much work remains.

In particular we addressed the known uncertainty surrounding two important datasets typically used in PEMs (Papers II and III). Land cover datasets have been shown to introduce potential uncertainty into model results ([McCallum, Wagner et al. 2009](#)). This comparison (Paper II) shows varying levels of agreement among the four global land cover datasets and suggests that users exercise caution when using any one particular product. In a study on global carbon sequestration, choice of land cover dataset influenced the model results by as much as 45% ([Benitez, McCallum et al. 2004](#)). Analysis using global land cover products should utilize several of these products in order to show the magnitude of possible differences. However, considerable disagreement among them and classification legends not primarily suited for specific applications such as carbon cycle model parameterizations pose significant challenges and uncertainties in the use of such data sets ([Jung, Henkel et al. 2006](#)). It may in fact be prudent to avoid the use of land cover datasets altogether in PEMs.

With the importance of fAPAR in PEMs and the existence of several global products, a quantitative comparison and analysis was warranted (Paper III). The difficulty in this study was the lack of in-situ data

for comparison with the satellite-based datasets. Analysis was performed based on a comparison of the datasets and a review of published studies describing or utilizing those datasets. This study identified the JRC fAPAR dataset as being most applicable to northern Eurasia. However, it was noted that dataset choice was very much land cover or biome dependent. The results of this study were applied in the seminal publication of ([Beer, Reichstein et al. 2010](#)) who demonstrated the strong effect different fAPAR datasets had on global GPP. For the time being, it is necessary to include multiple fAPAR products when performing global assessments, or to focus on specific regions and select the most suitable dataset.

With a variety of tools now available to model GPP globally, the accuracy of existing models is increasingly being called into question. Past intra- model comparisons pointed to broad agreement between model outputs, recognizing that large variability occurred within the models themselves. However, recent model-data comparisons have shown much more pessimistic results. As mentioned in the introduction, this is occurring for many reasons, including: (1) the majority of models have not been calibrated with in-situ data and hence cannot replicate the detailed in-situ estimates; (2) models generally operate at much coarser spatial resolution than in-situ measurements; and (3) models are designed to be generally applicable at the continental or global level.

Hence Paper IV set about to calibrate four GPP models against flux tower data. The results presented here (using cross validation) clearly demonstrate that accounting for temperature acclimation particularly at northern (temperature controlled) sites significantly improves the fit of modeled versus eddy covariance derived daily GPP values. These results indicate that inclusion of temperature acclimation on sites experiencing cold temperatures is imperative. It is important to note that the majority of GPP models currently do not account for temperature acclimation. Furthermore, models with a non-linear light response generally outperform models with a linear light response, increasingly so at the southern less temperature-controlled sites. Thus, developing models that address unique biome-level properties calibrated with EC data may help to improve the accuracy of global LUE-based models. The findings from this study are useful for the modeling community in general, who are perhaps not entirely aware of the impacts that including (in particular) temperature acclimation may have on model results.

In order to be able to measure our improvement in GPP modeling over northern Eurasia, it was necessary to establish a baseline measurement for the region. This was accomplished by comparison of the LEA/carbon accounting methodology, atmospheric measurements and DGVM results over central Siberia ([Quegan, Beer et al. 2011](#)). Results for NPP demonstrated broad agreement among the

approaches over central Siberia. However, results suggested that the flux partitioning derived by the LEA was more likely, on account of its use of empirical data. Hence the LEA was then applied across Russia and used in this study as the baseline assessment. It is important however to know that the LEA is based on long-term average data spanning several decades and hence does not represent a single year but a long-term mean value. Weaknesses in this approach include possible biases arising from unrepresentative sample data and temporal trends within the data.

Paper V resulted in a technique for regional gridded GPP mapping utilizing eddy covariance estimates over a region sparsely covered with in-situ sites. The diagnostic model used in this study was previously validated over this region ([McCallum, Franklin et al. 2013](#)). Furthermore, it utilises satellite-derived fAPAR (i.e. not NDVI or an LAI correlation) and the fAPAR product used was previously analyzed over Russia ([McCallum, Wagner et al. 2010](#)). Finally, results were compared against MOD17A2/A3 C5.1 and an independent inventory based approach ([Shvidenko, Schepashchenko et al. 2008](#)) demonstrating that this new method yields plausible results. The new predictions differ from the MODIS results and show the improvement that this methodology achieves over a large region. Assuming that the carbon accounting approach is a viable baseline estimate, these new results are consistently closer to the baseline than MODIS.

The most obvious difficulty with the method presented here is the lack of flux tower locations. Additional tower locations do exist (approximately 14 eddy covariance sites exist in Russia), but for a variety of reasons these could not be used. More tower locations would naturally increase the confidence in the results. All five eddy covariance locations used in the model parameterization were not water-limited, hence applied at water-limited sites, this model will likely over-estimate GPP. Thus this simple diagnostic model is most applicable over cold, non water-limited regions.

In summary, findings from this study are important as vegetation productivity is a key input variable in many ecosystem models. These models require, among other datasets, an accurate depiction of vegetation productivity in order to address a variety of global land use issues. Hence, reducing uncertainty in gross primary productivity estimates is a key goal within the scientific community. Future efforts should focus on up-scaling of the EC estimates. In order to facilitate this, there is a need for a substantial expansion (by several orders of magnitude) of the ground based observation network ([Ciais, Dolman et al. 2013](#)).

5.1 Conclusions

The main conclusions and scientific contributions derived from this dissertation are as follows:

- Improvements to the PEM approach were identified and addressed, including: LUE should not be assumed constant but should be varying; cautionary use of global land cover products; and the need to account for GPP saturation and frost stress via temperature. Additional improvements to the PEM approach were identified for future work, including: pursue relationships between satellite-derived variables and LUE or GPP; diffuse radiation; and soil moisture, among others.
- Large variation exists among available global fAPAR datasets. This study identified one fAPAR dataset as being most applicable to northern Eurasia. However, it was noted that dataset choice was very much land cover or biome dependent. The results of this study were used to demonstrate the strong effect different fAPAR datasets had on global GPP ([Beer, Reichstein et al. 2010](#)). For the time being, it appears necessary to include multiple fAPAR products when performing global assessments.
- Results clearly demonstrate that accounting for temperature acclimation particularly at northern (temperature controlled) sites significantly improves the fit of modeled versus eddy covariance derived daily GPP values. These results indicate that inclusion of temperature acclimation on sites experiencing cold temperatures is imperative. Furthermore, models with a non-linear light response generally outperform models with a linear light response, increasingly so at the southern less temperature-controlled sites. Thus, developing models that address unique biome-level properties calibrated with EC data may help to improve the accuracy of global LUE-based models.
- A new GPP model outperforms MODIS over northern Eurasia, matching closely the LEA. The approach presented in this study is better able to estimate GPP than a model parameterized globally. Furthermore it demonstrates that an up-scaling procedure, even using limited EC data, is effective.
- All these efforts are hampered by a lack of in situ measurements, particularly over regions such as northern Eurasia. Nonetheless, future efforts should focus on up-scaling of EC data, using statistical methods and semi-empirical models. In order to facilitate this, there is a need for a substantial expansion (by several orders of magnitude) of the ground based observation network.

5.2 Way Forward

Undoubtedly, a globally integrated carbon observation and analysis system is needed to improve the fundamental understanding of the global carbon cycle, to improve our ability to project future changes, and to verify the effectiveness of policies aiming to reduce greenhouse gas emissions and increase carbon sequestration (Ciais, Dolman et al. 2013). The current system is sparse from an in-situ standpoint in terms of geographical extent and temporal frequency, is exploratory in nature and to some extent ad-hoc, and lacks long-term commitment.

However, various initiatives are underway around the globe to address this situation, e.g. the European Eddy Fluxes Database Cluster (www.europe-fluxdata.eu). The European Eddy Fluxes Database Cluster is an initiative to improve standardization, integration and collaboration between databases that are part of European research projects. It has been created with the aim to host in a single infrastructure flux measurements between ecosystems and atmosphere and to provide standard and high quality data processing and data sharing tools.

Furthermore, new satellite missions are planned, including both the GOSAT-2 and OCO-2, both with enhanced CO₂ monitoring capabilities as compared to their predecessors. A key challenge is to bring remote sensing measurements to a level of long-term consistency and accuracy so that they can be efficiently combined in models to reduce uncertainties, in synergy with ground-based data (Ciais, Dolman et al. 2013).

Past intra-model comparisons of terrestrial NPP have tended to show high agreement between model results and inferred high accuracy from this agreement. However, recent studies demonstrating model-data comparisons have shown poor results, suggesting that our current monitoring and forecasting of terrestrial CO₂ fluxes are highly uncertain. With recent improvements in the global in-situ CO₂ monitoring network, and increasing availability and quality of biophysical and reanalysis meteorological datasets, new methods for reducing uncertainty hold great promise.

The FLUXCOM initiative aims at providing an array of improved data-driven flux products and includes pure machine learning based regression methods, and semi-empirical models, both trained at FLUXNET sites. A large number of predictor (explanatory) variables containing extensive remote sensing records such as reflectance, LAI and land surface temperature are now available for training and upscaling. Methods such as the model tree ensemble show great promise (Jung, Reichstein et al. 2010). Future upscaling studies are expected to advance toward incorporating the impacts of disturbance on

ecosystem carbon dynamics, quantifying uncertainties associated with gridded flux estimates, and comparing various upscaling methods and the resulting gridded flux fields ([Xiao, Chen et al. 2012](#)).

6 References

- Ahl, D. E., S. T. Gower, et al. (2004). "Heterogeneity of light use efficiency in a northern Wisconsin forest: implications for modeling net primary production with remote sensing." Remote Sensing of Environment **93**(1-2): 168-178.
- Alton, P. B. (2008). "Reduced carbon sequestration in terrestrial ecosystems under overcast skies compared to clear skies." Agricultural and Forest Meteorology **148**(10): 1641-1653.
- Anderson, M. C., J. M. Norman, et al. (2000). "An analytical model for estimating canopy transpiration and carbon assimilation fluxes based on canopy light-use efficiency." Agricultural and Forest Meteorology **101**(4): 265-289.
- Arneth, A., J. Kurbatova, et al. (2002). "Comparative ecosystem-atmosphere exchange of energy and mass in a European Russian and a central Siberian bog II. Interseasonal and interannual variability of CO₂ fluxes." Tellus, Series B: Chemical and Physical Meteorology **54**(5): 514-530.
- Baker, D. F. (2007). "Reassessing carbon sinks." Science **316**(5832): 1708-1709.
- Baldocchi, D., E. Falge, et al. (2001). "FLUXNET: A New Tool to Study the Temporal and Spatial Variability of Ecosystem-Scale Carbon Dioxide, Water Vapor, and Energy Flux Densities." Bulletin of the American Meteorological Society **82**(11): 2415-2434.
- Balzter, H., F. F. Gerard, et al. (2005). "Impact of the Arctic Oscillation pattern on interannual forest fire variability in Central Siberia." Geophysical Research Letters **32**(14): 1-4.
- Bartalev, S. A., A. S. Belward, et al. (2003). "A new SPOT4-VEGETATION derived land cover map of Northern Eurasia." International Journal of Remote Sensing **24**(9): 1977-1982.
- Bartsch, A., R. A. Kidd, et al. (2007). "Temporal and spatial variability of the beginning and end of daily spring freeze/thaw cycles derived from scatterometer data." Remote Sensing of Environment **106**(3): 360-374.
- Beer, C., M. Reichstein, et al. (2010). "Terrestrial gross carbon dioxide uptake: Global distribution and covariation with climate." Science **329**(5993): 834-838.
- Benitez, P., I. McCallum, et al. (2004). Global Supply for Carbon Sequestration: Identifying Least-Cost Afforestation Sites Under Country Risk Considerations. Laxenburg, IIASA. **IR-04-022**: 22 pp.
- Cao, M., S. D. Prince, et al. (2004). "Remotely sensed interannual variations and trends in terrestrial net primary productivity 1981-2000." Ecosystems **7**(3): 233-242.
- Chapin, F. S., P. A. Matson, et al. (2002). Principles of Terrestrial Ecosystem Ecology, Springer.
- Churkina, G. and S. W. Running (1998). "Contrasting climatic controls on the estimated productivity of global terrestrial biomes." Ecosystems **1**(2): 206-215.
- Ciais, P., A. J. Dolman, et al. (2013). "Current systematic carbon cycle observations and needs for implementing a policy-relevant carbon observing system." Biogeosciences Discuss. **10**(7): 11447-11581.
- Cihlar, J., S. Denning, et al. (2002). "Initiative to quantify terrestrial carbon sources and sinks." EOS, Transactions, American Geophysical Union **83**(1): 5-6.
- Corradi, C., O. Kolle, et al. (2005). "Carbon dioxide and methane exchange of a north-east Siberian tussock tundra." Global Change Biology **11**(11): 1910-1925.
- Cramer, W., D. W. Kicklighter, et al. (1999). "Comparing global models of terrestrial net primary productivity (NPP): Overview and key results." Global Change Biology **5**(SUPPL. 1): 1-15.
- Dee, D. P., S. M. Uppala, et al. (2011). "The ERA-Interim reanalysis: configuration and performance of the data assimilation system." Quarterly Journal of the Royal Meteorological Society **137**(656): 553-597.
- Di Gregorio, A. and L. J. M. Jansen (2000). Land Cover Classification System (LCCS): Classification Concepts and User Manual. Rome, Italy, FAO: 179 pp.

- Dolman, A., T. Maximov, et al. (2004). "Net ecosystem exchange of carbon dioxide and water of far eastern Siberian Larch (< i>Larix cajanderii</i>) on permafrost." Biogeosciences **1**(2): 133-146.
- Enting, I. G. and J. V. Mansbridge (1989). "Seasonal sources and sinks of atmospheric CO₂. Direct inversion of filtered data." Tellus, Series B **41 B**(2): 111-126.
- Franklin, O. (2007). "Optimal nitrogen allocation controls tree responses to elevated CO₂." New Phytologist **174**(4): 811-822.
- Friend, A. D., A. Arneeth, et al. (2007). "FLUXNET and modelling the global carbon cycle." Global Change Biology **13**(3): 610-633.
- Garrigues, S., R. Lacaze, et al. (2008). "Validation and intercomparison of global Leaf Area Index products derived from remote sensing data." Journal of Geophysical Research G: Biogeosciences **113** (2): **G02028** (2).
- Gobron, N., B. Pinty, et al. (2006). "Evaluation of fraction of absorbed photosynthetically active radiation products for different canopy radiation transfer regimes: Methodology and results using Joint Research Center products derived from SeaWiFS against ground-based estimations." Journal of Geophysical Research: Atmospheres **111**(D13): (D13110).
- Goetz, S. J. and S. D. Prince (1999). Modelling Terrestrial Carbon Exchange and Storage: Evidence and Implications of Functional Convergence in Light-use Efficiency. Advances in Ecological Research, Academic Press. **Volume 28**: 57-92.
- Goetz, S. J., S. D. Prince, et al. (1999). "Satellite remote sensing of primary production: An improved production efficiency modeling approach." Ecological Modelling **122**(3): 239-255.
- Goldammer, J. G. (1996). "The boreal forest, fire, and the global climate system: Achievements and needs in joint east-west boreal fire research and policy development." Combustion, Explosion and Shock Waves **32**(5): 544-557.
- Grace, J., C. Nichol, et al. (2007). "Can we measure terrestrial photosynthesis from space directly, using spectral reflectance and fluorescence?" Global Change Biology **13**(7): 1484-1497.
- Gu, L., D. Baldocchi, et al. (2002). "Advantages of diffuse radiation for terrestrial ecosystem productivity." Journal of Geophysical Research D: Atmospheres **107**(5-6): 2-1.
- Gurney, K. R., R. M. Law, et al. (2002). "Towards robust regional estimates of CO₂ sources and sinks using atmospheric transport models." Nature **415**(6872): 626-630.
- Heinsch, F. A., M. Zhao, et al. (2006). "Evaluation of remote sensing based terrestrial productivity from MODIS using regional tower eddy flux network observations." IEEE Transactions on Geoscience and Remote Sensing **44**(7): 1908-1923.
- Hirose, T., D. D. Ackerly, et al. (1997). "CO₂ elevation, canopy photosynthesis, and optimal leaf area index." Ecology **78**(8): 2339-2350.
- Hirose, T. and M. J. A. Werger (1987). "Nitrogen use efficiency in instantaneous and daily photosynthesis of leaves in the canopy of a *Solidago altissima* stand." Physiol. Plant. **70**: 215-222.
- Ibrom, A., A. Oltchev, et al. (2008). "Variation in photosynthetic light-use efficiency in a mountainous tropical rain forest in Indonesia." Tree Physiology **28**(4): 499-508.
- IPCC (2013). Working Group I Contribution to the IPCC Fifth Assessment Report . Climate Change 2013: The Physical Science Basis Summary for Policymakers.: 36 pp.
- Jenkins, J. P., A. D. Richardson, et al. (2007). "Refining light-use efficiency calculations for a deciduous forest canopy using simultaneous tower-based carbon flux and radiometric measurements." Agricultural and Forest Meteorology **143**(1-2): 64-79.
- Joos, F., I. Colin Prentice, et al. (2001). "Global warming feedbacks on terrestrial carbon uptake under the intergovernmental Panel on Climate Change (IPCC) emission scenarios." Global Biogeochemical Cycles **15**(4): 891-907.
- Jung, M., K. Henkel, et al. (2006). "Exploiting synergies of global land cover products for carbon cycle modeling." Remote Sensing of Environment **101**(4): 534-553.

- Jung, M., M. Reichstein, et al. (2010). "Recent decline in the global land evapotranspiration trend due to limited moisture supply." Nature **467**(7318): 951-954.
- Kajii, Y., S. Kato, et al. (2002). "Boreal forest fires in Siberia in 1998: Estimation of area burned and emissions of pollutants by advanced very high resolution radiometer satellite data." Journal of Geophysical Research D: Atmospheres **107**(24).
- Lafont, S., L. Kergoat, et al. (2002). "Spatial and temporal variability of land CO₂ fluxes estimated with remote sensing and analysis data over western Eurasia." Tellus, Series B: Chemical and Physical Meteorology **54**(5): 820-833.
- Landsberg, J. J. and R. H. Waring (1997). "A generalised model of forest productivity using simplified concepts of radiation-use efficiency, carbon balance and partitioning." Forest Ecology and Management **95**(3): 209-228.
- Lapenis, A., A. Shvidenko, et al. (2005). "Acclimation of Russian forests to recent changes in climate." Global Change Biology **11**(12): 2090-2102.
- Le Quere, C., M. R. Raupach, et al. (2009). "Trends in the sources and sinks of carbon dioxide." Nature Geosci **2**(12): 831-836.
- Loveland, T. R., B. C. Reed, et al. (2000). "Development of a global land cover characteristics database and IGBP DISCover from 1 km AVHRR data." International Journal of Remote Sensing **21**(6-7): 1303-1330.
- Mäkelä, A., M. Pulkkinen, et al. (2008). "Developing an empirical model of stand GPP with the LUE approach: Analysis of eddy covariance data at five contrasting conifer sites in Europe." Global Change Biology **14**(1): 92-108.
- Marchesini, L. B., D. Papale, et al. (2007). "Carbon balance assessment of a natural steppe of southern Siberia by multiple constraint approach." Biogeosciences **4**(4): 581-595.
- McCallum, I., O. Franklin, et al. (2013). "Improved light and temperature responses for light-use-efficiency-based GPP models." Biogeosciences **10**(10): 6577-6590.
- McCallum, I., O. Franklin, et al. (2013). "Improved light and temperature responses for light use efficiency based GPP models." Biogeosciences Discuss. **10**(5): 8919-8947.
- McCallum, I., M. Obersteiner, et al. (2006). "A spatial comparison of four satellite derived 1 km global land cover datasets." International Journal of Applied Earth Observation and Geoinformation **8**(4): 246-255.
- McCallum, I., W. Wagner, et al. (2009). "Satellite-based terrestrial production efficiency modeling." Carbon Balance and Management **4**: 8.
- McCallum, I., W. Wagner, et al. (2010). "Comparison of four global FAPAR datasets over Northern Eurasia for the year 2000." Remote Sensing of Environment **114**(5): 941-949.
- McGuire, A. D., F. S. Chapin III., et al. (2006). Integrated regional changes in arctic climate feedbacks: Implications for the global climate system. **31**: 61-91.
- Merbold, L., W. L. Kutsch, et al. (2009). "Artificial drainage and associated carbon fluxes (CO₂/CH₄) in a tundra ecosystem." Global Change Biology **15**(11): 2599-2614.
- Milyukova, I. M., O. Kolle, et al. (2002). "Carbon balance of a southern taiga spruce stand in European Russia." Tellus, Series B: Chemical and Physical Meteorology **54**(5): 429-442.
- Monteith, J. L. and M. H. Unsworth (1990). Principles of Environmental Physics. New York, Edward Arnold.
- Nabuurs, G. J., M. Lindner, et al. (2013). "First signs of carbon sink saturation in European forest biomass." Nature Climate Change **3**(9): 792-796.
- Nemani, R. R., C. D. Keeling, et al. (2003). "Climate-driven increases in global terrestrial net primary production from 1982 to 1999." Science **300**(5625): 1560-1563.
- Pan, Y., R. Birdsey, et al. (2006). "Improved estimates of net primary productivity from modis satellite data at regional and local scales." Ecological Applications **16**(1): 125-132.

- Papale, D., M. Reichstein, et al. (2006). "Towards a standardized processing of Net Ecosystem Exchange measured with eddy covariance technique: algorithms and uncertainty estimation." Biogeosciences **3**: 571-583.
- Papale, D. and R. Valentini (2003). "A new assessment of European forests carbon exchanges by eddy fluxes and artificial neural network spatialization." Global Change Biology **9**(4): 525-535.
- Prentice, I. C. (2001). Climate Change 2001: The Scientific Basis. Contribution of Working Group I to the Third Assessment Report of the Intergovernmental Panel on Climate Change. e. a. J. Houghton, Eds. , Cambridge University Press, Cambridge: pp. 183-237.
- Quegan, S., C. Beer, et al. (2011). "Estimating the carbon balance of central Siberia using a landscape-ecosystem approach, atmospheric inversion and Dynamic Global Vegetation Models." Global Change Biology **17**(1): 351-365.
- Reichstein, M., E. Falge, et al. (2005). "On the separation of net ecosystem exchange into assimilation and ecosystem respiration: review and improved algorithm." Global Change Biology **11**(9): 1424-1439.
- Ruimy, A., L. Kergoat, et al. (1999). "Comparing global models of terrestrial net primary productivity (NPP): Analysis of differences in light absorption and light-use efficiency." Global Change Biology **5**(SUPPL. 1): 56-64.
- Running, S. W., R. Nemani, et al. (1999). "MODIS daily photosynthesis (PSN) and annual net primary production (NPP) product (MOD17)." Algorithm Theoretical Basis Document (ATBD), Version 3.0.
- Running, S. W., R. R. Nemani, et al. (2004). "A continuous satellite-derived measure of global terrestrial primary production." BioScience **54**(6): 547-560.
- Running, S. W., Thornton, P. E., Nemani, R., & Glassy, J. M. (2000). Global terrestrial gross and net primary productivity from the Earth Observing System. Methods in ecosystem science. R. B. J. O. E. Sala, H. A. Mooney, & R. W. Howarth. New York, Springer-Verlag: 44-57.
- Schaefer, K., C. R. Schwalm, et al. (2012). "A model-data comparison of gross primary productivity: Results from the north American carbon program site synthesis." Journal of Geophysical Research G: Biogeosciences **117**(3).
- Schepaschenko, D., I. McCallum, et al. (2011). "A new hybrid land cover dataset for Russia: a methodology for integrating statistics, remote sensing and in situ information." Journal of Land Use Science **6**(4): 245-259.
- Seixas, J., N. Carvalhais, et al. (2007). Ecosystem production modelling in the Iberian Peninsula comparative analysis between MODIS and MERIS datasets. European Space Agency, (Special Publication) ESA SP.
- Shvidenko, A. and S. Nilsson (2003). "A synthesis of the impact of Russian forests on the global carbon budget for 1961-1998." Tellus, Series B: Chemical and Physical Meteorology **55**(2): 391-415.
- Shvidenko, A. and D. Schepaschenko (2013). "Climate Change and Wildfires in Russia." Contemporary Problems of Ecology **6**(7): 683-692.
- Shvidenko, A., D. Schepaschenko, et al. (2010). "Can the uncertainty of full carbon accounting of forest ecosystems be made acceptable to policymakers?" Climatic Change **103**(1-2): 137-157.
- Shvidenko A., S. D., McCallum I., Santoro M., Schmullius C. (2011). Use of remote sensing products in a terrestrial ecosystems verified full carbon account: Experiences from Russia. Proceedings: Earth Observation for Land-Atmosphere interaction Science, Frascati, Italy, ESA SP-688.
- Shvidenko, A. Z., D. G. Schepashchenko, et al. (2008). "Net primary production of forest ecosystems of Russia: A new estimate." Doklady Earth Sciences **421**(2): 1009-1012.
- Sims, D. A., A. F. Rahman, et al. (2008). "A new model of gross primary productivity for North American ecosystems based solely on the enhanced vegetation index and land surface temperature from MODIS." Remote Sensing of Environment **112**(4): 1633-1646.

- Sitch, S., B. Smith, et al. (2003). "Evaluation of ecosystem dynamics, plant geography and terrestrial carbon cycling in the LPJ dynamic global vegetation model." Global Change Biology **9**(2): 161-185.
- Sjoestroem, M., J. Ardoe, et al. (2011). "Exploring the potential of MODIS EVI for modeling gross primary production across African ecosystems." Remote Sensing of Environment **115**(4): 1081-1089.
- Stephens, B. B., K. R. Gurney, et al. (2007). "Weak northern and strong tropical land carbon uptake from vertical profiles of atmospheric CO₂." Science **316**(5832): 1732-1735.
- Still, C. J., J. T. Randerson, et al. (2004). "Large-scale plant light-use efficiency inferred from the seasonal cycle of atmospheric CO₂." Global Change Biology **10**(8): 1240-1252.
- Strahler, A., D. Muchoney, et al. (1999). MODIS Land Cover Product: Algorithm Theoretical Basis Document. Boston, MA, USA, Boston University: 72 pp.
- Tarnocai, C., J. G. Canadell, et al. (2009). "Soil organic carbon pools in the northern circumpolar permafrost region." Global Biogeochemical Cycles **23**(2).
- Tchebakova, N. M., O. Kolle, et al. (2002). "Inter-annual and seasonal variations of energy and water vapour fluxes above a Pinus sylvestris forest in the Siberian middle taiga." Tellus, Series B: Chemical and Physical Meteorology **54**(5): 537-551.
- Turner, D. P., W. D. Ritts, et al. (2006). "Evaluation of MODIS NPP and GPP products across multiple biomes." Remote Sensing of Environment **102**(3-4): 282-292.
- Turner, D. P., W. D. Ritts, et al. (2005). "Site-level evaluation of satellite-based global terrestrial gross primary production and net primary production monitoring." Global Change Biology **11**(4): 666-684.
- Turner, D. P., S. Urbanski, et al. (2003). "A cross-biome comparison of daily light use efficiency for gross primary production." Global Change Biology **9**(3): 383-395.
- van der Molen, M. K., J. van Huissteden, et al. (2007). "The growing season greenhouse gas balance of a continental tundra site in the Indigirka lowlands, NE Siberia." Biogeosciences **4**(6): 985-1003.
- Verstraeten, W. W., F. Veroustraete, et al. (2007). "Impact assessment of remotely sensed soil moisture on ecosystem carbon fluxes across Europe." 2nd International Workshop on Uncertainty in Greenhouse Gas Inventories.
- Vygodskaya, N. N., I. Milyukova, et al. (1997). "Leaf conductance and CO₂ assimilation of Larix gmelinii growing in an eastern Siberian boreal forest." Tree Physiology **17**(10): 607-615.
- Wagner, W., G. Blöschl, et al. (2007). "Operational readiness of microwave remote sensing of soil moisture for hydrologic applications." Nordic Hydrology **38**(1): 1-20.
- Xiao, J., J. Chen, et al. (2012). "Advances in upscaling of eddy covariance measurements of carbon and water fluxes." Journal of Geophysical Research G: Biogeosciences **117**(1).
- Zhao, M. and S. W. Running (2010). "Drought-induced reduction in global terrestrial net primary production from 2000 through 2009." Science **329**(5994): 940-943.
- Zhao, M., S. W. Running, et al. (2006). "Sensitivity of Moderate Resolution Imaging Spectroradiometer (MODIS) terrestrial primary production to the accuracy of meteorological reanalyses." Journal of Geophysical Research G: Biogeosciences **111**(1).

Appendices

Paper I: Satellite-based terrestrial production efficiency modeling

Paper II: Spatial comparison of global land cover datasets

Paper III: Comparison of four global fAPAR datasets

Paper IV: Improved light and temperature responses for GPP models

Paper V: Continental GPP mapping: use of a diagnostic model

Curriculum Vitae

Review

Open Access

Satellite-based terrestrial production efficiency modeling

Ian McCallum*¹, Wolfgang Wagner², Christiane Schmullius³,
Anatoly Shvidenko¹, Michael Obersteiner¹, Steffen Fritz¹ and Sten Nilsson¹

Address: ¹International Institute for Applied Systems Analysis, Schlossplatz 1, A-2361, Laxenburg, Austria, ²Institute of Photogrammetry and Remote Sensing, Technical University, Gufshausstraße 27 - 29, 1040 Vienna, Austria and ³Institute of Geography, Friedrich-Schiller-University, Grietgasse 6, 07743 Jena, Germany

Email: Ian McCallum* - mccallum@iiasa.ac.at; Wolfgang Wagner - ww@ipf.tuwien.ac.at; Christiane Schmullius - c.schmullius@uni-jena.de; Anatoly Shvidenko - shvidenk@iiasa.ac.at; Michael Obersteiner - oberstei@iiasa.ac.at; Steffen Fritz - fritz@iiasa.ac.at; Sten Nilsson - nilsson@iiasa.ac.at

* Corresponding author

Published: 18 September 2009

Received: 3 June 2009

Carbon Balance and Management 2009, **4**:8 doi:10.1186/1750-0680-4-8

Accepted: 18 September 2009

This article is available from: <http://www.cbjournal.com/content/4/1/8>

© 2009 McCallum et al; licensee BioMed Central Ltd.

This is an Open Access article distributed under the terms of the Creative Commons Attribution License (<http://creativecommons.org/licenses/by/2.0>), which permits unrestricted use, distribution, and reproduction in any medium, provided the original work is properly cited.

Abstract

Production efficiency models (PEMs) are based on the theory of light use efficiency (LUE) which states that a relatively constant relationship exists between photosynthetic carbon uptake and radiation receipt at the canopy level. Challenges remain however in the application of the PEM methodology to global net primary productivity (NPP) monitoring. The objectives of this review are as follows: 1) to describe the general functioning of six PEMs (CASA; GLO-PEM; TURC; C-Fix; MOD17; and BEAMS) identified in the literature; 2) to review each model to determine potential improvements to the general PEM methodology; 3) to review the related literature on satellite-based gross primary productivity (GPP) and NPP modeling for additional possibilities for improvement; and 4) based on this review, propose items for coordinated research.

This review noted a number of possibilities for improvement to the general PEM architecture - ranging from LUE to meteorological and satellite-based inputs. Current PEMs tend to treat the globe similarly in terms of physiological and meteorological factors, often ignoring unique regional aspects. Each of the existing PEMs has developed unique methods to estimate NPP and the combination of the most successful of these could lead to improvements. It may be beneficial to develop regional PEMs that can be combined under a global framework. The results of this review suggest the creation of a hybrid PEM could bring about a significant enhancement to the PEM methodology and thus terrestrial carbon flux modeling.

Key items topping the PEM research agenda identified in this review include the following: LUE should not be assumed constant, but should vary by plant functional type (PFT) or photosynthetic pathway; evidence is mounting that PEMs should consider incorporating diffuse radiation; continue to pursue relationships between satellite-derived variables and LUE, GPP and autotrophic respiration (Ra); there is an urgent need for satellite-based biomass measurements to improve Ra estimation; and satellite-based soil moisture data could improve determination of soil water stress.

Introduction

Carbon is removed from the atmosphere via photosynthesis by plants. Upon entering the terrestrial ecosystem it is termed gross primary productivity (GPP), with the difference between carbon gain via GPP and carbon loss through plant respiration defined as net primary productivity (NPP) [1]. At the regional or global scale, carbon fluxes (i.e. NPP) cannot be directly observed [2]. NPP is difficult to measure (in-situ) over large areas owing to spatial variability of environmental conditions and limitations in the accuracy of allometric equations [3]. Therefore, a variety of methods have been developed to estimate carbon fluxes, including flux towers e.g. [4], carbon accounting e.g. [5], global vegetation models e.g. [6], atmospheric measurements e.g. [7] and satellite-based techniques e.g. [8].

Among all these methods, only satellite observations provide globally consistent, spatially highly resolved observations of numerous surface variables that affect carbon exchanges [9]. However, models are required which can ingest this raw information and convert it into fluxes. Their interpretation of the underlying biochemical, biophysical and 3-D geometric properties of vegetation and soils is the main challenge in the application of satellite-based earth observation data for modeling the terrestrial carbon cycle [10].

Production efficiency models (PEM), sometimes referred to as diagnostic models, have been developed to monitor primary production, taking advantage of available satellite data. PEMs combine the meteorological constraint of available sunlight reaching a site with the ecological constraint of the amount of leaf-area absorbing that solar energy, avoiding many complexities of carbon balance theory [11]. PEMs are based on the theory of light use efficiency (LUE) which states that a relatively constant relationship exists between photosynthetic carbon uptake and radiation receipt at the canopy level [12]. In addition to LUE, PEMs typically require inputs of meteorological data (i.e. radiation, temperature and others) and the satellite-derived fraction of absorbed photosynthetically available radiation (FAPAR).

PEMs complement the many ecophysiological process models that simulate carbon exchange [13]. A model comparison of 17 global NPP models featured several PEMs whose results compared well with process models [2]. Currently two PEMs are producing NPP operationally at the global scale, namely C-fix [14] and MOD17 [8]. Challenges remain however in the application of the PEM methodology to global NPP monitoring. In particular, determination of LUE [15,16] and autotrophic respiration [17] remain somewhat uncertain. Additional uncertainties have been identified in the meteorological data [18]

and in the biophysical data [19], both key components in PEMs. Several recent studies suggest that simple regressions between GPP and remote sensing products might yield better results than those incorporating meteorological data [20]. All of these issues point to the need for a review of the current state of PEMs.

A variety of excellent reviews have addressed various aspects of PEMs in recent years: [2,3,21-24], however none have specifically reviewed the existing published models. The objectives of this review are as follows: 1) to describe the general functioning of six PEMs (CASA; GLO-PEM; TURC; C-Fix; MOD17; and BEAMS) identified in the literature; 2) to review each model to determine potential improvements to the general PEM methodology; 3) to review the related literature on satellite-based GPP and NPP modeling for additional possibilities for improvement; and 4) based on this review, propose items for coordinated research.

Production Efficiency Modeling

Background

Photosynthesis by plants provides the carbon and energy that drives most biological processes in ecosystems. Similar to photosynthesis by individual leaves, GPP varies diurnally and seasonally in response to changes in light, temperature, water and nitrogen supply while differences among ecosystems in annual GPP are determined primarily by the quantity of leaf area and the length of time that this leaf area is photosynthetically active [1]. While the relationship between photosynthesis and irradiance can be markedly non-linear for individual leaves, it approaches linearity at the canopy level, presumably because a smaller fraction of leaf area is operating under light-saturated conditions [12,25].

In 1953, the first steps were taken to calculate productivity of an entire plant community indirectly on the basis of light [26]. However, Monteith [27,28] is commonly credited with first proposing the existence of a conservative (linear) relationship between the rate of NPP and the rate at which solar energy is absorbed by the foliage, conducting experiments with crop species during the vegetative stages of growth under optimal growing conditions. The ratio between these two quantities has been called the conversion efficiency of absorbed radiation into dry matter, and was used in many simple models of crop growth, i.e. bypassing the complex process of photosynthesis and respiration known to depend on many environmental variables [21]. In crop canopies, where water and nutrients are highly available, the linear relationship between canopy carbon exchange and irradiance extends up to irradiance typical of full sunlight [1]. However in forest canopies, the relationship is not so simple and LUE is dependent upon other factors. An increasing number of

studies indicate that LUE fluctuates among vegetation species, stand age, soil fertility, etc [15,16,29]. It was noted, however, that light absorption and utilization are decoupled so that convergence is to be expected on gross production rather than net production, owing to differences in respiratory costs associated with synthesis and maintenance of plant constituents and associated 'payback intervals' on carbon investment in different functional types [3].

An attractive feature of the PEM concept is its suitability for use with remotely sensed observations [30], which provide both the timing of the active period and the quantitative values of FAPAR. The approximation that the annual photosynthetic activity is a conservative function of APAR permits monitoring of biospheric activity with little need for ancillary information [2]. While functional convergence provides a basis for the use of remote sensing of light absorption in measurement of primary production, models driven with light absorption must also include terms that describe the actual respiratory costs of maintenance and synthesis [3].

"Modern PEMs", however, should not be confused with early experimental models based solely on correlation relationships between spectral vegetation indices and crop yield [31]. They are now generally global, depend heavily on satellite and meteorological datasets and operate at high spatial and temporal resolution. They typically consider GPP and NPP separately and contain terms to describe plant respiration. A chronology of modeling efforts claims the first global PEM (CASA) appeared in 1993 [32].

PEM Algorithm

In general, all PEMs employ a similar basic methodology to calculate NPP. Typically this involves two steps, first calculating GPP (Equation 1) and then subtracting Autotrophic Respiration (R_a) (Equation 2) to derive NPP. Variation among the different methods generally appears in the determination of LUE, the use of scalars and R_a . Timesteps range from daily to yearly and spatial resolution from 1 km to 1 degree.

$$\text{GPP} = \text{PAR} * \text{FAPAR} * \text{LUE} * \text{Scalars} \quad (1)$$

$$\text{NPP} = \text{GPP} - R_a \quad (2)$$

where:

GPP Gross Primary Productivity (g C m^{-2})

PAR Photosynthetically Active Radiation (MJ m^{-2})

FAPAR Fraction of Absorbed PAR (dimensionless %)

LUE Light Use Efficiency (g C MJ^{-1})

Scalars Temperature, (VPD) Vapour Pressure Deficit, etc (0-1)

NPP Net Primary Production (g C m^{-2})

R_a Autotrophic respiration (g C m^{-2})

PAR

Photosynthetically active radiation (PAR) is the solar radiation reaching the canopy in the wavelength region of visible light (0.4 - 0.7 micrometers). This is typically derived from meteorological datasets, but may also come from satellite products [33]. At the global level, PAR is comprised of roughly equal amounts of direct (clear sky) and diffuse (cloudy, aerosols) radiation, while at the regional level large differences occur. Of crucial importance is the geometry of the incoming sunlight, which is comprised of direct and diffuse components [34-37].

FAPAR

The fraction of absorbed PAR (FAPAR) is defined as the fraction of PAR absorbed by green vegetation. FAPAR is difficult to measure directly, but is inferred from models describing the transfer of solar radiation in plant canopies, using remote sensing observations as constraints [25,38,39]. Comparisons between the actual FAPAR products derived by the various space agencies or projects reveal discrepancies: they are mainly due to the different strategies in the retrieval methodologies but also to the quality of input variables [38].

LUE

Light use efficiency (LUE) is typically defined in biology as the ratio between accumulated biomass and PAR (sometimes referred to as radiation use efficiency (RUE), a similar ratio but based on total solar radiation intercepted). LUE can be defined as measured on the basis of gross production, net production, environmentally stressed or hypothetically unstressed (i.e. maximum) production [40]. Difficulties arise with the lack of a universally agreed upon definition of LUE, a quotient where the numerator quantifies production and the denominator irradiance [41]. Historically, the numerator is either NPP (above-ground or total) or GPP, while incident, intercepted or absorbed total shortwave or PAR have been used as denominators. Literature derived LUE generally corresponds to above-ground LUE [42].

The conversion of absorbed radiation into dry matter can be computed from a variety of approaches: a constant 'conversion efficiency' or the product of an optimum value by other factors representing environmental stresses [42]. In most PEMs the potential (maximum) LUE value

is empirically derived, then reduced due to environmental constraints [2].

Scalars

Scalars representing environmental constraints are typically meteorologically derived (but may also be satellite-based) variables that serve to reduce the LUE value at a specific time and location due to predicted plant stress, e.g. high vapour pressure deficits (VPDs) have been shown to induce stomatal closure in many species, while low temperatures inhibit photosynthesis. Depending upon the PEM, scalars such as temperature, VPD and soil moisture are used to reduce the maximum LUE values, e.g. through linear ramp functions [43].

Ra

Autotrophic plant respiration (Ra) is a large, environmentally sensitive component of the ecosystem carbon balance, and net ecosystem carbon flux will change as the balance between photosynthesis and respiration changes [3,44,45]. Autotrophic respiration describes the respiration released from living plant tissues, including leaves, roots and wood. Plant respiration can be separated into three separate components: growth respiration; maintenance respiration and the respiratory cost of ion uptake - with modeling studies indicating that Ra is about half (48-60%) of GPP when a wide range of ecosystems are compared [1]. Ra is handled differently in each of the models, ranging from a simple linear function of temperature to empirical methods.

Model Descriptions

A review was made of the key attributes and results of six published PEMs (Table 1). A brief description of the unique properties of the six PEMs is given below.

CASA

The Carnegie Ames Stanford Approach (CASA) is a numerical model of monthly fluxes of water, carbon and nitrogen in terrestrial ecosystems. Estimates of terrestrial NPP fluxes depend on inputs of global satellite observa-

tions for land surface properties and on gridded model drivers from interpolated weather station records [46]. LUE is set uniformly at 0.39 g C MJ⁻¹ PAR, a value that derives from calibration of predicted annual NPP to previous field estimates. This model calibration has been assessed globally [47]. Temperature stress is computed with reference to derivation of optimal temperatures for plant production. CASA includes a water stress scalar estimated from monthly water deficits, based on a comparison of moisture supply to potential evapotranspiration demand [47]. This is the only model that does not separately calculate GPP. Instead it models NPP directly, thus avoiding a Ra calculation.

GLO-PEM

The Global Production Efficiency Model (GLO-PEM) consists of linked components that describe the processes of canopy radiation absorption, utilization, autotrophic respiration, and the regulation of these processes by environmental factors [48]. It was designed to run with both biological and environmental variables derived entirely from satellites and is thus unique as it is the only PEM to do so (except for distinguishing between C3 and C4 vegetation). The portion of C3 or C4 vegetation per pixel is calculated as a function of above ground biomass (calculated from the minimum annual visible channel reflectance [3]) and air temperature. In contrast to other modern PEMs, GLO-PEM estimates LUE rather than prescribing values based on limited field observations [31]. LUE is reduced by environmental factors that control stomatal conductance i.e. the effects of air temperature, VPD and soil moisture [48].

Autotrophic respiration is modeled for maintenance respiration using a semi-empirical relationship as a function of vegetation, biomass, air temperature and photosynthetic rate, while growth respiration is a constant of GPP (0.25). Below-ground biomass is not estimated, thus Ra is assumed to apply to the whole plant [31].

Table 1: Attributes and results of six global PEMs available from the literature.

PEM	Study period	Timestep	Cell-size	LUE Scalars	LUE-GPP (g C MJ ⁻¹)	NPP (Pg C yr ⁻¹)	Reference
CASA	1982-1998	Month	0.5°	T, AET, PET	0.39 ^e	48.0 ^c	[46]
GLO-PEM	1981-2000	10 days	8 km	T, SW, VPD	1.03-1.64 ^a	69.7 ^b	[48]
TURC	1998	Month	1°	No Scalars	1.10	64.0	[49]
C-Fix	1998-2008	10 days	1 km	T, CO ₂ , SW, EF	1.10	NA ^f	[14]
MOD17	2000-2008	Day/Year	1 km	T, VPD	0.68-1.159	56.0 ^d	[18]
BEAMS	1982-2000	Month	1°	T, h, SW	0.0-1.0		[53]

^a [13]; ^b [31]; ^c [78]; ^d [51]; ^e based on NPP; ^fNA (globally not available in published literature)

T Temperature; SW Soil Water; VPD Vapour Pressure Deficit; AET Actual Evapotranspiration; PET Potential Evapotranspiration; CO₂ fertilization factor; EF Evaporative Fraction; h Relative Humidity

TURC

When first published, the main originality of the model Terrestrial Uptake and Release of Carbon (TURC) was to relate light absorption to GPP (rather than to NPP), and to derive parameters from CO₂ exchange measurement (canopy fluxes for photosynthesis, chamber measurements for respiration) [49]. Originally, LUE was derived empirically (1.10 g C MJ⁻¹) and used to calculate GPP with environmental constraints applied to Ra [49]. Frost stress on photosynthesis was later included by reducing the conversion efficiency by 50% during the three days following a severe frost, defined by a daily mean air temperature lower than -2°C. Unique LUE values were also used for high latitude wetlands, which proved to be substantially reduced from non-wetlands and reduced the maximum LUE value based on values of low mean annual temperature [49].

Autotrophic respiration in TURC is the sum of maintenance (leaves, fine roots and wood) and growth respiration (a constant fraction (0.28) of GPP minus maintenance respiration). An average maintenance respiration coefficient at 20°C has been determined for each organ (using experimental data). Maintenance respiration is then scaled as a linear function of temperature and organ biomass. A vegetation map and normalized difference vegetation index (NDVI) data are used to estimate biomass for each cell [49].

C-Fix

The parametric PEM C-Fix, estimates carbon mass fluxes from local to global scales [14]. C-Fix is operational, providing global NPP since 1998. For a given point location, the original model estimates carbon fluxes on a daily basis. C-Fix is a mass balance model based on the parameterization of FAPAR derived from remotely sensed NDVI [14]. RUE is set equal to 1.10 g C MJ⁻¹. This is reduced by the normalized temperature dependency factor and the normalized CO₂ fertilization factor. Further refinements were introduced to C-Fix, namely integration of a water limitation; temperature buffering and estimates of soil temperature [14].

In C-Fix, the autotrophic respiration reduction factor is modeled as a simple linear function of daily mean atmospheric air temperature. This parametric model for respiratory losses is assumed state (phytomass) independent [50]. The dependency of maintenance respiration on the amount of living biomass is neglected.

MOD17

The Moderate Resolution Spectroradiometer (MODIS) sensor has provided near real-time global estimates of GPP and annual NPP (MOD17) since March 2000, on an operational basis. One of the largest assumptions made

(to implement MOD17 globally) is the use of a constant maximum RUE within each of the 12 biomes used [18]. A minimum temperature scalar reduces the conversion efficiency when cold temperatures limit plant function. The MOD17 GPP algorithm does not have a winter dormancy function to regulate winter productivity [18]. As a global generalisation, the algorithm truncates GPP on days when the minimum temperature is below 0°C [43]. A scalar is used to reduce the maximum conversion efficiency when the VPD is high enough to inhibit photosynthesis. The effect of soil water availability is not included in the GPP algorithm [18]. To partially account for this issue, sensitivity to VPD is increased in the model as a surrogate for drought effects. The model is parameterized with eddy covariance data.

In MOD17, maintenance respiration by leaves and fine roots is subtracted from GPP (on a daily basis). Annual NPP is then calculated by subtracting maintenance respiration by all other living parts except leaves and fine roots (e.g. livewood) and growth respiration [51]. Maintenance respiration and growth respiration components are derived from allometric relationships linking daily biomass (leaf biomass is calculated using leaf area index (LAI) and specific leaf area defined for each plant functional type (PFT) [43]) and annual growth of plant tissues to satellite-derived estimates of leaf area index.

BEAMS

The Biosphere model integrating Eco-physiological And Mechanistic approaches using Satellite data (BEAMS) is a diagnostic model requiring both satellite and climate data [52]. It includes a carbon cycle submodel to capture GPP and autotrophic respiration [53]. GPP was modeled based on the LUE concept using satellite-based monthly FAPAR data and a stress calculation which considered air temperature, relative humidity, soil moisture and atmospheric CO₂ concentrations. GPP is allocated into leaf, stem and root components by an empirical equation using climate parameters.

In BEAMS, the Ra of leaves, stems and roots consists of maintenance and growth respiration. Maintenance respiration is modeled in proportion to biomass (see MOD17) with temperature dependence ($Q_{10} = 2$), while growth respiration is modeled in proportion to the potential NPP [53].

Error Sources and Variability in PEMs

A variety of attempts at evaluation of PEMs have been published, most commonly at the global scale in the form of inter-comparison studies e.g. [2,42,53,54] or over the data-rich areas of North America e.g. [18] and Europe e.g. [14,55] with in-situ measurements. However, determining the uncertainty of carbon fluxes is difficult and

requires understanding of the uncertainties of model structure, data and model parameter uncertainties and particularly the temporal and spatial inaccuracy of the input data retrieval [56].

Early attempts at NPP modeling resulted in values for global NPP of approximately 60 Pg C yr⁻¹ [57]. An inter-comparison of global NPP models found values in the range of 40 - 80 Pg C yr⁻¹, with results from PEMs fitting well within this value [2]. However, while it appears that between model variability is relatively low, within model variability is likely much higher (more so at a regional scale). Models that agree on the value of certain outputs (e.g. annual NPP) may disagree on the underlying processes (e.g. differences in rates of photosynthesis vs. plant respiration) [42]. See Table 2 for a selection of PEM error sources and variability.

Too few studies exist that measure uncertainties in carbon flux modeling and remotely sensed data assimilation. However, error propagation and Monte-Carlo approaches to assess uncertainty in a PEM are available [56]. Additionally, a sensitivity analysis to assess which climate variables most influenced simulation differences of a PEM, via three climate datasets, found large differences [58]. Certainly, a more severe test of the models, including comparison with observed ecosystem fluxes at tower sites and with models driven by site meteorology, needs to be pursued [55].

Key Research Items

The following sections describe various shortcomings and potential improvements to the PEM methodology based on a review of the six models in this study (CASA; GLO-PEM; TURC; C-Fix; MOD17; and BEAMS) and related studies, along with suggested key research items.

Light Use Efficiency

Estimates of LUE are generally not well constrained and provide a large source of error in model estimates of global NPP, arising from different philosophies on the environmental and biological controls of LUE and the methods adopted to estimate this parameter [15]. One

Table 2: A selection of published error sources and variability from various input variables used in PEMs.

Dataset	Error Sources/Variability	Citation
Meteorology	16 - 43% difference in NPP	[58]
	28% difference in GPP	[18]
PAR	35-62% over predicted NPP	[107]
	13% difference in NPP	[33]
LUE	0.2 - 1.8 g C MJ ⁻¹ (in-situ)	[3]
FAPAR	RMSE 0.1 - 0.12	[108]
	8-20% greater than in-situ	[109]

major difference between models is the use of a constant versus biome, PFT or photosynthetic pathway specific LUE. Various studies suggest that LUE varies with factors such as forest stand age, species composition, soil fertility, foliar nutrients, drought, radiation, phenological stage, climatic condition, temperature, and others [3,16,29,49,59]. Therefore any model that incorporates the premise that LUE is constant can only be considered approximate and will be increasingly in error over shorter periods [40].

An understanding of the factors that control the efficiency with which forest canopies harvest available light to fix carbon via photosynthesis is necessary for the development of useful PEMs [29]. High LUE was found in boreal regions and in the northern hemisphere tropics [15]. Within boreal zones, Eurasian LUE is higher than North American LUE and has a distinctly different seasonal profile. More work is needed on the LUE of forested wetlands with different species mixtures [16], with low LUE found in high latitude wetlands [49]. In addition, LUE differed significantly among forest cover types and between years [16]. To date, there has been little work to account for variations in LUE introduced by herbivory, disease and differences in respiratory costs [3] although a benefit of using satellite data means that to some extent these elements are accounted for.

For large areas, in which the vegetation cover, LAI, physiognomy, and species are likely to be heterogeneous, field-plot scale empirical derivation of LUE is not appropriate [60]. However, it was suggested for model improvement, to selectively alter values for maximum LUE based on observations at eddy covariance flux towers [17]. This may work for areas with high sampling frequency, but for much of the globe will be too infrequent. Current efforts attempt to derive LUE directly from satellites [61-65] (see Recent Advances). Regular direct measurements of LUE would make it possible to capture the real variation of photosynthetic efficiency and then to assimilate it into PEMs [64].

Light Use Efficiency: key findings/research items

- LUE should not be assumed constant, but should vary by PFTs e.g. [18], photosynthetic pathway e.g. [48], or other means. LUE is most relevant in the context of GPP rather than NPP, due to differences in respiration among PFTs [3,13,31]
- More empirical studies are required to determine LUE under various environmental conditions - i.e. create a global publicly available database e.g. [22]
- Intensify efforts to derive LUE directly from satellites e.g. [61-65]

Biophysical, Meteorological and Atmospheric Variables

Only one of the six published PEMs in this review (GLO-PEM) relied purely on satellite-derived meteorological measurements - the rest have utilized observation-based meteorological datasets. The single largest error associated with GPP at most sites likely derives from meteorology, with a 28% difference between GPP generated from climatology data versus tower data [18]. The largest differences in temperature sensitivity among NPP estimates occurred in the northern latitudes [54].

Water stress is one of the primary limiting functions controlling photosynthesis by terrestrial ecosystems [66]. Under-estimation of VPD contributes greatly to overestimation of GPP [18]. High VPDs > 2000 Pa, have been shown to induce stomatal closure in many species. This level of daily atmospheric water deficit is commonly reached in semi-arid regions of the world for much of the growing season [43].

Additionally, models that do not directly account for soil water stress may be problematic at water-limited sites [18]. The accuracy of NPP estimates for forests more affected by soil water conditions than geographical moisture conditions, can be improved by using a soil water index [59]. The strong impact of soil moisture on the European carbon balance was demonstrated using a PEM [67]. Even if the water status of the leaf remains unchanged, stomatal conductance decreases with decreasing soil moisture [48]. Additionally, forest growth in high latitudes is not only limited by temperature, radiation and nutrient availability but also by the availability of liquid soil water, and it was, therefore, recommended to include permafrost in models [68]. In permafrost regions, a large amount of water is lost as runoff during spring and is hence not available for vegetation later in the growing season [68].

Accurate estimates of NPP are also highly dependent upon the quality of the global daily estimates of PAR [11]. A comparison of PAR products found biases and rms errors > 25% [33]. The importance of FAPAR data in model-data driven productivity estimation methods based on the PEM approach was also noted [19], especially as FAPAR is often the only satellite-based variable used in PEMs.

Three of the models reviewed here (GLO-PEM, C-Fix and BEAMS) account for CO₂. Elevated CO₂ increases both water use efficiency and RUE, even when those resources are at low-growth restrictive levels [69]. CO₂ fertilization is important for plant growth activity, and needs to be accounted for in satellite-based NPP models [53].

Biophysical, Meteorological and Atmospheric Variables: key findings/research items

- For both biophysical and meteorological variables a variety of datasets are available - here it would be beneficial to set standards in terms of input datasets, thus allowing for easier inter-model comparison
- Further investigation into meteorological remote sensing products such as land surface air temperature which can potentially be used as a measure of both temperature and VPD e.g. [70]
- Soil moisture available from satellite measurements e.g. [71], should be considered for inclusion in PEMs e.g. [67]. Additionally, regional effects of permafrost should be considered e.g. [68]
- CO₂ fertilization is important for plant growth activity, and needs to be accounted for in satellite-based NPP models [53]

Diffuse Radiation

Substantial evidence exists that the solar irradiance incident at the surface has declined substantially over the last 50 years (with a potential increase in diffuse radiation), pointing to the inclusion of diffuse radiation in models [72]. At the global level, PAR is comprised of roughly equal amounts of direct (clear sky) and diffuse (cloudy, aerosols) radiation, while at the regional level large differences occur. Diffuse and direct radiation differ in the way they transfer through plant canopies and affect the summation of non-linear processes like photosynthesis differently than what would occur at the leaf scale [35]. For example, conifer needles are particularly effective in absorbing diffuse light, which provides a more uniform illumination of the overall canopy.

Diffuse radiation results in higher LUE, with GPP dependent upon the composition of incident irradiation (the ratio of diffuse to direct light) [35,61]. LUE was found to be highest on overcast days and decreased on clear-sky days [36,37]. The relationship appears to be quite general, although the magnitude of the effect is related to the structural properties of the canopy and the productive capacity of the vegetation [37]. To the contrary, others consistently recorded a decrease in primary productivity, owing to the decline in total irradiance that occurs when clouds obscure the solar dish [73]. Additionally, current LUE approaches fail to predict GPP in a tropical rain forest as they neglect GPP saturation when radiation is high [74]. In general, systems adapted to large amounts of diffuse light (e.g. boreal) don't do well under high levels of direct light (and subsequent high VPD) and vice versa. To some extent, temporal integration gets around these issues that are most pronounced at short time scales.

It is a challenge for the next generation of production models - which rely on LUE, to develop new algorithms to accommodate diffuse radiation [35]. It was suggested that the inclusion of estimates of diffuse radiation as a scalar for LUE will substantially improve estimates of gross photosynthesis from PEMs, especially at daily time resolution [29]. An alternative formulation of the GPP algorithm was envisioned that specified a different maximum LUE under clear sky and overcast conditions, then ranged between those values depending on the degree of cloudiness [36].

Diffuse Radiation: key findings/research items

- Evidence is mounting that PEMs should consider incorporating diffuse radiation, especially at daily resolution e.g. [29,35-37], however caution should be applied e.g. [73]
- Several published methods which already incorporate diffuse light in PEMs should be further investigated e.g. [72,75]
- PEMs should also consider the need to account for GPP saturation when radiation is high e.g. [74]

Phenology

Phenology is to a certain extent captured in the current PEM models via the meteorological data and FAPAR. However, the timing of snowmelt and soil thaw, the onset of warming in the spring and other factors affecting phenology can have a large impact on the annual carbon balance in forests, in particular in cold climates [76,77]. Early in the season, efficiency may be reduced by the expense of leaf and fine root construction, while late in the season it may be reduced while transferring leaf metabolites into other tissues. For boreal systems there is an observed lag between the time temperatures permit photosynthesis and the time the photosynthetic machinery becomes active [78]. Seasonally, summer estimates of GPP are closest to tower data while spring estimates are the worst, most likely the result of the relatively rapid onset of leaf-out [18].

During winter and early spring, evergreen boreal conifers are severely stressed as light energy cannot be used when photosynthesis is preempted by low ambient temperatures. Severe intermittent low-temperature episodes during this period actually reversed physiological recovery [79]. Night frosts depress photosynthesis the following day and the effect of severe frost is visible for several days [80]. Frost stress on photosynthesis is included in the TURC model by reducing the conversion efficiency by 50% during the three days following a severe frost, defined by a daily mean air temperature lower than -2°C [49]. As a global generalisation, the MOD17 algorithm

truncates GPP on days when the minimum temperature is below 0°C [43].

The introduction of new techniques to better capture the start and finish of the growing season may improve a PEMs ability to detect these crucial transition periods. A method was developed using space-borne scatterometer measurements to detect the onset of spring thaw and the freeze/thaw cycle duration, based on the significance of diurnal differences with respect to long-term noise [81]. In general, backscatter is high and relatively stable during winter. During spring melt, however, rapid fluctuation is observed and only after the thaw does backscatter stabilize, albeit at a lower level. The onset of the spring thaw period coincides with the first days of increased CO_2 fluxes above the late winter baseline. The end of daily freeze thaw cycles corresponds to the switch from source to sink in evergreen boreal forest [81].

Phenology: key findings/research items

- Investigate incorporating scatterometer data to account for spring thaw and the freeze/thaw cycle duration e.g. [81]. This data could be used to prevent assigning carbon uptake too early in the spring due to e.g. rising FAPAR values
- Consider some form of frost stress, perhaps via air temperature e.g. [49], if not already included

Vegetation Morphology

Among the PEMs, land cover is currently only used in MOD17 for the assignment of LUE. However, this was noted as a potential source of error because of landscape heterogeneity at the sub pixel scale [18], leading to overestimation of GPP in complex ecosystems. Additionally, large discrepancies occur among land cover datasets, and choice of one dataset over another will affect model outcome [82,83]. Vegetation related disturbances should however be adequately represented e.g. [84], with various satellite-based options available [85]. It may be, however, that FAPAR is capturing this adequately - perhaps crucial only at shorter timescales.

An important detail which could introduce uncertainty into PEMs is the fact that they generally consider whole forest stands via the notion of convergence, largely ignoring canopy layers. In some high latitude regions for certain species, forest understory and a green forest floor can generate up to 50% of total NPP [86].

Several authors have suggested that leaf area index (LAI) is the principal scaling variable for both gross photosynthesis and ecosystem respiration of northern deciduous and coniferous forests e.g. [76]. Problems exist however with the quality of global satellite-derived LAI products [87],

currently making this a difficult variable to include in PEMs. Saturation at high LAI values together with biases due to soil reflectance, vegetation clumping and others have limited performance [88].

Vegetation Morphology: key findings/research items

- Exercise caution if utilizing land cover products or LAI in PEMs [18,82,87]
- Consider methods to account for disturbance effects on vegetation morphology e.g. [85]

Autotrophic Respiration

Plant respiratory regulation is too complex for a mechanistic representation in current terrestrial productivity models [89]. Of the six PEMs compared in this review, all but one separately account for autotrophic respiration (R_a), needed to convert GPP into NPP. All but one of these define R_a as the sum of growth and maintenance respiration, estimating R_a for leaves, wood and roots. Variation in maintenance respiration is the most likely cause for variability in the efficiency of converting GPP into NPP. According to [17], over prediction in NPP is a problem of underestimating R_a rather than overestimating GPP.

PEMs that assume maintenance respiration is dependent upon the amount of living biomass obviously require some measure of biomass. Previous efforts have relied on correlations of biomass with optical reflectance measurements. However, forest biomass is poorly quantified across most parts of the planet [90]. Owing to the difficulty in estimating above ground wood (of live trees), it was suggested for forests, to make stemwood R_a a fixed proportion of total R_a .

Work is ongoing to determine whether autotrophic respiration can be estimated from remote sensing data alone [91]. For densely forested sites, respiration is strongly related to land surface temperature (LST), with relatively little variation in this relationship between sites [92].

Autotrophic Respiration: key findings/research items

- There is an urgent need for satellite-based biomass measurements to improve R_a estimation - efforts such as BIOMASS [93] and various RADAR and LiDAR [94] research efforts could be applied here
- Pursue studies attempting to link plant respiration to satellite-derived variables e.g. [91]
- The research community could benefit from a comprehensive literature review specifically focused on autotrophic respiration modeling with satellite data.

Recent Advances

New methods are currently under development which will perhaps enhance or replace the PEM methodology in the future; however at present these are largely not operational. The general trend is to develop new methods from satellite-based tools that measure LUE or GPP directly. Several proposed (presently unsupported) satellite missions from the European Space Agency (ESA) (i.e. FLEX and ASCOPE) [93] specifically target this issue. In addition, the GOSAT http://www.jaxa.jp/projects/sat/gosat/index_e.html and OCO <http://oco.jpl.nasa.gov> missions will provide global measurements of CO_2 fluxes which could be used to help calibrate and/or validate PEMs.

The use of chlorophyll content measured from satellite to predict crop productivity was proposed; however variation in GPP due to short term stress cannot be detected [61]. It was therefore recommended to combine other products along with the use of a red-edge. A continuous-field LUE retrieved from satellite data using the photochemical reflectance index (PRI) was developed [95]. Indices such as the PRI and the enhanced vegetation index (EVI) have been shown to correlate with LUE, however the relationship between LUE and PRI varies considerably between vegetation types and years [63,64]; and LUE and EVI are not well correlated for evergreen sites. The relationship between PRI and LUE improves when the analysis is restricted to small changes of viewing angles [65]. Combining the LST product from MODIS with the EVI for 16-day means, [91] found an improved correlation to flux tower GPP data for 11 sites as compared to MOD17.

Replacing the LUE approach with a more general PAR-response approach was advocated by [74] - one that includes common response features of vegetation canopies to environmental conditions (particularly light saturation), based on work in a tropical biome. Another approach was presented to estimate GPP using FAPAR in conjunction with GPP estimates from eddy covariance measurements, suggesting that use of simple regression between GPP and a remote sensing product yield more robust results than models additionally based on meteorological input [20]. In a related study, flux data were used to constrain and parameterize a neural network structure using a limited number of driving variables to estimate spatial and temporal carbon fluxes for European forests [96]. Additionally, hyperspectral remote sensing offers the possibility of sensing changes in the xanthophyll cycle and fluorescence, both related to photosynthesis [64].

Recent Advances: key findings/research items

- Continue to pursue relationships between satellite-derived variables and LUE or GPP e.g. [64,91]

- Results from proposed satellite missions i.e. FLEX and ASCOPE [93] could improve the capability to model productivity from space - these efforts should be pursued
- Results from the GOSAT/OCO missions should be used to improve validation efforts by comparison with PEM outputs - a potential improvement over the current sparse network of FLUXNET [97] towers currently used for validation

Discussion

Progress in PEMs and related development has been steady since the earliest models were proposed [26,30]. The first global PEMs utilizing satellite data appeared in the early 1990s [32] i.e. CASA, GLO-PEM and TURC. Some of these models were already quite sophisticated (i.e. GLO-PEM derived the majority of its inputs from satellite data), and they have continued to be improved and updated e.g. [48]. Recently, a new generation of PEMs has emerged (i.e., C-Fix, MOD17 and BEAMS) of which C-Fix and MOD17 are operational. They incorporate generally higher resolution (spatial and temporal) data, or are more comprehensive in terms of input requirements (i.e. BEAMS). Operational models must however remain at a moderate level of complexity in order to be practical. Additionally, many regional models exist which can be used to test new ideas e.g. [72] for potential inclusion into global PEMs. Furthermore, a lot of effort among the research community is resulting in different satellite-based techniques which could be utilized in the PEM approach i.e. LST, EVI, PRI, etc.

This review aims to examine existing global PEMs and related literature in an attempt to extract key elements from each of the models to establish a proposed framework for coordinated research. Several reviews have addressed various aspects of PEMs in recent years, e.g. [3,21-24] although none have specifically reviewed the existing published models. The earliest reviews of global PEMs involved inter-comparison studies of NPP models (i.e. CASA, TURC and GLO-PEM) [2,42,54]. More recently, a comparison was made of BEAMS, MOD17 and CASA [53]. Additionally, the carbon sink archives <http://www.cger.nies.go.jp/cger-e/db/enterprise/csa/index.html>, were designed for inter-comparison of terrestrial carbon models and include three PEMs (GLO-PEM, BEAMS and MOD17).

Although the focus of this study was on primary productivity, the ultimate goal of carbon flux modeling is to estimate net ecosystem productivity (NEP), the central term used to describe imbalances in carbon uptake and loss by ecosystems [98]. NEP is typically defined as NPP less heterotrophic respiration (Rh). Rh is generally known to be

difficult to model, because it depends upon many interacting factors in the soil, such as soil carbon content, soil humidity, soil pH, soil oxidation potential, soil temperature and the micro-fauna and flora activity of the soil [50].

Of the six PEMs discussed in this review, four produce estimates of global NEP (i.e. CASA, TURC, C-Fix and BEAMS):

- CASA has a similar structure to the CENTURY [99] model, accounting for the soil profile, production and decomposition
- In TURC, Rh is related to soil temperature through a Q_{10} relationship ($Q_{10} = 2$) [49]. Soil moisture impact on the decomposition rate follows the CENTURY model
- C-Fix accounts for the impact of temperature on soil respiration, using a temperature dependency factor and a site-specific rate constant (based on flux measurements) [100]
- BEAMS parameterizes soil decomposition as a function of soil temperature and water content i.e. CENTURY

Soil respiration is often modeled as a simple Q_{10} or Arrhenius type function of temperature, sometimes modified by a water scalar e.g. [101]. More recently, soil respiration was modeled using a temperature, precipitation and LAI model, providing compatibility with remote sensing approaches [102]. However, prior to global application the approach needs to be tested in boreal, cold-temperate and tropical biomes, as well as for non-woody vegetation. Additionally, research suggests that differences between the apparent and intrinsic temperature sensitivity of soil respiration may be due to a correlation between soil respiration and photosynthetic rates (i.e. GPP) [103], offering another possibility for remote sensing based solutions. Research into these methods should continue with the aim of further linking soil respiration and remote sensing measurements.

Conclusion

Since the influential work of Monteith [30], founded on the relationship between the rate of NPP and the rate at which solar energy is absorbed by foliage, the application of satellite-based PEMs for NPP monitoring has consistently evolved. With constant advances in satellite-based measurements, in-situ methods and computational ability, the PEM methodology has been refined and now delivers operational measurements of global terrestrial primary productivity at high temporal and spatial resolution. Simplification of the estimation of LUE enables

remote sensing to utilize a robust approach, based in evolutionary ecology, while exploring the key advantage of a spatially and temporally contiguous monitoring capability [3].

A review of six global PEMs available in the literature (CASA; GLO-PEM; TURC; C-Fix; MOD17; and BEAMS) revealed the use of a similar conceptual framework based on the LUE methodology. However, review of the approaches and screening of the related literature have identified potential improvements that could be implemented to enhance the results of existing or new PEMs. Based upon this review, key research items were identified that appear crucial to improve the PEM methodology, including:

- LUE should not be assumed constant, but should vary by PFTs e.g. [18], photosynthetic pathway e.g. [48], or other means
- Continue to pursue relationships between satellite-derived variables and LUE or GPP e.g. [64,91]
- Evidence is mounting that PEMs should consider incorporating diffuse radiation, especially at daily resolution e.g. [29,35-37], however caution should be applied e.g. [73]
- Exercise caution if utilizing land cover products or LAI in PEMs [18,82,87]
- There is an urgent need for satellite-based biomass measurements to improve autotrophic respiration estimation
- Investigate incorporating scatterometer data to account for spring thaw and the freeze/thaw cycle duration e.g. [81]
- Soil moisture available from satellite measurements e.g. [71], should be considered for inclusion in PEMs e.g. [67]

The results of this review and the above indicated key research items suggest the creation of a global hybrid PEM could bring about a significant improvement to the PEM methodology and thus terrestrial carbon flux modeling. Each of the six PEMs reviewed apply somewhat different techniques to determine NPP. Based on this review, it is possible to identify certain features of some of the models which, if combined into a hybrid PEM, could potentially generate improved estimations. In addition, recent research has also led to the creation of datasets that were not available when most of these models were first published, and incorporation of these datasets could poten-

tially lead to improvements, i.e. soil moisture, freeze-thaw, improved meteorology, FAPAR, and others.

It may, however, be beneficial to develop regional PEMs that can be combined under a global framework. As global PEMs were intended for application across different vegetation systems, they address only the most fundamental and universal factors governing plant growth [104]. Unique ecophysiological characteristics are therefore not accounted for, which may introduce errors. Current PEMs typically treat the globe similarly in terms of physiology. In an effort to produce global (and in the case of C-Fix and MOD17) operational PEMs with reasonable spatial/temporal resolution, certain assumptions have been made. It is well documented, however, that regional phenomena e.g. permafrost, disturbances, etc have a large influence on NPP. Incorporating these features in regional PEMs under a global framework may lead to improved results.

To date there are few examples of direct empirical validation of PEMs for large territories, due to the evident difficulties of implementing such a procedure. Those that do exist, e.g. [18], rely on eddy covariance measurements and thus the quality of the validation is dependent upon the number and distribution of towers. An alternative approach to validation might include the use of inventory-based NPP datasets where available, which provide complete spatial coverage [105]. Recent efforts to establish a global carbon flux database for forest ecosystems will be helpful [106]. In general, more studies on evaluation of global PEMs are required. Choice of input datasets (e.g. PAR, FAPAR, and others) can have a large impact on the results; therefore more effort is needed here.

Finally, new techniques are being developed to measure rates of photosynthesis and GPP directly, although these are not yet operational. With the recent launch of GOSAT and several proposed ESA/NASA missions, new techniques for carbon flux estimation and PEM calibration and validation will be available in the near future. In the interim, PEMs will likely remain a useful tool in the suite of carbon flux modeling techniques.

Competing interests

The authors declare that they have no competing interests.

Authors' contributions

IM conceived the review and drafted the majority of the manuscript. Remaining authors read, edited, and approved the final manuscript.

Acknowledgements

Thanks to six anonymous reviewers and the Handling Editor for additional reference materials. The IIASA library team provided invaluable help with the literature search. The FP6 Project Geobene <http://www.geo-bene.eu>.

the FP7 Project CC-TAME <http://www.cctame.eu> and the IIASA Forestry Program provided support. Thanks to M. Gusti for helpful comments.

References

- Chapin FS, Matson PA, Mooney HA: *Principles of Terrestrial Ecosystem Ecology* Springer; 2002.
- Cramer W, Kicklighter DW, Bondeau A, Moore Iii B, Churkina G, Nemry B, Ruimy A, Schloss AL: **Comparing global models of terrestrial net primary productivity (NPP): Overview and key results.** *Global Change Biology* 1999, **5**:1-15.
- Goetz SJ, Prince SD: **Modelling Terrestrial Carbon Exchange and Storage: Evidence and Implications of Functional Convergence in Light-use Efficiency.** In *Advances in Ecological Research Volume 28*. Academic Press; 1999:57-92.
- Friend AD, Arneth A, Kiang NY, Lomas M, Ogee J, Roedenbeck C, Running SW, Santaren JD, Sitch S, Viovy N, et al.: **FLUXNET and modelling the global carbon cycle.** *Global Change Biology* 2007, **13**:610-633.
- Shvidenko A, Nilsson S: **A synthesis of the impact of Russian forests on the global carbon budget for 1961-1998.** *Tellus, Series B: Chemical and Physical Meteorology* 2003, **55**:391-415.
- Beer C, Lucht W, Schmullius C, Shvidenko A: **Small net carbon dioxide uptake by Russian forests during 1981-1999.** *Geophysical Research Letters* 2006, **33**:L15403.
- Stephens BB, Gurney KR, Tans PP, Sweeney C, Peters W, Bruhwiler L, Ciais P, Ramonet M, Boussquet P, Nakazawa T, et al.: **Weak northern and strong tropical land carbon uptake from vertical profiles of atmospheric CO₂.** *Science* 2007, **316**:1732-1735.
- Running SW, Nemani RR, Heinsch FA, Zhao M, Reeves M, Hashimoto H: **A continuous satellite-derived measure of global terrestrial primary production.** *BioScience* 2004, **54**:547-560.
- Cihlar J, Denning S, Ahern F, Arino O, Belward A, Bretherton F, Cramer W, Dedieu G, Field C, Francey R, et al.: **Initiative to quantify terrestrial carbon sources and sinks.** *EOS, Transactions, American Geophysical Union* 2002, **83**:5-6.
- Lindner M, Lucht W, Bouriaud O, Green T, Janssens I: **Specific study on forest greenhouse gas budget.** *Carbo Europe* 2004:62.
- Running SW, Nemani R, Glassy JM, Thornton PE: **MODIS daily photosynthesis (PSN) and annual net primary production (NPP) product (MOD17).** *Algorithm Theoretical Basis Document (ATBD), Version 30* 1999.
- Anderson MC, Norman JM, Meyers TP, Diak GR: **An analytical model for estimating canopy transpiration and carbon assimilation fluxes based on canopy light-use efficiency.** *Agricultural and Forest Meteorology* 2000, **101**:265-289.
- Goetz SJ, Prince SD, Goward SN, Thawley MM, Small J: **Satellite remote sensing of primary production: An improved production efficiency modeling approach.** *Ecological Modelling* 1999, **122**:239-255.
- Verstraeten WW, Veroustraete F, Feyen J: **On temperature and water limitation of net ecosystem productivity: Implementation in the C-Fix model.** *Ecological Modelling* 2006, **199**:4-22.
- Still CJ, Randerson JT, Fung IY: **Large-scale plant light-use efficiency inferred from the seasonal cycle of atmospheric CO₂.** *Global Change Biology* 2004, **10**:1240-1252.
- Ahl DE, Gower ST, Mackay DS, Burrows SN, Norman JM, Diak GR: **Heterogeneity of light use efficiency in a northern Wisconsin forest: implications for modeling net primary production with remote sensing.** *Remote Sensing of Environment* 2004, **93**:168-178.
- Turner DP, Ritts WD, Cohen WB, Maeirsperger TK, Gower ST, Kirschbaum AA, Running SW, Zhao M, Wofsy SC, Dunn AL, et al.: **Site-level evaluation of satellite-based global terrestrial gross primary production and net primary production monitoring.** *Global Change Biology* 2005, **11**:666-684.
- Heinsch FA, Zhao M, Running SW, Kimball JS, Nemani RR, Davis KJ, Bolstad PV, Cook BD, Desai AR, Ricciuto DM, et al.: **Evaluation of remote sensing based terrestrial productivity from MODIS using regional tower eddy flux network observations.** *IEEE Transactions on Geoscience and Remote Sensing* 2006, **44**:1908-1923.
- Seixas J, Carvalhais N, Nunes C, Benali A: **Ecosystem production modelling in the Iberian Peninsula comparative analysis between MODIS and MERIS datasets.** *European Space Agency, (Special Publication) ESA SP* 2007.
- Jung M, Verstraete M, Gobron N, Reichstein M, Papale D, Bondeau A, Robustelli M, Pinty B: **Diagnostic assessment of European gross primary production.** *Global Change Biology* 2008, **14**:2349-2364.
- Ruimy A, Jarvis PG, Baldocchi DD, Saugier B: **CO₂ fluxes over plant canopies and solar radiation: A review.** *Advances in Ecological Research* 1996, **26**:1-68.
- Gower ST, Kucharik CJ, Norman JM: **Direct and indirect estimation of leaf area index, f(APAR), and net primary production of terrestrial ecosystems.** *Remote Sensing of Environment* 1999, **70**:29-51.
- Glenn EP, Huete AR, Nagler PL, Nelson SG: **Relationship between remotely-sensed vegetation indices, canopy attributes and plant physiological processes: What vegetation indices can and cannot tell us about the landscape.** *Sensors* 2008, **8**:2136-2160.
- Hilker T, Coops NC, Wulder MA, Black TA, Guy RD: **The use of remote sensing in light use efficiency based models of gross primary production: A review of current status and future requirements.** *Science of the Total Environment* 2008, **404**:411-423.
- Sellers PJ: **Canopy reflectance, photosynthesis, and transpiration, II. The role of biophysics in the linearity of their interdependence.** *Remote Sensing of Environment* 1987, **21**:143-183.
- Monsi M, Saeki T, Schortemeyer M: **On the factor light in plant communities and its importance for matter production.** *Annals of Botany* 2005, **95**:549-567.
- Monteith JL: **Solar radiation and productivity in tropical ecosystems.** *J Appl Ecol* 1972, **9**:747-766.
- Monteith JL: **Climate and the efficiency of crop production in Britain.** *Philos Trans R Soc London, Ser B* 1977, **281**:277-294.
- Jenkins JP, Richardson AD, Braswell BH, Ollinger SV, Hollinger DY, Smith ML: **Refining light-use efficiency calculations for a deciduous forest canopy using simultaneous tower-based carbon flux and radiometric measurements.** *Agricultural and Forest Meteorology* 2007, **143**:64-79.
- Kumar M, Monteith JL: **Remote sensing of crop growth.** *Plants and the Daylight Spectrum* 1981:133-144.
- Goetz SJ, Prince SD, Small J, Gleason ACR: **Interannual variability of global terrestrial primary production: Results of a model driven with satellite observations.** *Journal of Geophysical Research D: Atmospheres* 2000, **105**:20077-20091.
- Alexandrov GA, Matsunaga T: **Normative productivity of the global vegetation.** *Carbon Balance Manag.* 2008, **3**:8.
- Dye DG, Shibasaki R: **Intercomparison of global PAR data sets.** *Geophysical Research Letters* 1995, **22**:2013-2016.
- Roderick ML: **The ever-flickering light.** *Trends in Ecology & Evolution* 2006, **21**:3-5.
- Gu L, Baldocchi D, Verma SB, Black TA, Vesala T, Falge EM, Dowty PR: **Advantages of diffuse radiation for terrestrial ecosystem productivity.** *Journal of Geophysical Research D: Atmospheres* 2002, **107**:2-1.
- Turner DP, Ritts WD, Cohen WB, Gower ST, Running SW, Zhao M, Costa MH, Kirschbaum AA, Ham JM, Saleska SR, Ahl DE: **Evaluation of MODIS NPP and GPP products across multiple biomes.** *Remote Sensing of Environment* 2006, **102**:282-292.
- Turner DP, Urbanski S, Bremer D, Wofsy SC, Meyers T, Gower ST, Gregory M: **A cross-biome comparison of daily light use efficiency for gross primary production.** *Global Change Biology* 2003, **9**:383-395.
- Gobron N, Verstraete M: **ECV T10: Fraction of Absorbed Photosynthetically Active Radiation (FAPAR).** In *Essential Climate Variables Rome: Global Terrestrial Observing System*; 2008.
- Myneni RB, Ross J: **Photon-vegetation interactions.** *Applications in Optical Remote Sensing and Plant Ecology* 1991.
- Prince SD: **A model of regional primary production for use with coarse resolution satellite data.** *International Journal of Remote Sensing* 1991, **12**:1313-1330.
- Schwalm CR, Black TA, Amiro BD, Arain MA, Barr AG, Bourque CPA, Dunn AL, Flanagan LB, Giasson MA, Lafleur PM, et al.: **Photosynthetic light use efficiency of three biomes across an east-west continental-scale transect in Canada.** *Agricultural and Forest Meteorology* 2006, **140**:269-286.
- Ruimy A, Kergoat L, Bondeau A: **Comparing global models of terrestrial net primary productivity (NPP): Analysis of differences in light absorption and light-use efficiency.** *Global Change Biology* 1999, **5**:56-64.

43. Heinsch FA, Reeves M, Votava P, Kang S, Milesi C, Zhao M: *Users Guide: GPP and NPP (MOD17A2/A3) Products NASA MODIS Land Algorithm* 2003.
44. Ryan MG: **Effects of climate change on plant respiration.** *Ecological Applications* 1991, **1**:157-167.
45. Goetz SJ, Prince SD: **Variability in carbon exchange and light utilization among boreal forest stands: Implications for remote sensing of net primary production.** *Canadian Journal of Forest Research* 1998, **28**:375-389.
46. Potter C, Klooster S, Tan P, Steinbach M, Kumar V, Genovesi V: **Variability in terrestrial carbon sinks over two decades: Part 2 - Eurasia.** *Global and Planetary Change* 2005, **49**:177-186.
47. Potter C, Klooster S, Myneni R, Genovesi V, Tan PN, Kumar V: **Continental-scale comparisons of terrestrial carbon sinks estimated from satellite data and ecosystem modeling 1982-1998.** *Global and Planetary Change* 2003, **39**:201-213.
48. Cao M, Prince SD, Small J, Goetz SJ: **Remotely sensed interannual variations and trends in terrestrial net primary productivity 1981-2000.** *Ecosystems* 2004, **7**:233-242.
49. Lafont S, Kergoat L, Dedieu G, Chevillard A, Karstens U, Kolle O: **Spatial and temporal variability of land CO₂ fluxes estimated with remote sensing and analysis data over western Eurasia.** *Tellus, Series B: Chemical and Physical Meteorology* 2002, **54**:820-833.
50. Veroustraete F, Sabbe H, Rasse DP, Bertels L: **Carbon mass fluxes of forests in Belgium determined with low resolution optical sensors.** *International Journal of Remote Sensing* 2004, **25**:769-792.
51. Zhao M, Heinsch FA, Nemani RR, Running SV: **Improvements of the MODIS terrestrial gross and net primary production global data set.** *Remote Sensing of Environment* 2005, **95**:164-176.
52. Sasai T, Okamoto K, Hiyama T, Yamaguchi Y: **Comparing terrestrial carbon fluxes from the scale of a flux tower to the global scale.** *Ecological Modelling* 2007, **208**:135-144.
53. Sasai T, Ichii K, Yamaguchi Y, Nemani R: **Simulating terrestrial carbon fluxes using the new biosphere model BEAMS: Biosphere model integrating Eco-physiological And Mechanistic approaches using Satellite data.** *J Geophys Res* 2005, **110**:G02014.
54. Schloss AL, Kicklighter DW, Kaduk J, Wittenberg U: **Comparing global models of terrestrial net primary productivity (NPP): Comparison of NPP to climate and the Normalized Difference Vegetation Index (NDVI).** *Global Change Biology* 1999, **5**:25-34.
55. Reichstein M, Ciais P, Papale D, Valentini R, Running S, Viovy N, Cramer W, Granier A, Ogee J, Allard V, et al.: **Reduction of ecosystem productivity and respiration during the European summer 2003 climate anomaly: A joint flux tower, remote sensing and modelling analysis.** *Global Change Biology* 2007, **13**:634-651.
56. Verstraeten WW, Veroustraete F, Heyns W, Roey TV, Feyen J: **On uncertainties in carbon flux modelling and remotely sensed data assimilation: The Brasschaat pixel case.** *Advances in Space Research* 2008, **41**:20-35.
57. Leith H: **Primary productivity in ecosystems: Comparative analysis of global patterns.** *Unifying Concepts in Ecology* 1975:67-88.
58. Ito A, Sasai T: **A comparison of simulation results from two terrestrial carbon cycle models using three climate data sets.** *Tellus, Series B: Chemical and Physical Meteorology* 2006, **58**:513-522.
59. Pan Y, Birdsey R, Hom J, McCullough K, Clark K: **Improved estimates of net primary productivity from modis satellite data at regional and local scales.** *Ecological Applications* 2006, **16**:125-132.
60. Hanan NP, Prince SD, Begue A: **Estimation of absorbed photosynthetically active radiation and vegetation net production efficiency using satellite data.** *Agricultural and Forest Meteorology* 1995, **76**:259-276.
61. Gitelson AA, Vina A, Verma SB, Rundquist DC, Arkebauer TJ, Keydan G, Leavitt B, Ciganda V, Burba GG, Suyker AE: **Relationship between gross primary production and chlorophyll content in crops: Implications for the synoptic monitoring of vegetation productivity.** *Journal of Geophysical Research D: Atmospheres* 2006, **111**(8):D08S11.
62. Rahman AF, Cordova VD, Gamon JA, Schmid HP, Sims DA: **Potential of MODIS ocean bands for estimating CO₂ flux from terrestrial vegetation: A novel approach.** *Geophysical Research Letters* 2004, **31**(10):L10503.
63. Sims DA, Rahman AF, Cordova VD, El-Masri BZ, Baldocchi DD, Flanagan LB, Goldstein AH, Hollinger DY, Misson L, Monson RK, et al.: **On the use of MODIS EVI to assess gross primary productivity of North American ecosystems.** *Journal of Geophysical Research G: Biogeosciences* 2006, **111**(4):G04015.
64. Grace J, Nichol C, Disney M, Lewis P, Quaife T, Bowyer P: **Can we measure terrestrial photosynthesis from space directly, using spectral reflectance and fluorescence?** *Global Change Biology* 2007, **13**:1484-1497.
65. Goerner A, Reichstein M, Rambal S: **Tracking seasonal drought effects on ecosystem light use efficiency with satellite-based PRI in a Mediterranean forest.** *Remote Sensing of Environment* 2009, **113**:1101-1111.
66. Mu Q, Zhao M, Heinsch FA, Liu M, Tian H, Running SW: **Evaluating water stress controls on primary production in biogeochemical and remote sensing based models.** *Journal of Geophysical Research G: Biogeosciences* 2007, **112**(1):G01012.
67. Verstraeten WW, Veroustraete F, Wagner W, Van Roey T, Heyns W, Verbeiren S, Sande CJ van der, Feyen J: **Impact assessment of remotely sensed soil moisture on ecosystem carbon fluxes across Europe.** *2nd International Workshop on Uncertainty in Greenhouse Gas Inventories* 2007.
68. Beer C, Lucht W, Gerten D, Thonicke K, Schmullius C: **Effects of soil freezing and thawing on vegetation carbon density in Siberia: A modeling analysis with the Lund-Potsdam-Jena Dynamic Global Vegetation Model (LPJ-DGVM).** *Global Biogeochemical Cycles* 2007, **21**(1):GB1012.
69. Gifford RM: **The global carbon cycle: A viewpoint on the missing sink.** *Australian Journal of Plant Physiology* 1994, **21**:1-15.
70. Hashimoto H, Dungan JL, White MA, Yang F, Michaelis AR, Running SW, Nemani RR: **Satellite-based estimation of surface vapor pressure deficits using MODIS land surface temperature data.** *Remote Sensing of Environment* 2008, **112**:142-155.
71. Wagner W, Blöschl G, Pampaloni P, Calvet JC, Bizzarri B, Wigneron JP, Kerr Y: **Operational readiness of microwave remote sensing of soil moisture for hydrologic applications.** *Nordic Hydrology* 2007, **38**:1-20.
72. Roderick ML, Farquhar GD, Berry SL, Noble IR: **On the direct effect of clouds and atmospheric particles on the productivity and structure of vegetation.** *Oecologia* 2001, **129**:21-30.
73. Alton PB: **Reduced carbon sequestration in terrestrial ecosystems under overcast skies compared to clear skies.** *Agricultural and Forest Meteorology* 2008, **148**:1641-1653.
74. Ibrom A, Oltchev A, June T, Kreilein H, Rakkibu G, Ross T, Panferov O, Gravenhorst G: **Variation in photosynthetic light-use efficiency in a mountainous tropical rain forest in Indonesia.** *Tree Physiology* 2008, **28**:499-508.
75. Cook BD, Bolstad PV, Martin JG, Heinsch FA, Davis KJ, Wang W, Desai AR, Teclaw RM: **Using light-use and production efficiency models to predict photosynthesis and net carbon exchange during forest canopy disturbance.** *Ecosystems* 2008, **11**:26-44.
76. Lindroth A, Lagergren F, Aurela M, Bjarnadottir B, Christensen T, Dellwik E, Grelle A, Ibrom A, Johansson T, Lankreijer H, et al.: **Leaf area index is the principal scaling parameter for both gross photosynthesis and ecosystem respiration of Northern deciduous and coniferous forests.** *Tellus, Series B: Chemical and Physical Meteorology* 2008, **60 B**:129-142.
77. Kimball JS, McDonald KC, Running SW, Frolking SE: **Satellite radar remote sensing of seasonal growing seasons for boreal and subalpine evergreen forests.** *Remote Sensing of Environment* 2004, **90**:243-258.
78. Field CB, Randerson JT, Malmström CM: **Global net primary production: Combining ecology and remote sensing.** *Remote Sensing of Environment* 1995, **51**:74-88.
79. Ensminger I, Sveshnikov D, Campbell DA, Funk C, Jansson S, Lloyd J, Shibistova O, Oquist G: **Intermittent low temperatures constrain spring recovery of photosynthesis in boreal Scots pine forests.** *Global Change Biology* 2004, **10**:995-1008.
80. Makela A, Hari P, Berninger F, Hanninen H, Nikinmaa E: **Acclimation of photosynthetic capacity in Scots pine to the annual cycle of temperature.** *Tree Physiology* 2004, **24**:369-376.
81. Bartsch A, Kidd RA, Wagner W, Bartalis Z: **Temporal and spatial variability of the beginning and end of daily spring freeze/**

- thaw cycles derived from scatterometer data. *Remote Sensing of Environment* 2007, **106**:360-374.
82. McCallum I, Obersteiner M, Nilsson S, Shvidenko A: **A spatial comparison of four satellite derived 1 km global land cover datasets.** *International Journal of Applied Earth Observation and Geoinformation* 2006, **8**:246-255.
 83. Fritz S, McCallum I, Schill C, Perger C, Grillmayer R, Achard Fdr, Kraxner F, Obersteiner M: **Geo-Wiki.Org: The Use of Crowdsourcing to Improve Global Land Cover.** *Remote Sensing* 2009, **1**:345-354.
 84. Sitch S, Smith B, Prentice IC, Arneth A, Bondeau A, Cramer WW, Kaplan JO, Levis S, Lucht WW, Sykes MT, et al.: **Evaluation of ecosystem dynamics, plant geography and terrestrial carbon cycling in the LPJ dynamic global vegetation model.** *Global Change Biology* 2003, **9**:161-185.
 85. Tansey K, Gregoire JM, Defourny P, Leigh R, Pekel JF, van Bogaert E, Bartholome E: **A new, global, multi-annual (2000-2007) burnt area product at 1 km resolution.** *Geophysical Research Letters* 2008, **35**(1):L01401.
 86. Shvidenko AZ, Schepashchenko DG, Vaganov EA, Nilsson S: **Net primary production of forest ecosystems of Russia: A new estimate.** *Doklady Earth Sciences* 2008, **421**:1009-1012.
 87. Garrigues S, Lacaze R, Baret F, Morisette JT, Weiss M, Nickeson JE, Fernandes R, Plummer S, Shabanov NV, Myneni RB, et al.: **Validation and intercomparison of global Leaf Area Index products derived from remote sensing data.** *Journal of Geophysical Research G: Biogeosciences* 2008, **113**(2):G02028.
 88. Fernandes R, Canisius F, Rochdi N, Khurshid S: **Integrating a priori in-situ information within satellite based LAI products.** *Geophysical Research Abstracts* 2008, **10**:2-2.
 89. Gifford RM: **Plant respiration in productivity models: Conceptualisation, representation and issues for global terrestrial carbon-cycle research.** *Functional Plant Biology* 2003, **30**:171-186.
 90. Houghton RA: **Aboveground forest biomass and the global carbon balance.** *Global Change Biology* 2005, **11**:945-958.
 91. Sims DA, Rahman AF, Cordova VD, El-Masri BZ, Baldocchi DD, Bolstad PV, Flanagan LB, Goldstein AH, Hollinger DY, Misson L, et al.: **A new model of gross primary productivity for North American ecosystems based solely on the enhanced vegetation index and land surface temperature from MODIS.** *Remote Sensing of Environment* 2008, **112**:1633-1646.
 92. Rahman AF, Sims DA, Cordova VD, El-Masri BZ: **Potential of MODIS EVI and surface temperature for directly estimating per-pixel ecosystem C fluxes.** *Geophysical Research Letters* 2005, **32**:1-4.
 93. Bézy JL, Bensi P, Berger M, Carnicero B, Davidson M, Drinkwater M, Durand Y, Hélie F, Ingmann P, Langen J, et al.: **ESA future earth observation explorer missions.** *Proceedings of SPIE - The International Society for Optical Engineering* 2008.
 94. Goetz SJ, Baccini A, Laporte NT, Johns T, Walker W, Kellendorfer J, Houghton RA, Sun M: **Mapping and monitoring carbon stocks with satellite observations: A comparison of methods.** *Carbon Balance and Management* 2009, **4**:2.
 95. Gamon JA, Penuelas J, Field CB: **A narrow-waveband spectral index that tracks diurnal changes in photosynthetic efficiency.** *Remote Sensing of Environment* 1992, **41**:35-44.
 96. Papale D, Valentini R: **A new assessment of European forests carbon exchanges by eddy fluxes and artificial neural network spatialization.** *Global Change Biology* 2003, **9**:525-535.
 97. Baldocchi D, Falge E, Gu L, Olson R, Hollinger D, Running S, Anthoni P, Bernhofer C, Davis K, Evans R, et al.: **FLUXNET: A New Tool to Study the Temporal and Spatial Variability of Ecosystem-Scale Carbon Dioxide, Water Vapor, and Energy Flux Densities.** *Bulletin of the American Meteorological Society* 2001, **82**:2415-2434.
 98. Chapin FS III, Woodwell GM, Randerson JT, Rastetter EB, Lovett GM, Baldocchi DD, Clark DA, Harmon ME, Schimel DS, Valentini R, et al.: **Reconciling carbon-cycle concepts, terminology, and methods.** *Ecosystems* 2006, **9**:1041-1050.
 99. Parton WJ: **Observations and modeling of biomass and soil organic matter dynamics for the grassland biome worldwide.** *Global Biogeochemical Cycles* 1993, **7**:785-809.
 100. Veroustraete F, Sabbe H, Eerens H: **Estimation of carbon mass fluxes over Europe using the C-Fix model and Euroflux data.** *Remote Sensing of Environment* 2002, **83**:376-399.
 101. Lloyd J, Taylor JA: **On the temperature dependence of soil respiration.** *Functional Ecology* 1994, **8**:315-323.
 102. Reichstein M, Rey A, Freibauer A, Tenhunen J, Valentini R, Banza J, Casals P, Cheng Y, Grunzweig JM, Irvine J, et al.: **Modeling temporal and large-scale spatial variability of soil respiration from soil water availability, temperature and vegetation productivity indices.** *Global Biogeochemical Cycles* 2003, **17**:15-11.
 103. Sampson DA, Janssens IA, Curriel Yuste J, Ceulemans R: **Basal rates of soil respiration are correlated with photosynthesis in a mixed temperate forest.** *Global Change Biology* 2007, **13**:2008-2017.
 104. Goward SN, Dye DG: **Evaluating North American net primary productivity with satellite observations.** *Advances in Space Research* 1987, **7**:165-174.
 105. Nilsson S, Shvidenko A, Jonas M, McCallum I, Thomson A, Balzter H: **Uncertainties of a regional terrestrial biota full carbon account: A systems analysis.** *Water, Air, and Soil Pollution: Focus* 2007, **7**:425-441.
 106. Luyssaert S, Inglima I, Jung M, Richardson AD, Reichstein M, Papale D, Piao SL, Schulze ED, Wingate L, Matteucci G, et al.: **CO2 balance of boreal, temperate, and tropical forests derived from a global database.** *Global Change Biology* 2007, **13**:2509-2537.
 107. Zhang K, Kimball JS, Zhao M, Oechel WC, Cassano J, Running SW: **Sensitivity of pan-Arctic terrestrial net primary productivity simulations to daily surface meteorology from NCEP-NCAR and ERA-40 reanalyses.** *J Geophys Res* 2007, **112**:G01011.
 108. Weiss M, Baret F, Garrigues S, Lacaze R: **LAI and fAPAR CYCLOPES global products derived from VEGETATION. Part 2: validation and comparison with MODIS collection 4 products.** *Remote Sensing of Environment* 2007, **110**:317-331.
 109. Fensholt R, Sandholt I, Rasmussen MS: **Evaluation of MODIS LAI, fAPAR and the relation between fAPAR and NDVI in a semi-arid environment using in situ measurements.** *Remote Sensing of Environment* 2004, **91**:490-507.

Publish with **BioMed Central** and every scientist can read your work free of charge

"BioMed Central will be the most significant development for disseminating the results of biomedical research in our lifetime."

Sir Paul Nurse, Cancer Research UK

Your research papers will be:

- available free of charge to the entire biomedical community
- peer reviewed and published immediately upon acceptance
- cited in PubMed and archived on PubMed Central
- yours — you keep the copyright

Submit your manuscript here:
http://www.biomedcentral.com/info/publishing_adv.asp



A spatial comparison of four satellite derived 1 km global land cover datasets

Ian McCallum*, Michael Obersteiner, Sten Nilsson, Anatoly Shvidenko

International Institute for Applied Systems Analysis (IIASA), Schlossplatz 1, A-2361 Laxenburg, Austria

Received 17 August 2005; accepted 2 December 2005

Abstract

Global change issues are high on the current international political agenda. A variety of global protocols and conventions have been established aimed at mitigating global environmental risks. A system for monitoring, evaluation and compliance of these international agreements is needed, with each component requiring comprehensive analytical work based on consistent datasets. Consequently, scientists and policymakers have put faith in earth observation data for improved global analysis. Land cover provides in many aspects the foundation for environmental monitoring [FAO, 2002a. Proceedings of the FAO/UNEP Expert Consultation on Strategies for Global Land Cover Mapping and Monitoring, FAO, Rome, Italy, 38 pp.]. Despite the significance of land cover as an environmental variable, our knowledge of land cover and its dynamics is poor [Foody, G.M., 2002. Status of land cover classification accuracy assessment. *Rem. Sens. Environ.* 80, 185–201]. This study compares four satellite derived 1 km land cover datasets freely available from the internet and in wide use among the scientific community. Our analysis shows that while these datasets have in many cases reasonable agreement at a global level in terms of total area and general spatial pattern, there is limited agreement on the spatial distribution of the individual land classes. If global datasets are used at a continental or regional level, agreement in many cases decreases significantly. Reasons for these differences are many—ranging from the classes and thresholds applied, time of data collection, sensor type, classification techniques, use of in situ data, etc., and make comparison difficult. Results of studies based on global land cover datasets are likely influenced by the dataset chosen. Scientists and policymakers should be made aware of the inherent limitations in using current global land cover datasets, and would be wise to utilise multiple datasets for comparison.

© 2005 Elsevier B.V. All rights reserved.

Keywords: Land cover; Earth observation; Global change; Environmental monitoring

1. Introduction

An increasing number of international environmental agreements place global change at the top of international scientific and political agendas, including the Kyoto Protocol, the Convention on Biological Diversity, the Convention to Combat Desertification and the Ramsar Convention on Wetlands. There are over

700 multi-lateral environmental agreements and over 1000 bilateral agreements dealing with different aspects of the environment and global change (Mitchell, 2003). Each of these agreements requires a unique set of information for implementation, monitoring and compliance. The needed information is currently coming from in situ data, models and remotely sensed data. A key component of the data needed within the global change framework is ecosystem-based information. However, while our knowledge of ecosystems has increased dramatically, it has not kept pace with our ability to alter them (WRI, 2000). One crucial parameter of the needed ecosystem information is land

* Corresponding author. Tel.: +43 2236 807328;
fax: +43 2236 807559.

E-mail address: mccallum@iiasa.ac.at (I. McCallum).

cover. Land cover is defined as the observed (bio) physical cover on the earth's surface (Di Gregorio and Jansen, 2000). In spite of the significance of land cover as a key environmental parameter our knowledge about it and in particular its dynamics is poor and to some extent infantile (Foody, 2002). We are far from producing geospatially consistent high-quality data at an operational level (Giri et al., 2005).

Both the policy and the science communities, with a manifold of disciplines, have great expectations that satellite observations can provide improvements with respect to our knowledge on continental and global land cover issues. Remote sensing can deliver data in a transparent and repeatable fashion without bias. Scientists, international organizations, NGOs and policy-makers have had increased access to satellite-based land cover descriptions of the globe over the last decade with more products planned for delivery in the near future. Users must therefore increase their understanding of the potential differences between the available global land cover products before they are used in monitoring, compliance and estimating conditions and trends.

The purpose of this study is to highlight for the user community some of the potential differences between the four existing (freely downloadable) global land cover datasets when compared at the global level. Armed with this information, the user may choose to more carefully select one dataset versus another for a particular study, or to use multiple datasets. We do not indicate preference of one map over another, nor do we identify the accuracy of any of the individual datasets.

2. Global land cover mapping

Prior to the existence of global satellite measurements suitable for deriving land cover maps, land cover

datasets were assembled from a wide variety of data sources (Matthews, 1983; Henderson-Sellers et al., 1986). Townsend et al. (1991) found the information from conventional ground-based data contained significant deficiencies. Not only did the total area occupied by different classes vary substantially between datasets, but the detailed spatial distribution often varied substantially even where the total global estimates of a cover were similar. The absence of suitable land cover information at the global scale led in part to the attempts to retrieve this information from satellite observations. These efforts have thus far produced the following four freely available global satellite-based 1 km land cover products which are in wide use by the international science community (see Table 1): (1) International Geosphere Biosphere Project (IGBP) (Loveland et al., 2000) http://edcns17.cr.usgs.gov/glcc/globe_int.html; (2) University of Maryland (UMD) (Hansen et al., 2000) <http://www.geog.umd.edu/landcover/1km-map.html>; (3) Global Land Cover 2000 (GLC2000) (Fritz et al., 2003) <http://www-gvm.jrc.it/glc2000/>; and (4) MODerate resolution Imaging Spectroradiometer (MODIS) (Strahler et al., 1999) <http://duckwater.bu.edu/lc/mod12q1.html>.

Three of the four datasets utilized the IGBP land cover classification (UMD utilised a simplified IGBP approach), which includes 11 categories of natural vegetation covers distinguished by life form, 3 classes of urban and cropland mosaic lands and 3 classes of non-vegetated lands for a total of 17 classes (Strahler et al., 1999). The legend aimed to be exhaustive, so that every part of the earth's surface was assigned to a class; exclusive so that classes would not overlap; and structured so classes are equally interpretable with 1-km data, higher resolution satellite imagery or ground observation (Loveland et al., 2000). Alternatively, the GLC2000 classification utilises the Land Cover

Table 1
Characteristics of the four satellite derived global land cover datasets compared in this study

	IGBP	UMD	GLC2000	MODIS
Sensor	AVHRR	AVHRR	SPOT Vegetation	Terra MODIS
Time of data collection	April 1992–March 1993	April 1992–March 1993	November 1999–December 2000	October 2000–October 2001
Input data	12 Monthly NDVI composites	41 Metrics derived from NDVI and bands 1–5	Daily mosaics of 4 spectral channels and NDVI	12, 32-Day composites of 8 input parameters
Classification technique	Unsupervised clustering	Supervised classification decision tree	Generally unsupervised classification	Supervised decision-tree classifier, neural networks
Classification scheme	IGBP (17 classes)	Simplified IGBP (14 classes)	FAO LCCS (23 classes)	IGBP (20 classes)
Validation	High resolution satellite images	Used other digital datasets	Statistical sampling	Confusion matrices, confidence values
Supplemental data	DEM, ecoregions, vegetation, land cover	Coarse/fine resolution satellite data	Data from other sensors	Fine resolution imagery with ancillary data

Classification System (LCCS) of the Food and Agricultural Organization (FAO) (Di Gregorio and Jansen, 2000) producing a total of 23 land cover classes. The LCCS is a comprehensive, standardised a priori classification system that describes land cover according to a hierarchical series of classifiers and attributes. In doing so, it separates vegetated or non-vegetated surfaces; terrestrial or aquatic/flooded; cultivated and managed; natural and semi-natural; life-form; cover; height; spatial distribution; leaf type and phenology (Fritz et al., 2003).

The first of these datasets produced was the IGBP dataset. This was developed through a continent by continent unsupervised classification of 1-km monthly advanced very high resolution radiometer (AVHRR) normalized difference vegetation index (NDVI) composites covering 1991–1993 (Loveland et al., 2000). This dataset employed 17 IGBP land cover classes. Problem areas include global wetlands which were underrepresented in the database due to difficulty in separating trees, shrubs and water along with the small size of many wetland areas (Loveland et al., 2000). The overall area-weighted accuracy of the dataset was determined to be 66.9% (Scepan, 1999).

The IGBP dataset creation was followed shortly by the UMD global land cover dataset. The UMD approach involves a supervised method where the entire globe was classified using a classification tree algorithm. The tree predicts class memberships from metrics derived from the same AVHRR data employed by Loveland et al. (2000) except that all five spectral bands as well as NDVI values were used (Hansen et al., 2000). The UMD utilised a simplified IGBP classification with 14 classes. The classes permanent wetlands, cropland/natural vegetation mosaic and ice and snow were not used. Problem areas included those of low biomass agriculture, high-latitude broadleaf forest and temperate pastures within areas of agriculture. The agreements for all classes varied from an average of 65% when viewing all pixels to an average of 82% when viewing only those 1-km pixels consisting of greater than 90% one class within the high-resolution datasets (Hansen et al., 2000).

A major global effort concluded with the recent release of the GLC2000 global land cover dataset. In contrast to former global mapping initiatives the GLC2000 project is a bottom-up approach to global mapping (Fritz et al., 2003). Regional experts were identified from around the globe to classify 19 regional windows (each with a unique regional legend), which were then combined into a global product. The dataset was based on daily data from the VEGETATION sensor

on-board SPOT4, though mapping of some regions involved use of data from other Earth observing sensors to resolve specific issues. The GLC2000 utilises a global classification based on the LCCS legend of 23 classes. The product has been visually validated by a number of experts and the overall response has been very positive. A comparison of overlapping regions between Eurasia, Asia and Europe recorded a maximum of 64.26% agreement (Fritz et al., 2003). The accuracy assessment relied on quality control based on a comparison with ancillary data and a quantitative accuracy assessment based on a stratified random sampling of reference data (Landsat ETM imagery). First results of the accuracy assessment indicate similar accuracies as the IGBP dataset (GOFC-GOLD, 2004).

The latest global land cover dataset made available is from MODIS. Land cover classes are produced by processing the 32-day database using decision tree and artificial neural network classification algorithms to assign land cover classes based on training data (Strahler et al., 1999). The MODIS dataset was classified according to the IGBP legend with 20 classes in total. The estimated accuracy of the IGBP layer of the Consistent-Year Land Cover product (V003) is 75–80% globally; 70–85% by continental regions; and from 60 to 90% for individual classes (MODIS, 2003).

Obvious and sometimes major differences exist between the four datasets including sensor-type, temporal scales, classification methods, etc. Both the IGBP and UMD datasets are based on 1992–1993 data, while the GLC2000 and MODIS datasets use year 2000/2001 data. Because the variability between estimates substantially exceeds that of actual land cover changes (Defries and Townshend, 1994), it is not possible to identify change by comparing these datasets. However, it is likely that sub-pixel changes affect in some cases the classification of a pixel. Latifovic et al. (2004) noted that changes in forested area in North America caused largely by forest fires occurring between 1992 and 2000, accounted for a significant part of the differences between the IGBP/UMD and GLC2000/MODIS datasets. Forest harvesting and fire could also have an impact across the worlds other large forest regions, namely Russia and Brazil. Additionally, the IGBP and UMD datasets use variations of the NDVI. With the eruption of Mt. Pinatubo in June 1991, satellite observations through December 1992 were affected and the impact can be seen in the NDVI data (Stowe et al., 1992). While the NDVI is appropriate for the identification of vegetated land cover patterns and characteristics, it is not suited to the discrimination of cover patterns within non-vegetated landscapes, and

faces difficulty in separating classes of minimal vegetation (Loveland et al., 2000).

3. Methodology

The initial step involved downloading the four datasets from the internet. Minor differences existed between the datasets regarding geo-registration, however these were resolved using geo-processing software.

In order to compare the datasets a common legend was assigned to all four datasets based on the IGBP classification (see Table 2). The IGBP and MODIS datasets were downloaded with an IGBP classification. The UMD dataset is provided in a modified IGBP classification. Hansen et al. (2000) provided the conversion from the UMD into the IGBP classification.

A document describing the conversion from the GLC2000 into the IGBP classification (GLC2000-LCSS_global-legend_overview.doc) was downloaded from the Joint Research Centre website in March, 2003 and used to aid in IGBP assignment. Additionally, we referred to the comparison of the IGBP, UMD, GLC2000 and MODIS products over North and Central America, where Latifovic et al. (2004) assigned each of the four products to an IGBP class. As well, Giri et al. (2005) and Fritz and See (2005) made comparisons of the GLC2000 and MODIS products. Fritz and See (2005) presented a fuzzy approach to comparing these datasets, thus alleviating the difficulties of matching the legends. In our study, we made no attempt to modify the classes in any of the datasets. Whole classes were assigned to the most suitable IGBP class based on the

Table 2

A description of the classification used in each of the four spatial land cover datasets, in relation to the IGBP classification

IGBP/MODIS	UMD	GLC-2000
Evergreen needleleaf forest ^a	Evergreen needleleaf forest ^b	Tree cover, needleleaf, evergreen, closed-open; tree cover, burnt (mainly boreal) ^c
Evergreen broadleaf forest ^a	Evergreen broadleaf forest ^b	Tree cover, broadleaf, evergreen, closed-open ^c ; tree cover, regularly flooded, fresh water ^c ; tree cover, regularly flooded, saline water ^c
Deciduous needleleaf forest ^a	Deciduous needleleaf forest ^b	Tree cover, needleleaf, deciduous ^c
Deciduous broadleaf forest ^a	Deciduous broadleaf forest ^b	Tree cover, broadleaf, deciduous, closed (tree canopy >40%, height > 3 m)
Mixed forest (no one type >60%) ^a	Mixed forest (no one type <25% or >75%) ^b	Tree cover, mixed leaf type, closed-open ^c
Closed shrublands (shrub canopy >60%, height < 2 m, evergreen or deciduous)	Closed shrubland (tree canopy <10%)	Mosaic: tree cover/other natural vegetation (crop component possible) shrub cover, closed-open, evergreen
Open shrublands (shrub canopy 10–60%, height < 2 m, evergreen or deciduous)	Open shrubland (shrub canopy 10–40%, height < 2 m, evergreen or deciduous)	Sparse herbaceous or sparse shrub cover
Woody savannas (forest 30–60%, height > 2 m)	Woodland (forest 40–60%, height > 5 m)	Tree cover, broadleaf, deciduous, open (tree canopy 15–40%, height > 3 m)
Savannas (forest 10–30%, height > 2 m)	Wooded grassland/shrub forest 10–30%, height > 5 m	Shrub cover, closed-open, deciduous (broadleaf)
Grasslands, herbaceous (tree and shrub cover <10%)	Grassland	Herbaceous cover, closed-open
Permanent wetlands (water/herbaceous or woody vegetation)	No such class	Regularly flooded shrub and/or herbaceous cover (flooded > 2 months)
Croplands (single and multiple crop systems)	Cropland (>80% crop-producing fields)	Cultivated and managed areas
Urban and built-up	Urban and built-up	Artificial surfaces and associated areas
Cropland/natural vegetation mosaic (cropland, forest, shrub, grass: no one type >60%)	No such class	Mosaic: cropland/tree cover/other natural vegetation; mosaic: cropland/shrub or grass cover
Snow and ice, permanent barren or sparsely vegetated (soil, sand, rocks or snow, <10% vegetated cover)	Bare ground (including ice)	Snow and ice bare areas

^a IGBP forest canopy cover >60%, tree height > 2 m.

^b UMD forest canopy cover >60%, tree height > 5 m.

^c GLC2000 forest canopy cover >15%, tree height > 3 m.

best available information. This was done intentionally, to show the differences between the available datasets using the IGBP classification. It is also unlikely that users will have the time or tools at hand to perform such a comparison and if at all will use the IGBP legend if using multiple datasets.

For the purposes of this study, water was not included in the comparison; however significant differences occur between the products for inland water. Specifically, many small water bodies exist in northern boreal regions. In addition, we merged IGBP classes 15 and 16 (snow and ice, and barren or sparsely vegetated) into one class, due to the fact that the UMD dataset does not distinguish between snow and ice. Antarctica was excluded from the analysis.

Once the datasets were assigned to the IGBP classification according to Table 2, the four datasets were merged. A comparison was performed to identify the level of agreement between each 1 km² pixel in the four datasets using the IGBP classification. Four levels of agreement were distinguished: no agreement—pixels containing a unique IGBP class in each dataset; partial agreement—pixels where two of the four datasets are in agreement (it is possible that the other two pixels are identical to each other—no distinction was made); high agreement—where three of the datasets agree for the same pixel; and full agreement—where all four datasets within a pixel were in agreement.

In addition to the global comparison, seven test sites were selected (5 × 5 degree areas) across the globe representing the continents. These sites allow for a regional comparison of the datasets. In addition, the heterogeneity of the landscape was measured in order to further explain some of the differences between the datasets. Using an eight neighbour rule (McGarigal et al., 2002), patches (contiguous areas of similar land cover class) were delineated and counted for each land cover dataset based on the standard IGBP classification.

4. Results and analyses

Initially, a total percent area comparison of the four land cover datasets assigned to each of the original IGBP land cover classes was performed (Fig. 1). In Fig. 1, there is reasonable agreement across the datasets for evergreen forest classes, open shrub lands, grasslands, croplands, urban classes and snow/ice/barren. However, disagreement occurs across the datasets between the deciduous and mixed forest classes, closed shrub lands, savannas, woody savannas and cropland/vegetation mosaic. Neither permanent wetlands nor

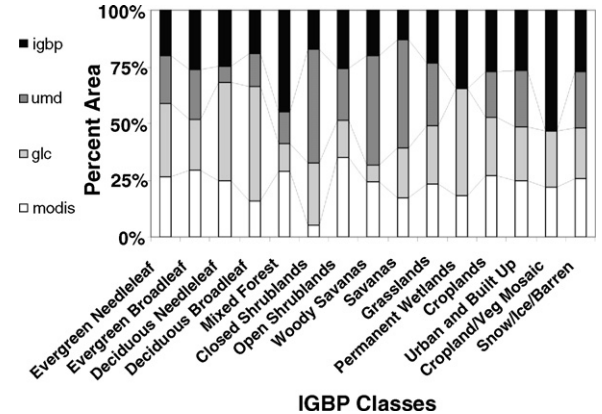


Fig. 1. The percent area comparison of IGBP, UMD, GLC2000 and MODIS land cover datasets over the globe, classified according to the IGBP classification.

cropland/vegetation mosaic are present in the UMD dataset and therefore comparison is not possible.

In order to better visualise the legend assignment in Table 2, and the percent area composition in Fig. 1, Fig. 2 provides a spatial comparison of each dataset, according to its assigned IGBP class. Overall, general patterns of land cover across the globe viewed at this scale are obvious. In particular, forest classes: (1) evergreen needleleaf, (2) evergreen broadleaf and (3) deciduous needleleaf are similarly identified across the four datasets. Major differences appear in the assignment of the UMD map to the IGBP classification (based on Hansen and Reed, 2000), created in part by the lack of the cropland/natural vegetation mosaic in the UMD classification. By collapsing the IGBP legend further, improvement could be made in harmonization, albeit at the cost of detail.

A different picture emerges when a spatial comparison is made on the level of agreement between the global datasets (Fig. 3). According to Fig. 3, the only major regions classified similarly in all four datasets were the snow/ice regions over Greenland, the barren/sparsely vegetated regions over Africa and the tropical evergreen broadleaf forests of Brazil, amounting to a total of 26% of the globe.

Reasons for the lack of agreement are many. An obvious reason visible in Fig. 2 is the missing UMD class of croplands/natural vegetation mosaic, which creates a possible overestimation in other classes. Less obvious are the errors introduced in the assignment of the various datasets to the IGBP legend. In addition, basic differences between the datasets outlined in Table 1 are significant and play a role.

Latifovic et al. (2004) noted that for North America, central/core forested areas were in good agreement,

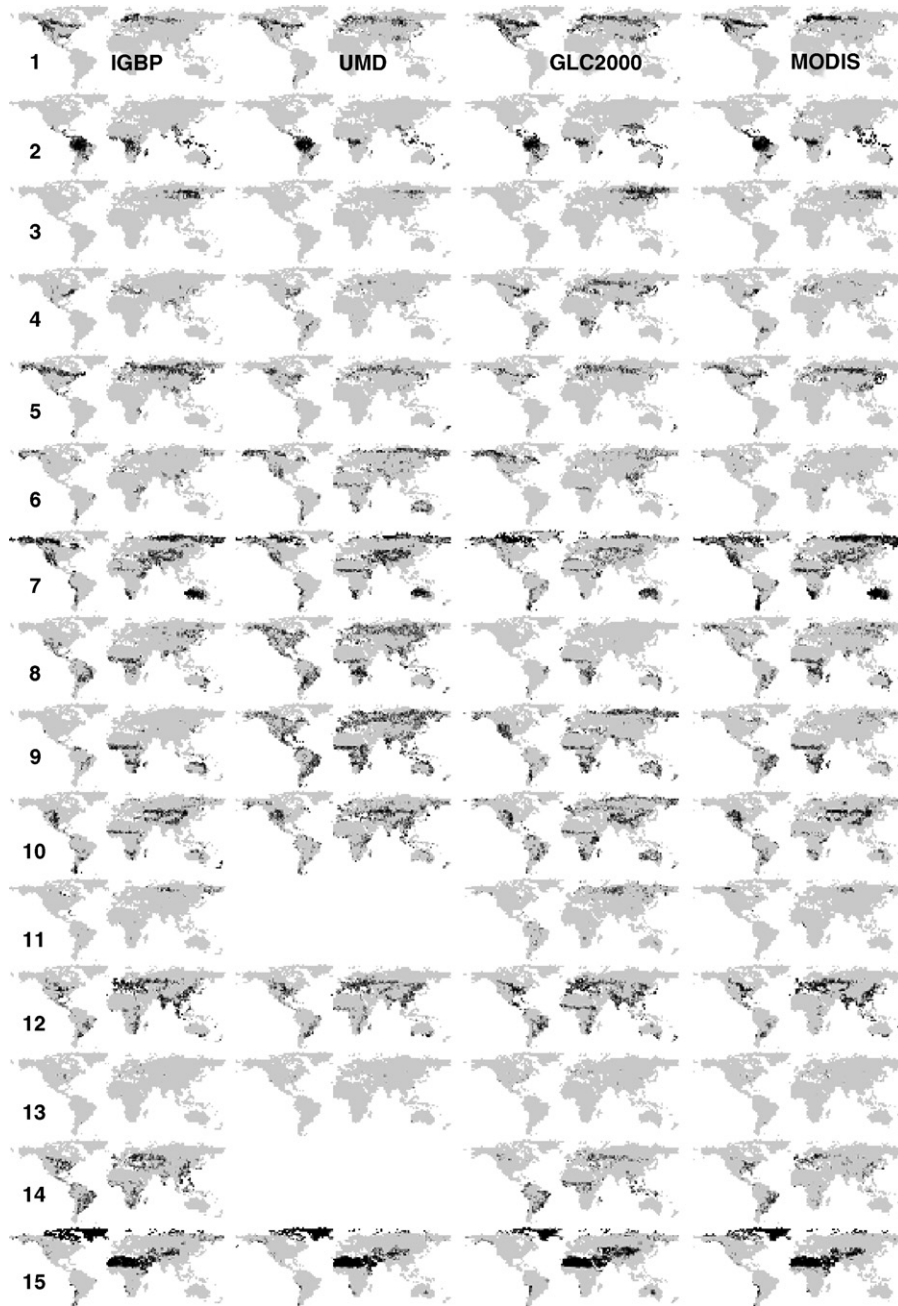


Fig. 2. Comparison of the 15 (ascending order) IGBP classes for the IGBP, UMD, GLC2000 and MODIS land cover datasets (1, evergreen needleleaf forest; 2, evergreen broadleaf forest; 3, deciduous needleleaf forest; 4, deciduous broadleaf forest; 5, mixed forest; 6, closed shrublands; 7, open shrublands; 8, woody savannas; 9, savannas; 10, grasslands; 11, permanent wetlands; 12, croplands; 13, urban and built-up; 14, cropland/natural vegetation mosaic; 15, snow and ice barren or sparsely vegetated).

while disagreement occurred mostly along edges and transition zones. Often in the global comparison, areas of full agreement are adjacent to areas of high agreement (where only three datasets agree), and areas of no agreement are adjacent to areas of low agreement (when only two datasets agree). It appears

that in many cases, major patterns of land cover are similarly identified among the varying datasets. One explanation is the application of different thresholds for separating various classes [Latifovic and Olthof \(2004\)](#). One of the key differences among the land cover datasets are the use of thresholds for separating

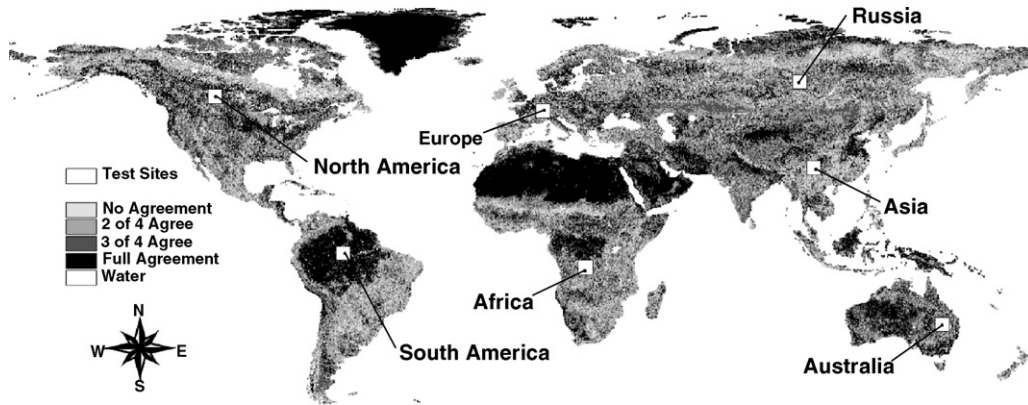


Fig. 3. Global levels of agreement among the IGBP, UMD, GLC2000 and MODIS land cover datasets, compared according to the IGBP classification. In addition, seven test sites are identified for continental comparison at the regional level.

the classes. Forest classes for example are distinguished in the IGBP dataset with a height > 2 m, in UMD with a height > 5 m and in GLC2000 with a height > 3 m.

In addition to global studies, global land cover datasets are often used for analyses at the continental, country and regional levels regardless of whether or not they were intended for this purpose. Therefore, it is of importance to have an awareness of the possible differences between the datasets at these scales, as differences will arise between regions based on many factors. In an effort to better describe and understand the levels of agreement between the datasets, seven test sites were identified across the globe for comparison. The European test site was selected in particular for closer observation (Fig. 4).

As expected, agreement within the European test site among the classes is poorer than at the global level, with

practically all classes having unbalanced proportions of agreement. It is however very difficult to expect that in such a heterogeneous and anthropogenic landscape as Central Europe that comparisons of a 1 km global land cover dataset will be in full agreement. This emphasises the importance of looking at smaller areas within a global dataset, as many classes are not represented by some of the datasets at this scale, causing disagreement. Specifically, the evergreen broadleaf class appears in the MODIS dataset, although representing a very small area. This appears to be an error in the classification algorithm. Additionally, areas of deciduous needleleaf, closed shrublands, savannas and grasslands have poor agreement across the datasets. When using these global datasets for regional studies the user should make use of more than one dataset and review the datasets prior to use.

Maps of agreement were created for four of the seven test sites (Fig. 5), and the levels of agreement were calculated for all seven test sites (Table 3). The South American test site provided high levels of agreement (82% full agreement) due to the dominance of evergreen broadleaf forests, while the Asian test site provided very low agreement (4% full agreement), due in part to disagreement among forest and anthropogenic classes between the datasets.

In order to compare the heterogeneity of the four products, we calculated the total number of patches in the European test site for each of the land cover datasets (Table 4). As the total area of each dataset is equal, this provides a comparable measure of the fragmentation of each of the datasets for this test site. Based on the number of patches, the IGBP dataset (11,926) is the most homogenous dataset, while the MODIS dataset (31,385) is the most heterogeneous dataset. This adds

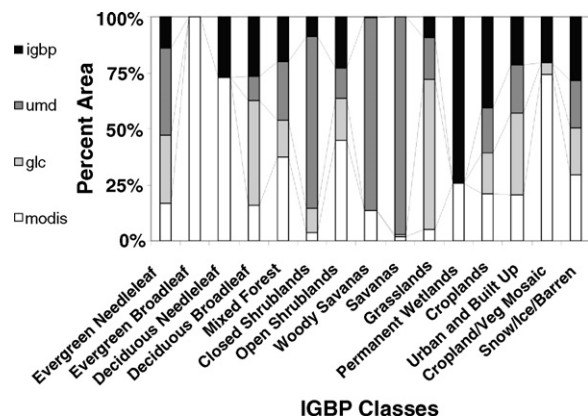


Fig. 4. The percent area comparison of the IGBP, UMD, GLC2000 and MODIS land cover datasets for the European test site, classified according to the IGBP classification.

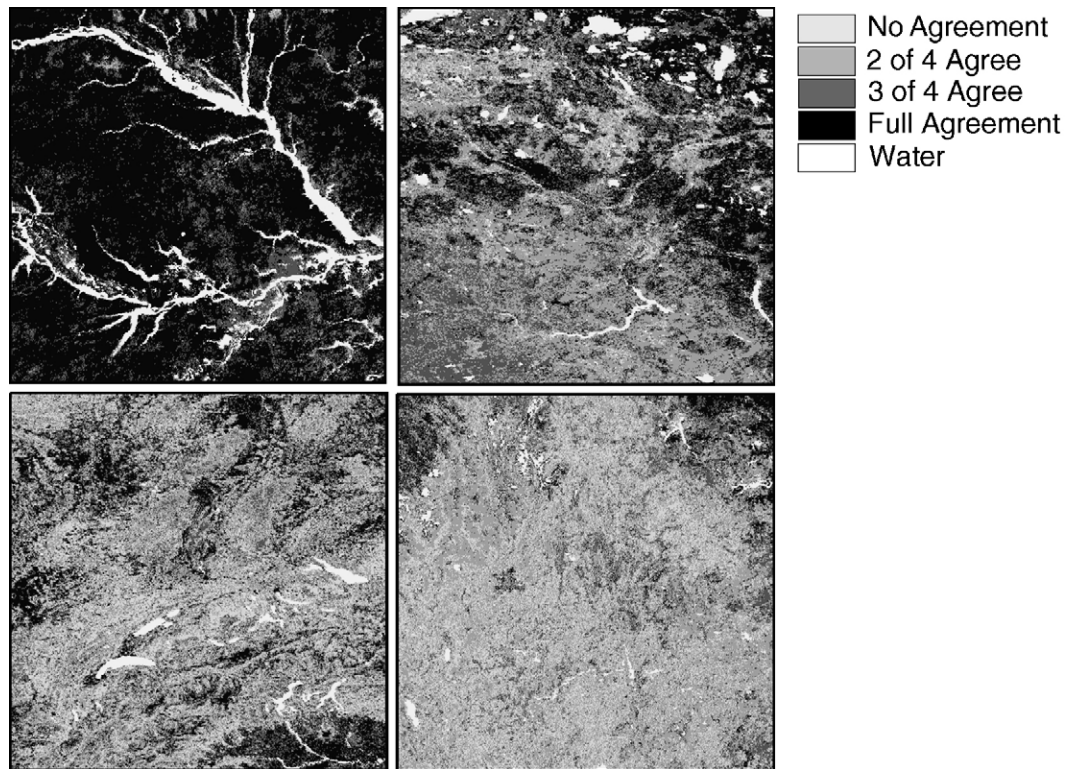


Fig. 5. Levels of agreement among the IGBP, UMD, GLC2000 and MODIS land cover datasets over the South American (upper left), North American (upper right), European (lower left) and Asian (lower right) test sites, classified according to the IGBP classification.

Table 3

Percent agreement of the four global land cover datasets (IGBP, UMD, GLC2000 and MODIS) across the seven (5×5 degree) test sites in decreasing order of full agreement

Test sites	No agreement	2 of 4 agree	3 of 4 agree	Full agreement	Longitude (center)	Latitude (center)
South America	0	2	16	82	-62.5	-2.5
North America	4	37	34	25	-107.5	52.5
Europe	19	42	24	15	7.5	47.5
Africa	10	49	30	11	22.5	-7.5
Australia	8	49	33	10	147.5	-27.5
Russia	5	49	37	9	97.5	57.5
Asia	26	55	15	4	102.5	27.5

Table 4

The number of patches (contiguous areas of similar land cover classes) for each of the four land cover datasets within the European test site

Land cover dataset	No. of patches
IGBP	11,926
GLC2000	15,289
UMD	28,134
MODIS	31,385

another level of complexity when comparing these datasets and analyzing the differences.

5. Conclusions

Following on previous studies comparing two global land cover datasets (e.g. Hansen and Reed, 2000; Giri et al., 2005) this study compares four (IGBP, UMD, GLC2000 and MODIS) freely downloadable satellite-based global land cover datasets at the global level. All land cover datasets were created using different

classification methods, but with the same purpose of providing accurate land cover information for environmental modellers and policy makers (Latifovic and Olthof, 2004). The datasets compared in this study all have inherent strengths and weaknesses. Areas of disagreement among the compared datasets could be true disagreement, or could simply be due to differences in their original classification, the assignment to the IGBP classification, the sensor, temporal period, etc. It is also important to remember that pixels with 100% agreement could be entirely wrong (Hansen and Reed, 2000).

Aside from the input variables, algorithms and classification schemes, a number of external factors create variability which makes it difficult to clearly compare the methodologies used to create global land cover, including reliance on ancillary data sources, data artefacts such as clouds, data gaps, etc. (Hansen and Reed, 2000). The relationship between land cover and temporal-spectral data is frequently ambiguous; the phenological dynamics of the Earth's land cover are complex, with similar land cover types having quite variable seasonal properties; and land cover spectral and temporal characteristics in many parts of the world are affected by atmospheric contaminants (Loveland et al., 2000).

Remote sensing has been advocated as a means of producing more consistent, repeatable and unbiased products than were previously possible with traditional ground-based methods. This comparison shows varying levels of agreement among the four global land cover datasets and suggests that users exercise caution when using any one particular product. In a study on global carbon sequestration by Benitez et al. (2004), choice of land cover dataset influenced the model results by as much as 45%. Analysis using global land cover products should utilise several of these products in order to show the magnitude of possible differences. This becomes even more crucial if these datasets are being used for analysis at the continental or regional scales. Aggregating original classes will improve agreement between the datasets; however valuable spatial information is lost in this process. For some applications, disagreement will have significant consequences, while for others, where only a coarse description of land surface is required, it may be of lesser consequence (DeFries and Los, 1999). Users who need a certain level of detail should examine the data themselves in order to judge which dataset is most useful for their purposes (Hansen and Reed, 2000).

At present there is no internationally accepted land cover classification system in use (GLCN, 2005).

Current remotely sensed land cover maps can only set a framework for global change analysis and will only help us to a limited extent in understanding the ongoing global change process. By comparing different products as they become available we gain insights into better methodologies for mapping and utilising land cover. Experience thus far points to an urgent need for harmonisation between the different satellite-based land cover products (FAO, 2002a), specifically an intensification of the process of harmonizing land cover related definitions used by different stakeholders (FAO, 2002b). It would be beneficial if future datasets provided linkages to both a common standard (i.e. FAO LCCS) and previous classifications (i.e. IGBP).

This study utilised the IGBP land cover classification legend to compare the datasets. It is likely that with further study of the various IGBP classes assigned to each of the datasets, improvements to the agreement level could be made. In the conversion to a common legend, classification accuracy may be reduced due to the transferability of classes from one legend to another (Latifovic and Olthof, 2004). Use of the IGBP legend may slightly favour the IGBP, UMD and MODIS products in such a comparison. A fairer comparison involving the GLC2000 might be to use the regional land cover datasets and assign them directly to a common legend (i.e. IGBP), thereby better incorporating the regional differences and knowledge and perhaps having more flexibility in class assignment before comparison. The use of fuzzy logic (Fritz and See, 2005) and prior knowledge offers a solution to improve agreement between the datasets. One solution might be the creation of a composite “best-of” global 1km land cover dataset which includes all existing products, along with other related datasets (e.g. climate, elevation, etc.)—essentially a land cover probability map that could be continuously updated and improved.

Acknowledgements

The authors would like to thank three reviewers for helpful comments.

References

- Benitez, P., McCallum, I., Obersteiner, M., Yamagata, Y., 2004. Global Supply for Carbon Sequestration: Identifying Least-Cost Afforestation Sites Under Country Risk Considerations. IIASA, IR-04-022, Laxenburg, Austria, 22 pp.
- DeFries, R.S., Los, S.O., 1999. Implications of land-cover misclassification for parameter estimates in global land-surface models: an example from the Simple Biosphere Model (SiB2). *Photogramm. Eng. Rem. Sens.* 65, 1083–1088.

- Defries, R.S., Townshend, J.R.G., 1994. NDVI-derived land cover classifications at a global scale. *Int. J. Rem. Sens.* 15 (17), 3567–3586.
- Di Gregorio, A., Jansen, L.J.M., 2000. Land Cover Classification System (LCCS): Classification Concepts and User Manual. FAO, Rome, Italy, 179 pp.
- FAO, 2002a. Proceedings of the FAO/UNEP Expert Consultation on Strategies for Global Land Cover Mapping and Monitoring. FAO, Rome, Italy, 38 pp.
- FAO, 2002b. Expert Meeting on Harmonizing Forest-Related Definitions for Use by Various Stakeholders, 23–25 January. FAO, Rome, Italy, 193 pp.
- Footy, G.M., 2002. Status of land cover classification accuracy assessment. *Rem. Sens. Environ.* 80, 185–201.
- Fritz, S., Bartholomé, E., Belward, A., Hartley, A., Stibig, H.J., Eva, H., Mayaux, P., Bartalev, S., Latifovic, R., Kolmert, S., Roy, P.S., Agrawal, S., Bingfang, W., Wenting, X., Ledwith, M., Pekel, J.F., Giri, C., Múcher, S., de Badts, E., Tateishi, R., Champeaux, J.L., Defourny, P., 2003. Harmonization, Mosaicing and Production of the Global Land Cover 2000 Database (Beta Version). European Commission, Joint Research Centre, Ispra, Italy, 41 pp.
- Fritz, S., See, L., 2005. Comparison of land cover maps using fuzzy agreement. *Int. J. Geogr. Sci.* 19 (7), 787–807.
- Giri, C., Zhu, Z., Reed, B., 2005. A Comparative Analysis of the Global Land Cover 2000 and MODIS Land Cover Data Sets. *Rem. Sens. Environ.* 94, 123–132.
- GLCN, 2005. Global Land Cover Network—Land Cover Topic Centre, September. Website: <http://www.glcnc-lcss.org>.
- GOFC-GOLD, 2004. Land Cover and Change: Newsletter of the GOFC-GOLD Land Cover Project Office. Newsletter 4, 8 pp.
- Hansen, M.C., Defries, R.S., Townsend, R.G., Sohlberg, R., 2000. Global land cover classification at 1km spatial resolution using a classification tree approach. *Int. J. Rem. Sens.* 21 (6/7), 1331–1364.
- Hansen, M.C., Reed, B., 2000. A comparison of the IGBP DISCover and University of Maryland 1km global land cover products. *Int. J. Rem. Sens.* 21, 1365–1373.
- Henderson-Sellers, A., Wilson, M.F., Thomas, G., Dickinson, R.E., 1986. Current Global Land-Surface Data Sets for Use in Climate-Related Studies. Report NCAR/TN. 272. National Center for Atmospheric Research, Boulder CO., USA.
- Latifovic, R., Olthof, I., 2004. Accuracy assessment using sub-pixel fractional error matrices of global land cover products derived from satellite data. *Rem. Sens. Environ.* 90, 153–165.
- Latifovic, R., Zhu, Z.L., Cihlar, J., Giri, C., Olthof, I., 2004. Land cover mapping of North and Central America—Global Land Cover 2000. *Rem. Sens. Environ.* 89, 116–127.
- Loveland, T.R., Reed, B.C., Brown, J.F., Ohlen, D.O., Zhu, Z., Yang, L., Merchant, J.W., 2000. Development of a global land cover characteristics database and IGBP DISCover from 1 km AVHRR data. *Int. J. Rem. Sens.* 21 (6/7), 1303–1330.
- Mattews, E., 1983. Global vegetation and land-use: new-high resolution databases for climate studies. *J. Clim. Appl. Meteorol.* 22, 474–487.
- McGarigal, K., Cushman, S.A., Neel, M.C., Ene, E., 2002. FRAGSTATS: Spatial Pattern Analysis Program for Categorical Maps. Computer Software Program Produced by the Authors at the University of Massachusetts, Amherst. Website: <http://www.umass.edu/landeco/research/fragstats/fragstats.html>.
- Mitchell, R.B., 2003. International environmental agreements: a survey of their features, formation and effects. *Ann. Rev. Environ. Resour.* 28, 429–461.
- MODIS, 2003. Validation of the Consistent-year V003 MODIS Land Cover Product, 9 pp. Website: <http://geography.bu.edu/landcover/userguide/c/consistent.pdf>.
- Scepan, J., 1999. Thematic validation of high-resolution Global Land-Cover Data Sets. *Photogramm. Eng. Rem. Sens.* 65 (9), 1051–1060.
- Stowe, L.L., Carey, R.M., Pelegrino, P.P., 1992. Monitoring the Mt. Pinatubo aerosol layer with NOAA-11 AVHRR data. *Geophys. Res. Lett.* 19, 159–162.
- Strahler, A., Muchoney, D., Borak, J., Friedl, M., Gopal, S., Lambin, E., Moody, A., 1999. MODIS Land Cover Product: Algorithm Theoretical Basis Document, Version 5.0. Boston University, Boston, MA, USA, 72 pp.
- Townsend, J., Justice, C., Li, W., Gurney, C., McManus, J., 1991. Global land cover classification by remote sensing: present capabilities and future possibilities. *Rem. Sens. Environ.* 35, 243–255.
- WRI, 2000. World Resources 2000–2001—People and Ecosystems: The Fraying Web of Life. WRI, Washington, DC, USA, 389 pp.



Comparison of four global FAPAR datasets over Northern Eurasia for the year 2000

Ian McCallum^{a,*}, Wolfgang Wagner^b, Christiane Schmullius^c, Anatoly Shvidenko^a, Michael Obersteiner^a, Steffen Fritz^a, Sten Nilsson^a

^a International Institute for Applied Systems Analysis, Schlossplatz 1, A-2361, Laxenburg, Austria

^b Institute of Photogrammetry and Remote Sensing, Technical University, Gußhausstraße 27 - 29, 1040 Vienna, Austria

^c Institute of Geography, Friedrich-Schiller-University, Grietgasse 6, 07743 Jena, Germany

ARTICLE INFO

Article history:

Received 30 December 2008

Received in revised form 7 December 2009

Accepted 12 December 2009

Keywords:

Fraction of Absorbed Photosynthetically Active Radiation (FAPAR)

Northern Eurasia

MODIS

CYCLOPES

JRC

GLOBCARBON

ABSTRACT

The Fraction of Absorbed Photosynthetically Active Radiation (FAPAR) has been identified as one of several key satellite-derived biophysical datasets. With multiple global FAPAR datasets now available and a lack of in-situ measurements and comparison studies in the far north, this study attempts to provide the reader with an indication of the performance of four global FAPAR datasets (MODIS, CYCLOPES, JRC and GLOBCARBON) over Northern Eurasia in the year 2000 via comparison. Within the year 2000 growing season, both the MODIS and CYCLOPES datasets recorded on average similar but substantially higher values than the JRC and GLOBCARBON datasets. Among three of the four datasets, a high level of agreement in deciduous broadleaf forests and croplands was observed. Largest disagreement occurred among needleleaf forests and grassland/shrubland. Potential reasons for discrepancies among the datasets include different retrieval methods, use of LAI and land cover, snow effects and others. Findings from this study and other published results suggest that overall, JRC best captures FAPAR over northern Eurasia in the year 2000. However, when considering individual landcover types, any one or more of the four products may be suitable. There exists a real need for more in-situ measurements in this region – the lack of such measurements makes evaluation extremely difficult. It appears that areas north of 60° urgently require further investigation.

© 2010 Elsevier Inc. All rights reserved.

1. Introduction

In recent years the scientific community has witnessed a significant increase in the availability of global satellite-derived biophysical datasets. Sensors such as AVHRR (launched in 1981), VEGETATION (launched in 1998) and MODIS (launched in 1999) have been contributing to long-term records of spectral reflectance, allowing for the continual creation of products and the refinement and reprocessing of algorithms. Examples of global biophysical satellite-derived products now available from multiple sources include the Normalised Difference Vegetation Index (NDVI), Leaf Area Index (LAI) and the Fraction of Absorbed Photosynthetically Active Radiation (FAPAR). The Global Climate Observing System (GCOS, 2006) has identified FAPAR as one of several key terrestrial products to be derived from satellite observations, and it is the focus of this paper.

FAPAR is generally defined as the fraction of Photosynthetically Active Radiation (PAR) absorbed by vegetation, where PAR is the solar radiation reaching the vegetation in the wavelength region 0.4–0.7 μm (FAO, 2007). It excludes the fraction of incident PAR reflected from the canopy and the fraction absorbed by the soil surface, but includes the portion of PAR which is reflected by the soil/understorey

and absorbed by the canopy on its return to space (CCRS, 2007). FAPAR is thus a physically-based, quantitative variable with a clear, unambiguous meaning, directly related to the maintenance of life systems on the planet (GCOS, 2006). FAPAR acts as an integrated indicator of the status and health of the plant canopy, and can be reasonably well derived by remote sensing techniques (Gobron et al., 2002). FAPAR is difficult to measure directly, but is inferred from models describing the transfer of solar radiation in plant canopies, using remote sensing observations as constraints (Gobron & Verstraete 2008).

FAPAR is useful in a number of applications, ranging from agriculture (e.g. crop-yield forecasting) and forestry to environmental stress and sustainability monitoring; it has potential to be used in the areas of food security, land degradation (e.g. desertification), and land cover mapping (GCOS, 2006) and is a key state variable in ecosystem productivity models and in global models of climate, hydrology, biogeochemistry and ecology (Myneni, et al., 2003). In particular, FAPAR plays a key role in the family of diagnostic terrestrial carbon models known as Production Efficiency Models (PEMs) used to calculate Gross and Net Primary Productivity (GPP/NPP) (e.g. Prince & Goward, 1995; Veroustraete et al., 2002; Running et al., 2004; Potter et al., 2005; and others). FAPAR is often the only satellite derived variable used in PEMs and as such it provides the only link between ecosystem function and structure in these models (Asner et al., 1998). Absolute values, seasonal trend and spatial pattern are all important features of any FAPAR dataset.

* Corresponding author. IIASA, A-2361, Laxenburg, Austria.

E-mail address: mccallum@iiasa.ac.at (I. McCallum).

With multiple global FAPAR datasets now available from several initiatives (including those analysed in this study from: Boston University (MODIS); MEDIAS-France (CYCLOPES); Joint Research Center (JRC) and the European Space Agency (GLOBCARBON)), it is becoming increasingly important to analyze these datasets in terms of compatibility, standards, convergence, etc. The few comparison studies performed to date have indicated large differences between the products (GCOS, 2006).

Unfortunately, existing in-situ FAPAR measurements appear limited (FAO, 2007). Both Yang et al. (2006) and Weiss et al. (2007) found that most of the field data are limited to LAI, with only a few containing FAPAR measurements. Regional examples of FAPAR evaluation exist (Fensholt et al., 2004; Steinberg et al., 2006), however there is, in particular, a lack of such information across Northern Eurasia – a unique region that presents many challenges for monitoring. The projects EUROSIBERIAN CARBONFLUX and TCOS-Siberia have provided some data (Heimann, 2002), but remaining gaps are large. Initiatives such as VALERI (<http://www.avignon.inra.fr/valeri/>) are attempting to address this issue at the global level. In the meantime, efforts such as comparison between products as well as evaluation of their temporal and spatial consistency (Weiss et al., 2007), may prove useful. This study attempts to provide the reader with an indication of the performance of four global FAPAR datasets over Northern Eurasia in the year 2000 through quantitative comparison and analysis.

2. Study region

The study region was chosen to approximate the extent of Northern Eurasia, with coordinates 50°N, 30°E; and 70°N, 180°E. The boreal forests of Russia comprise almost one fourth of the world's forest cover, making Russian forests a unique natural phenomenon at the global scale (Shvidenko et al., 2007). Their large land area undergoes great annual changes in albedo, productivity, and fresh water as seasonal temperatures swing well above and below 0 °C – thus they are active contributors to the major cycles (energy, biogeochemical and hydrological) that regulate Earth's environment (Apps et al., 2006). This region in particular is home to the world's only large homogeneous tract of deciduous needleleaf or Larch (*Larix gmelinii* and *Larix kajaneri*) forests. Additionally, large regions lie in various stages of permafrost and the area is prone to catastrophic disturbances including fire (Goldammer 1996; Kajii et al., 2002; Balzter et al., 2005), drastically altering the landscape and releasing large amounts of greenhouse gases into the atmosphere.

Pronounced warming in high latitudes has been occurring for the past several decades and has consequences for carbon storage of northern ecosystems (Myneni et al., 2001; Nemani, et al., 2003; Balshi, et al., 2007). However, Lapenis et al. (2005) suggest a possible overestimation by remote sensing methods of the carbon sink for living biomass across this region. Existing estimates of NPP for the region vary about three fold (Shvidenko et al., 2008). Biophysical variables such as FAPAR which can be used to infer productivity are therefore important for monitoring such large regions. In particular, field measurements are difficult to obtain over such a large region and satellite-based methods often provide the only alternative.

3. Methodology

Initially, four global FAPAR datasets (MODIS, CYCLOPES, JRC, and GLOBCARBON) were obtained (see Table 1). After reviewing all available products, the year 2000 with a monthly time-step and 0.25° resolution was chosen for comparison. Some products have a resolution as fine as 1-km and an 8-day frequency, however owing to both the size of the region and the lack of finer information from some datasets, the 0.25° and monthly time-step was deemed appropriate for this analysis. Datasets with resolution finer than 0.25° were aggregated to 0.25°, based on the mean value of all cells

Table 1

Description of global FAPAR datasets acquired for this study.

Project/Provider	Sensor	Repeat	Size ^a	Ver.	URL
Boston Uni.	MODIS	Month	0.25°	5.0	ftp://primavera.bu.edu
CYCLOPES	VGT	10Day	1 km ²	3.1	postel.mediasfrance.org
JRC	SeaWifs	Month	0.25°	2.0	fapar.jrc.it
GLOBCARBON	VGT	Day	0.25°	3.1	geofront.vgt.vito.be

^a Approximate grid-cell size of the original reflectance data 1 km².

falling within the resultant 0.25° cell. Datasets with a time-step more frequent than monthly were aggregated into monthly values by taking the mean of all values recorded within the month. In the case of GLOBCARBON, a quality flag was used to assign the monthly mean.

Additionally, to aid in comparison of the various products and to better identify where differences related to land cover are occurring, we made use of the Global Land Cover 2000 product (GLC2000) (Bartalev et al., 2003). This product was specifically created for Russia by regional experts and should, therefore, adequately represent the distribution of vegetation types (see Fig. 1). We aggregated the 23 GLC2000 classes into the following six classes to obtain the basic land cover types and simplify the analysis (percent vegetated area represented by each aggregated class): deciduous broadleaf forest (3%); evergreen needleleaf forest (14%); deciduous needleleaf forest (33%); mixed forest (14%); shrubs/grasses (26%); and cropland (10%). This distribution is similar to the areal statistics in the land and forest account of Russia (MNRFF, 2003).

Owing to the lack of in-situ data, we focus in this study on indirect evaluation in order to examine the various global products and their applicability to Northern Eurasia. Techniques applied include measures of temporal and spatial consistency, including spatial correlation and root mean square error (RMSE). An overview of the four FAPAR products analyzed in this study is provided in Table 2 and further explanation follows.

3.1. Boston University (MODIS)

Boston University Climate and Vegetation Group provide FAPAR mosaics utilising the Moderate Resolution Imaging Radiometer (MODIS). FAPAR is defined as the instantaneous FAPAR at the time of satellite overpass (Weiss et al., 2007) using direct and diffuse incoming radiation (Gobron & Verstraete 2008). The operational MODIS algorithm ingests up to seven atmosphere-corrected surface spectral Bi-directional Reflectance Factors (BRFs) and their uncertainties and outputs the most probable values per grid-cell of LAI and FAPAR (Myneni et al., 2002). LAI is required as input to the MODIS FAPAR algorithm (Knyazikhin et al., 1998).

A look-up-table method is used to achieve inversion of the three-dimensional radiative transfer problem (Myneni et al., 2002). The retrieval technique compares observed and modelled BRFs for a suite of canopy structures and soil patterns that represent an expected range of typical conditions for a given biome type (Yang et al., 2006). MODIS FAPAR relies on the MOD12 biome map (8 global biomes). The products are produced at 1 km spatial resolution (daily) and composited over an 8 day period based on the maximum FAPAR (Yang et al., 2006). When this method fails to localize a solution, a back-up method based on empirical relations between the NDVI and LAI/FAPAR is utilized (Myneni et al., 2002). The success rate of the main radiative transfer algorithm in Collection 4 was 67% with the quality of retrievals from the back-up NDVI method noted as poor (Yang et al., 2006).

3.2. CYCLOPES

The Carbon Cycle and Change in Land Observational Products from an Ensemble of Satellites (CYCLOPES) project relies on the Vegetation (VGT)

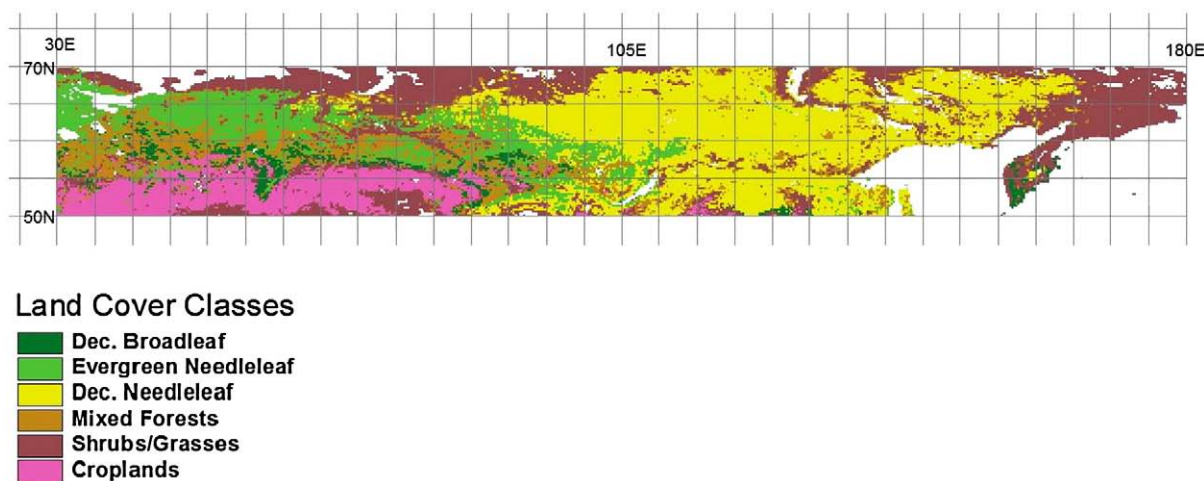


Fig. 1. Aggregated GLC2000 land cover dataset showing the six classes used within the study region.

sensor. The FAPAR CYCLOPES products correspond to a black-sky (no diffuse illumination) at 10:00 (instantaneous) local solar time absorption of visible radiation by the green vegetation elements. Four steps are necessary to derive the FAPAR, namely, cloud screening (utilizing the GLC2000 land cover), atmospheric correction, generation of BRFs and temporal compositing, followed by the algorithm itself (Baret et al., 2007). The biophysical algorithm is based on radiative transfer model inversion. The CYCLOPES algorithm is designed to be applied to any surface type conversely to the MODIS or GLOBCARBON products for which the algorithm is tuned for each biome type. Reflectance values of soils were simulated using five typical soil reflectance spectra, multiplied by a brightness coefficient (Baret et al., 2007).

3.3. Joint Research Center (JRC)

The Joint Research Center (Global Environmental Monitoring Unit) produces an FAPAR product utilising (among other sensors) the Sea-viewing Wide Field-of-view Sensor (SeaWiFS). FAPAR is defined here as 'green' instantaneous FAPAR under direct illumination (Gobron & Verstraete 2008). The generic FAPAR algorithm implements a two-step procedure where the spectral BRFs measured in the red and near-infrared bands are, first, rectified in order to ensure their optimal decontamination from atmospheric and angular effects and, second, combined together to estimate the instantaneous FAPAR value at the time of acquisition (Gobron et al., 2006). The JRC dataset uses the median value (not the maximum composite) in generating the statistics. Illumination conditions adopted in the algorithm training set do not significantly exceed 50° in sun zenith angle (Gobron et al., 2006). Similar to CYCLOPES, the JRC algorithm is not biome specific thus requiring no land cover product.

3.4. GLOBCARBON

The European Space Agency coordinates the GLOBCARBON project, utilising among other datasets, VGT. LAI and FAPAR are derived using a constrained model-based look-up table established for different vegetation types based on GLC2000 land cover (Plummer et al., 2007). FAPAR is derived from the smoothed LAI values using a modified Beer-Bouguer law. The algorithm calculates FAPAR as the difference between the total Top Of Canopy (TOC) PAR absorbance minus the PAR absorbance of soil. Only instantaneous FAPAR at the view and illumination angle is produced (Plummer et al., 2007). The TOC PAR absorbance is estimated by the red surface reflectance while the PAR absorbance of soil is calculated from the single scattering term reflected by the soil and passing through the canopy without suffering any further scattering. The soil reflectance is taken from a look-up table according to a soil map. The transmission through the vegetation canopy is assumed an exponential function of the effective LAI, also depending on the solar zenith angle. For soil slope higher than 5° both the soil slope and its aspect, as provided by a global Digital Elevation Model (DEM), are taken into account for the transmission exponential term calculation (Geosuccess, 2007).

4. Results and discussion

To date only a few studies have attempted to compare results between available global FAPAR datasets (e.g. Gobron, et al., 2007; Weiss et al., 2007), even fewer over Northern Eurasia (e.g. Pinty et al., 2008). Here we have compared the results of four available global datasets over northern Eurasia, using the latest versions of these products available at the time of analysis.

Table 2

Description of key input, retrieval and output methods employed by the four FAPAR products. Table based on Gobron and Verstraete (2008).

FAPAR dataset	Input reflectance	Input data	Retrieval method	Output
MODIS	TOC surface reflectance in 7 spectral bands	Land: MOD12 (8 biomes), LAI	Inversion of 3D model versus land cover (NDVI backup)	Instantaneous green FAPAR direct and diffuse radiation
CYCLOPES	TOC surface reflectance in blue, red, NIR and SWIR	Cloud screening: GLC2000	Neural network trained with radiative transfer models	Instantaneous green FAPAR (at 10:00 solar local time) direct radiation
JRC	TOA BRFs in blue, red and NIR	No <i>a priori</i> data	Optimization formulae based on radiative transfer models	Instantaneous green FAPAR direct radiation
GLOBCARBON	TOC surface reflectance in red, NIR and SWIR	Land:GLC2000, Soil, DEM, LAI	Parametric relation with LAI as function of land cover	Instantaneous green FAPAR direct radiation

TOC Top of Canopy; TOA Top of Atmosphere; NIR Near Infrared; SWIR Short-wave infrared.

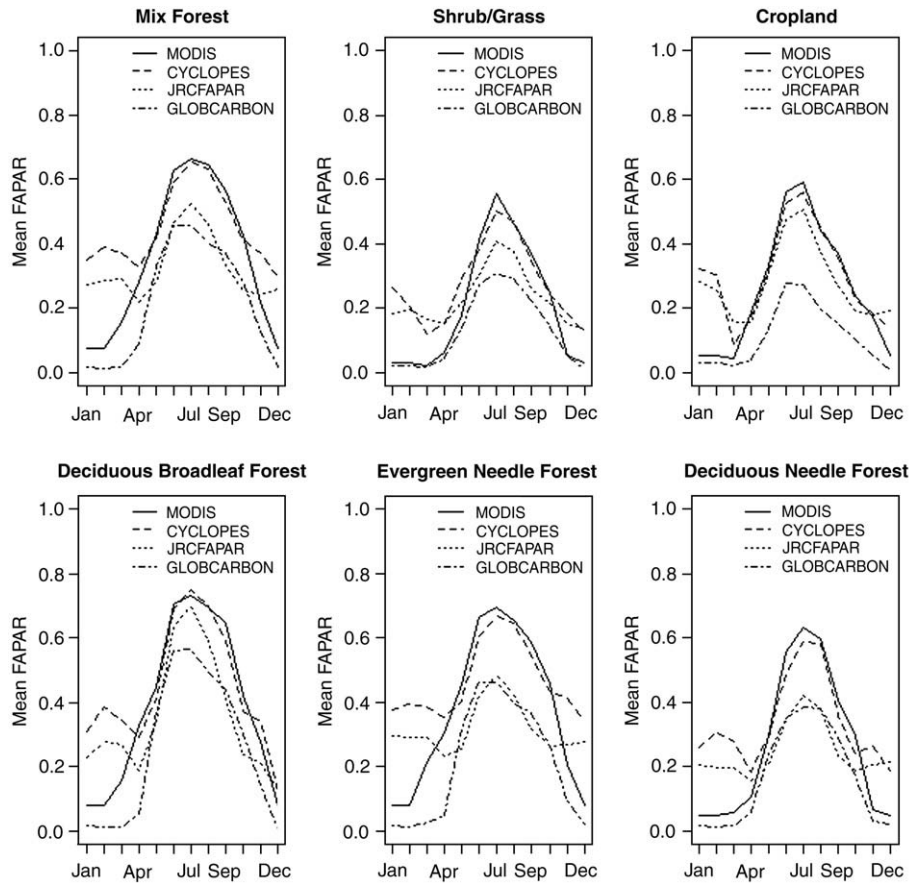


Fig. 2. Comparison of monthly mean values from four global FAPAR datasets over northern Eurasia for the year 2000, by land cover type. Datasets from MODIS for January and February are not available, thus values for December were applied.

4.1. Seasonal trend and absolute values

The seasonal trend of the four global FAPAR datasets monthly mean values over the entire study region by land cover type in the year 2000 is displayed in Fig. 2. For deciduous broadleaf, evergreen needleleaf and mixed forests, MODIS begins to absorb FAPAR a full 1–2 months ahead of other products. The peak in mean FAPAR values across Northern Eurasia for all datasets and land cover types occurs in July. However, the MODIS (as in previous studies) and CYCLOPES datasets have substantially higher growing season mean values compared to the JRC and GLOBCARBON datasets. Highest agreement occurs during green-up (May) and senescence (October), however the rates of change are also largest in these two periods. Large variation occurs during the winter months, with values ranging from 0.0 to 0.4. Winter values in evergreen forests generally remain higher than deciduous values, grassland/shrublands and croplands, as expected. CYCLOPES tends to record the highest values in winter, while MODIS and GLOBCARBON the lowest.

Across all six land cover classes, FAPAR mean values are highest in the forest classes, with the highest values occurring in the deciduous broadleaf class. This is particularly significant as the level of agreement among three of the datasets is also high (GLOBCARBON is significantly lower), although the deciduous broadleaf forest class represents only 3% of the vegetative area. Additionally, three of the datasets agree in croplands, again pointing to potential difficulties in the remaining dataset (GLOBCARBON) to record FAPAR in croplands. This implies that the datasets are in fact utilising a similar definition of FAPAR, and that disagreement among the remaining classes is due to algorithm and/or sensor related differences. In the remaining classes the gap between the datasets is often large. In needleleaved

and mixed forests, MODIS and CYCLOPES are in close agreement, but consistently higher than JRC and GLOBCARBON (also in close agreement).

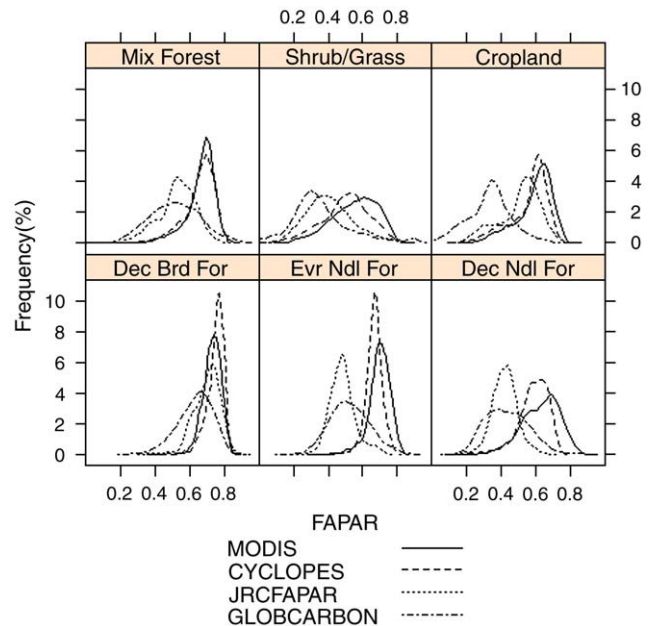


Fig. 3. Frequency histograms of four global FAPAR datasets for July 2000, per land cover class (from left to right, starting lower-left: 1: deciduous broadleaf forest; 2: evergreen needleleaf forest; 3: deciduous needleleaf forest; 4: mixed forest; 5: shrub/grass; and 6: croplands).

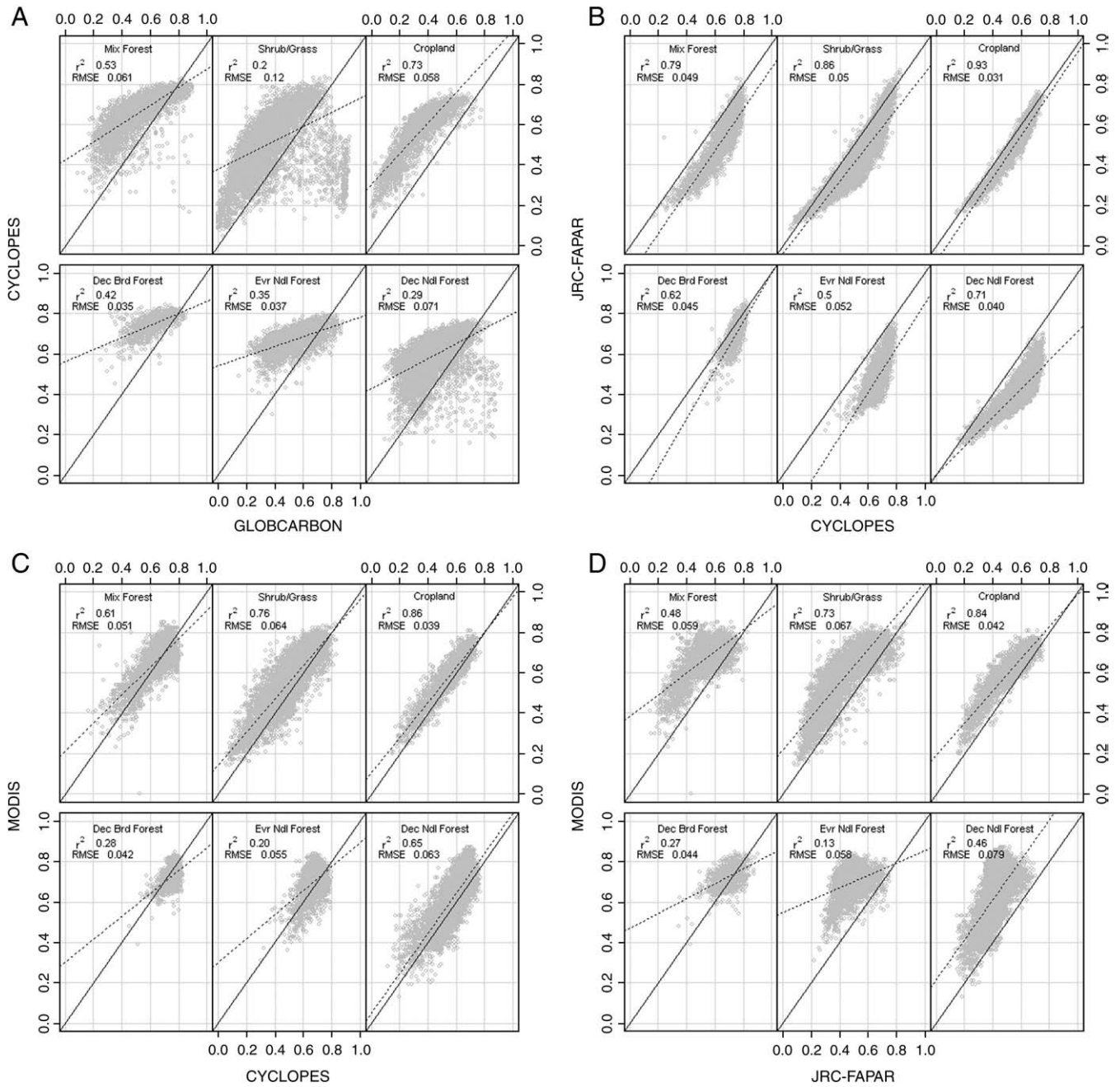


Fig. 4. A comparison of four global FAPAR datasets over northern Eurasia for July, 2000 by major land cover. Dashed line represents linear fit.

Frequency histograms of FAPAR values for each of the four datasets are presented by land cover type in Fig. 3 for July 2000. Some of the poorest agreement among the datasets occurs in deciduous needleleaf forests and shrubland/grassland. In the case of Northern Eurasia, this is significant as deciduous needleleaf forests and shrubland/grassland represent a large portion (33% and 26% respectively) of the total vegetated area. The shrubland/grassland class generates substantial disagreement among all four products as it includes vegetation spread over a wide latitudinal range, making this class difficult to compare.

4.2. Spatial comparison

Scatterplots of FAPAR values comparing the datasets were made by land cover type for July 2000 (Fig. 4). Reassuring among all datasets (excluding GLOBCARBON) is the high level of correlation among croplands, accompanied by a high r^2 value. This would again suggest

that the datasets are comparable, and disagreement in other classes is potentially a result of error. Not obvious from previous figures, CYCLOPES and JRC are highly correlated across all land cover types, although JRC values are on average lower (highest correlation among all datasets in croplands 0.93 r^2). The GLOBCARBON product appears to detect a wide range of values within the shrubland/grassland and deciduous needleleaf forest classes in particular.

Fig. 5 displays the spatial pattern of absolute FAPAR values across the region for each of the datasets in July, 2000. General spatial patterns among the datasets appear similar. Absolute FAPAR values are however different among the datasets, and on average in decreasing order from MODIS to CYCLOPES to JRC and GLOBCARBON. MODIS and CYCLOPES are very similar, reaching peaks of 0.8. JRC and GLOBCARBON show strong decreases in FAPAR moving north and record significantly lower values than MODIS and CYCLOPES in deciduous needleleaf forests and shrubland/grassland. GLOBCARBON

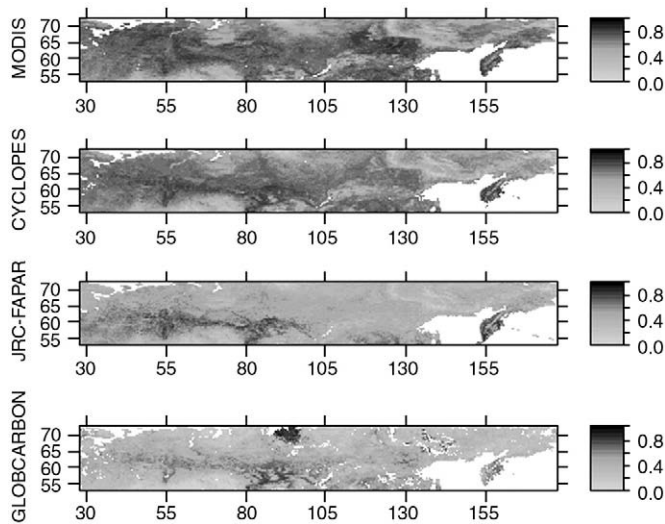


Fig. 5. Four global FAPAR products (absolute values) for July, 2000 over northern Eurasia.

contains some very high values (anomaly) in the far north. This may be explained by difficulties with the algorithm when encountering elevation at high latitudes.

Difference maps (subtraction) for each combination of the four FAPAR products were produced to target spatial dissimilarity (Fig. 6). MOD-GCB, CYC-GCB and JRC-GCB showed the greatest spatial disagreement, especially in the north and south. MOD-JRC and CYC-JRC both displayed disagreement largely in the eastern deciduous needleleaf forests, along with the northern latitudinal belt of coniferous forests. MOD-CYC displayed a very smooth figure with similar results overall.

Additionally, a map of each FAPAR product was created after subtracting the mean of the four products, per grid-cell (Fig. 7). In general, MODIS appears significantly above the mean, specifically in the far north. CYCLOPES records values slightly above the mean. JRC lies below the mean in deciduous and evergreen needleleaf forests, elsewhere displaying generally mean values. GLOBCARBON lies generally well below the mean, with anomalies previously mentioned.

An RMSE map of the four global FAPAR datasets was made for July, 2000 over northern Eurasia, highlighting agreement/disagreement appearing in latitudinal bands, particularly noticeable in the far north (Fig. 8). Below 60°N, agreement among datasets improves. Again the anomaly from GLOBCARBON is strongly visible in the far north. Agreement appears highest over the deciduous broadleaf and mixed forests, and lowest over the deciduous needleleaf forests (mean RMSE 0.16).

An RMSE map of only the MODIS, CYCLOPES and JRC datasets produced a mean RMSE of 0.13 (Fig. 9). Removing GLOBCARBON from

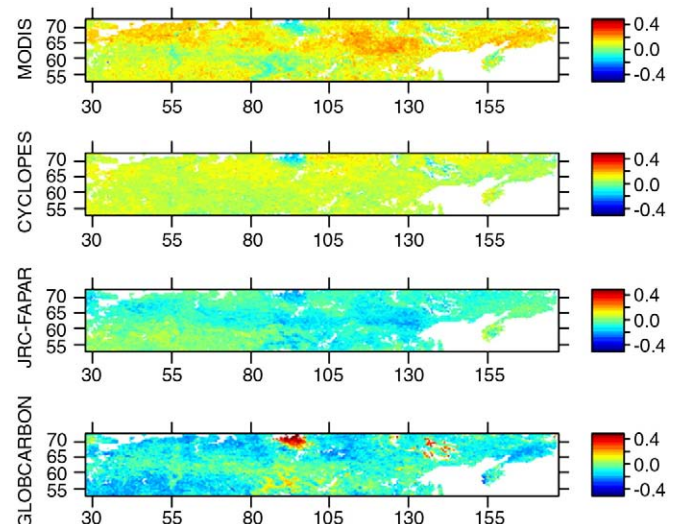


Fig. 7. Maps of four global FAPAR datasets, with the mean (per grid-cell) of all four subtracted from each dataset.

the calculation provides a substantial improvement in the RMSE map. The largest RMSE values lie over eastern Siberia in deciduous needleleaf forests and in general to the north.

4.3. FAPAR definition

In order to explain some of the differences among the products it is necessary to consider the definition of FAPAR used in each dataset. Although two of the datasets (CYCLOPES and GLOBCARBON) utilise the identical sensor (see Table 1), all four products define and calculate FAPAR differently. However, Weiss et al. (2007) noted that although differences are observed between satellite products, the consequences on FAPAR values are far less important than in the case of LAI.

From Table 2, we are able to derive a number of factors that may contribute to some of the noted differences among the FAPAR products. Both MODIS and GLOBCARBON apply somewhat similar approaches – but with different results. Both products employ a land cover/biome dataset, albeit different datasets, using a lookup table approach based on those land cover/biome classes. Additionally, both datasets require LAI in order to calculate FAPAR. Both of these factors may be affecting results. GLOBCARBON additionally employs a soil map and DEM, introducing perhaps further uncertainty as witnessed in the anomaly (see Fig. 5). Furthermore, MODIS utilizes an empirical NDVI approach as a backup solution, which gets applied typically in

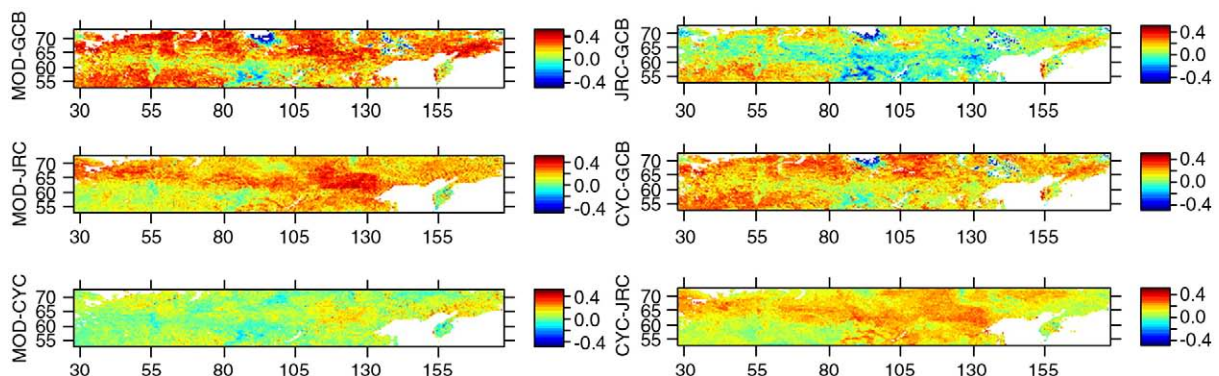


Fig. 6. Difference maps of all four FAPAR products, where each of the datasets was subtracted from the others (MOD = MODIS; CYC = CYCLOPES; JRC = JRC; and GCB = GLOBCARBON).

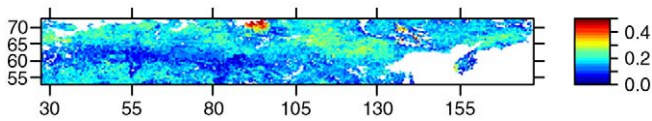


Fig. 8. RMSE map of four global FAPAR datasets (MODIS, CYCLOPES, JRC and GLOBCARBON) for July, 2000 over northern Eurasia.

the far north in spring and autumn conditions, but contains known errors (Yang et al., 2006).

Conversely, the CYCLOPES and JRC approaches generally avoid *a priori* data and employ neural network and optimization techniques, respectively. Although these two datasets generally disagree over forest sites in absolute terms, correlation among them is highest across all land cover types.

4.4. Comparison to other studies

Although few studies exist comparing FAPAR products over northern Eurasia, Pinty et al. (2008) examined several products over a site in Eastern Russia (including MODIS and JRC). In particular, they estimated FAPAR over a deciduous needleleaf larch forest in the range of 0.0–0.5, reporting that MODIS grossly overestimated these values while JRC values were similar. Several authors have noted that previous versions of MODIS FAPAR tended towards overestimation, in particular having difficulty describing low FAPAR values (Steinberg et al., 2006; Wang et al., 2004; Weiss et al., 2007). Similar results occurred over boreal coniferous needleleaf forests, while agreement was much higher over temperate deciduous broadleaf forests. They showed that the availability of a snow indicator is beneficial to the analysis of products generated under winter and early spring seasons, especially at high latitudes. The findings by Pinty et al. (2008) help to explain the results from this study, suggesting that in high latitudes in certain land classes, unique conditions must be accounted for. Using the JRC FAPAR product, Jung et al. (2008) demonstrated that the cumulative FAPAR of the growing season was directly linked to gross carbon uptake in European evergreen forests (including measurements north of 60°N), suggesting that JRC FAPAR is correctly capturing this variable. Comparison of GLOBCARBON LAI with AVHRR, MODIS and CYCLOPES, found that GLOBCARBON LAI values were lower than other datasets – a fact that would translate into low FAPAR values (GIM, 2006).

Kobayashi et al. (2007) also noted that reflectance in sparse deciduous needleleaf forests (typical for eastern Siberia) is affected by various changes in surface conditions, such as snow melt, canopy LAI, tree density and forest floor conditions. In Northern Eurasia in particular, a substantial part of NPP falls on lower layers, owing to generally sparse canopies – undergrowth and shrubs (6.5%) and green forest floor (16.8%) (Shvidenko et al., 2008). In these regions it is likely that sparse forest canopies with a green forest floor and understorey confound both LAI and FAPAR measurements.

4.5. Study limitations

A major limitation in this study is the lack of FAPAR in-situ measurements. Such a comparison relies to some extent on similarity – if all products are different, and in-situ data is lacking, it is difficult to know which product better represents reality. There is, however, a need to

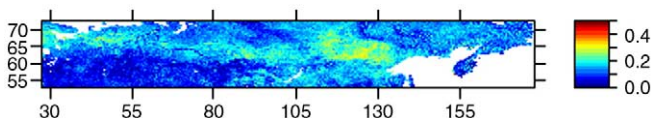


Fig. 9. RMSE map of three global FAPAR datasets (MODIS, CYCLOPES and JRC) for July, 2000 over northern Eurasia.

acquire these values more systematically in space and time, taking into account the heterogeneity and 3-D structure of canopies in different ecosystems (Gobron & Verstraete, 2008). Additional possibilities for validation of FAPAR beyond those attempted in this study might include some measure of phenology, freeze-thaw and others.

Additionally, all data compared in this study were aggregated to monthly 0.25° resolution. This naturally has the effect of grossly smoothing the data, as FAPAR is a rapidly changing variable – with values changing over the course of the day. A benefit, however, of this averaging is to lessen the effects surrounding the comparison of different instantaneous values, and differences in illumination and observer angles. Considering only the year 2000 is also a limitation, as running this analysis for multiple years might reveal more information. However, the year 2000 is representative of the long-term trend between 1976 and 2008 for temperature, precipitation and radiation (Roshydromet, 2008). Although the MODIS FAPAR algorithm utilises the MOD12 biome map, we selected the GLC2000 product in order to generate statistics and analyze all four datasets. Tests using the MOD12 biome map made little difference to the analysis – presumably because the basic thematic classes were relatively similar. The greatest difference lies in the existence of a savanna biome in MOD12 in the far north, which overlaps with grasses, shrubs and needleleaf forest in GLC2000.

4.6. Novelty of study

To the authors' knowledge, this is the only study to compare these four products (MODIS, CYCLOPES, JRC and GLOBCARBON) exclusively over Northern Eurasia. Previous comparisons of the aforementioned products were made over areas of Europe and North America. However, over those areas, ample in-situ data is available for comparison, sun-zenith angle and snow effects are less problematic, large tracts of sparse needleleaf forests are rare and generally comparisons reveal better results. The novelty of this study is that it focuses on data retrieved from a large and significant part of the globe from which in-situ data is difficult to obtain and conditions of measurement are challenging.

5. Conclusions

The productivity of a vegetated surface is related, among other factors, to the fraction of incident photosynthetically active radiation (0.4–0.7 μm) absorbed by the photosynthesizing tissue in a canopy (Myneni & Williams, 1994). Therefore, when modeling carbon accumulation over large regions such as Northern Eurasia, satellite-derived measures of FAPAR are a key biophysical variable. In recent years the availability of FAPAR datasets has increased, with constant improvements in both spatial and temporal resolution. When faced with multiple choices of input datasets, selection of one versus another may have significant effects upon model results (McCallum et al., 2006). As is the case in PEMs, where the FAPAR dataset is integral to the resulting output, choice of an FAPAR dataset likely has a significant effect. Seixas et al. (2007) emphasized the importance of FAPAR in data-driven ecosystem productivity estimation methods. The user therefore faces the dilemma of choosing the most appropriate product to suit an application (Weiss et al., 2007).

This study focused on comparison of four global FAPAR datasets over Northern Eurasia for the year 2000, namely MODIS, CYCLOPES, JRC, and GLOBCARBON. Monthly versions of these datasets at 0.25° spatial resolution were used. Reassuring is the high level of agreement among the MODIS, CYCLOPES and JRC datasets in deciduous broadleaf forests and croplands. This suggests that these datasets are similarly and potentially correctly recording FAPAR in these classes, and that disagreement in other land cover types is the result of problems in several or all of the datasets. Agreement among datasets does not imply accuracy; however the more datasets agree over a particular area, the

greater the likelihood that those datasets are correctly capturing the variable.

Poorest agreement among the datasets over forest land cover occurs within mixed and needleleaf forests. In the case of Northern Eurasia this is significant as needleleaf forests represent 61% of the study region. MODIS and CYCLOPES record similarly high values, while the JRC and GLOBCARBON datasets are similar but significantly lower. The lack of published FAPAR in-situ measurements highlights the need to increase the measurements in the near future over this region. Spatial comparison of the datasets also highlights the wide range of values across the datasets over northern Eurasia. The RMSE maps (Figs. 8 and 9) clearly demonstrate this discrepancy and identify regional differences that appear to be land cover related. In addition, an anomaly was observed in the far north of the GLOBCARBON dataset, indicating potential problems with the algorithm.

Based on the results of this study and other published findings (Jung et al., 2008; Pinty et al., 2008), it appears that the JRC FAPAR algorithm produces a conservative estimate that can be generally applied across northern Eurasia in the year 2000. Application of the remaining datasets (MODIS, CYCLOPES and GLOBCARBON) is dependent upon land cover type. Potential reasons for discrepancies among the datasets include different retrieval methods, use of LAI and land cover, snow effects and others.

In addition to FAPAR related studies, new remote sensing methods are under investigation which may provide better tools to detect the amount of photosynthesis occurring within vegetation. These include hyperspectral remote sensing (sensing changes in the xanthophyll cycle) along with the remote detection of fluorescence, however these methods are not yet operational (Grace et al., 2007).

The majority of global FAPAR evaluation efforts have focused to date on Europe, North America and regions below 60°N, largely because it is in these regions where the majority of in-situ measurements exist. Here the findings are generally better and agreement higher among the datasets. Based on the findings of this study, it appears that areas north of 60°N urgently require further investigation.

Acknowledgements

Four anonymous reviewers provided helpful comments. N. Gobron (Joint Research Center) provided FAPAR data in 0.25° Plate Carree format for the year 2000. The IIASA FOR Program and the EC FP7 Projects EuroGEOSS (www.eurogeoss.eu) and CC-TAME (www.cctame.eu) supported this work. E. Moltchanova provided statistical consultation. The IIASA Library provided reference materials.

References

- Aps, M. J., Shvidenko, A., & Vaganov, E. A. (2006). Boreal forests and the environment: A foreword. *Mitigation and Adaptation Strategies for Global Change*, 11, 1–4.
- Asner, G. P., Wessman, C. A., & Archer, S. (1998). Scale dependence of absorption of photosynthetically active radiation in terrestrial ecosystems. *Ecological Applications*, 8(4), 1003–1021.
- Balshi, M. S., McGuire, A. D., Zhuang, Q., Melillo, J., Kicklighter, D. W., Kasichke, E., et al. (2007). The role of historical fire disturbance in the carbon dynamics of the pan-boreal region: a process-based analysis. *Journal of Geophysical Research*, 112, G02029.
- Balster, H., Gerard, F. F., George, C. T., Rowland, C. S., Jupp, T. E., McCallum, I. R., et al. (2005). Impact of the Arctic Oscillation pattern on interannual forest fire variability in Central Siberia. *Geophysical Research Letters*, 32(14), L14709.
- Baret, F., Hagolle, O., Geiger, B., Bicheron, P., Miras, B., Huc, M., et al. (2007). LAI, fAPAR and fCover CYCLOPES global products derived from VEGETATION Part 1: Principles of the algorithm. *Remote Sensing of Environment*, 110, 275–286.
- Bartalev, S. A., Belward, A. S., Erchov, D. V., & Isaev, A. S. (2003). A new SPOT4-VEGETATION derived land cover map of Northern Eurasia. *International Journal of Remote Sensing*, 24(9), 1977–1982.
- CCRS (2007). Canadian Centre for Remote Sensing. Fraction of Photosynthetically Active Radiation (FPAR) Downloaded 15.10.07 from: www.ccrs.nrcan.gc.ca/optic/veg.
- FAO (2007). Development of Standards for Essential Climate Variables: Fraction of Absorbed Photosynthetically Active Radiation (FAPAR) 5 pp. Downloaded 19.09.07 from: www.fao.org/gtos/doc/ECVs/T10/ECV-T10-FAPAR-report-v02.doc.
- Fensholt, R., Sandholt, I., & Rasmussen, M. S. (2004). Evaluation of MODIS LAI, fAPAR and the relation between fAPAR and NDVI in a semi-arid environment using in situ measurements. *Remote Sensing of Environment*, 91, 490–507.
- GCOS (2006). Systematic Observation requirements for satellite-based products for climate. GCOS-107 90pp.
- Geosuccess. (2007). fAPAR. <http://geofront.vgt.vito.be/geosuccess>. Accessed on 11.09.07.
- GIM (2006). GLOBCARBON Demonstration Products and Qualification Report. : European Space Agency 161 pp.
- Gobron, N., Knorr, W., Aussenat, O., Pinty, B., Scholze, M., & Taberner, M. (2007). Relevance of global remote-sensing FAPAR products to carbon flux estimates. *Proceedings Envisat Symposium 2007, Montreux, Switzerland. ESA SP-636*.
- Gobron, N., Pinty, B., Aussenat, O., Chen, J., Cohen, W., Fensholt, R., et al. (2006). Evaluation of fraction of absorbed photosynthetically active radiation products for different canopy radiation transfer regimes: Methodology and results using Joint Research Center products derived from SeaWiFS against ground-based estimations. *Journal of Geophysical Research*, 111, D13110, doi:10.1029/2005JD006511.
- Gobron, N., Pinty, B., Melin, F., Taberner, M., & Verstraete, M. (2002). Sea Wide Field-of-View Sensor – An optimized FAPAR algorithm theoretical basis document. JRC Pub. No. EUR 20148 20 pp.
- Gobron, N., & Verstraete, M. (2008). ECV T10: Fraction of Absorbed Photosynthetically Active Radiation (FAPAR). *Essential Climate Variables. Rome: Global Terrestrial Observing System* 23 pp.
- Goldammer, J. G. (1996). The boreal forest, fire, and the global climate system: Achievements and needs in joint east–west boreal fire research and policy development. *Combustion, Explosion and Shock Waves*, 32, 544–557.
- Grace, J., Nichol, C., Disney, M., Lewis, P., Quaife, T., & Bowyer, P. (2007). Can we measure terrestrial photosynthesis from space directly, using spectral reflectance and fluorescence? *Global Change Biology*, 13, 1484–1497.
- Heimann, M. (2002). Foreword: The EUROSIBERIAN CARBONFLUX Project. *Tellus*, 54B(5), 417–419.
- Jung, M., Verstraete, M., Gobron, N., Reichstein, M., Papales, D., Bondeau, A., et al. (2008). Diagnostic assessment of European gross primary production. *Global Change Biology*, 14, 2349–2364.
- Kajii, Y., Kato, S., Streets, D. G., Tsai, N. Y., Shvidenko, A., Nilsson, S., et al. (2002). Boreal forest fires in Siberia in 1998: Estimation of area burned and emissions of pollutants by advanced very high resolution radiometer satellite data. *Journal of Geophysical Research*, 107, doi:10.1029/2001JD001078.
- Knyazikhin, Y., Martohchik, J. V., Myneni, R. B., Diner, D. J., & Running, S. W. (1998). Synergistic algorithm for estimating vegetation canopy leaf area index and fraction of absorbed photosynthetically active radiation from MODIS and MISR data. *Journal of Geophysical Research*, 103 98JD02462.
- Kobayashi, H., Suzuki, R., & Kobayashi, S. (2007). Reflectance seasonality and its relation to the canopy leaf area index in an eastern Siberian larch forest: Multi-satellite data and radiative transfer analyses. *Remote Sensing of Environment*, 106, 238–252.
- Lapenis, A., Shvidenko, A., Shepaschenko, D., Nilsson, S., & Aiyyer, A. (2005). Acquisition of Russian forests to recent changes in climate. *Global Change Biology*, 11, 2090–2102.
- McCallum, I., Obersteiner, M., Nilsson, S., & Shvidenko, A. (2006). A spatial comparison of four satellite derived 1 km global land cover datasets. *International Journal of Applied Earth Observation and Geoinformation*, 8, 246–255.
- MNRRF. (2003). *State forest account of Russia*. Moscow: Ministry of Natural Resources of the Russian Federation 637 pp.
- Myneni, R. B., & Williams, D. L. (1994). On the relationship between FAPAR and NDVI. *Remote Sensing of Environment*, 49, 200–211.
- Myneni, R. B., Dong, J., Tucker, C. J., Kaufmann, R. K., Kauppi, P. E., Liski, J., et al. (2001). A large carbon sink in the woody biomass of Northern forests. *Proceedings of the National Academy of Sciences, USA*, 98, 14784–14789.
- Myneni, R. B., Hoffman, S., Knyazikhin, Y., Privette, J. L., Glassy, J., Tian, Y., et al. (2002). Global products of vegetation leaf area and fraction absorbed PAR from year one of MODIS data. *Remote Sensing of Environment*, 83, 214–231.
- Myneni, R. B., Knyazikhin, Y., Glassy, J., Votava, P., & Shabanov, N. (2003). *User's Guide – FPAR, LAI 8-day composite NASA MODIS land algorithm*. Terra MODIS Land Team 17 pp.
- Nemani, R., Keeling, C., Hashimoto, H., Jolly, W., Piper, S., Tucker, C., et al. (2003). Climate driven increases in global terrestrial net primary production from 1982 to 1999. *Science*, 300, 1560–1563.
- Pinty, B., Lavergne, T., Kaminski, T., Aussenat, O., Giering, R., Gobron, N., et al. (2008). Partitioning the solar radiant fluxes in forest canopies in the presence of snow. *Journal of Geophysical Research*, 113, D04104, doi:10.1029/2007JD009096.
- Plummer, S., Arino, O., Ranera, F., Tansey, K., Chen, J., Dedieu, G., et al. (2007). An Update on the GlobCarbon Initiative: Multi-Sensor Estimation of Global Biophysical Products for Global Terrestrial Carbon Studies. *Proceedings ENVISAT Symposium 2007, ESA SP-636*.
- Potter, C., Klooster, S., Tan, P., Steinbach, M., Kumar, V., & Genovesi, V. (2005). Variability in terrestrial carbon sinks over two decades: Part 2 – Eurasia. *Global and Planetary Change*, 49, 177–186.
- Prince, S. D., & Goward, S. N. (1995). Global primary production: A remote sensing approach. *Journal of Biogeography*, 22, 815–835.
- Roshydromet (2008). The Assessment Report on Climate Changes and their Consequences in territories of the Russian Federation. Vol. 1, *Climate Change*. Moscow in Russian.
- Running, S. W., Nemani, R. R., Heinsch, F. A., Zhao, M., Reeves, M., & Hashimoto, H. (2004). A continuous satellite-derived measure of global terrestrial primary production. *BioScience*, 54(6), 547–560.
- Seixas, J., Carvalhais, N., Nunes, C., & Benali, A. (2007). Ecosystem production modelling in the Iberian Peninsula: Comparative analysis between MODIS and MERIS datasets. *Proceedings Envisat Symposium 2007, Montreux, Switzerland, ESA SP-636*.
- Shvidenko, A., Schepaschenko, D., McCallum, I., & Nilsson, S. (2007). CD-ROM "Russian Forests and Forestry", International Institute for Applied Systems Analysis and the Russian Academy of Science, Laxenburg, Austria www.iiasa.ac.at/Research/FOR.

- Shvidenko, A., Schepaschenko, D., Nilsson, S., & Vaganov, E. (2008). Net primary production of forest ecosystems of Russia: A new estimate. *Doklady Earth Sciences*, 421(2), 1009–1012.
- Steinberg, D. C., Goetz, S. J., & Hyer, E. J. (2006). Validation of MODIS FPAR products in boreal forests of Alaska. *IEEE Transactions on Geoscience and Remote Sensing*, 44(7), 1818–1828.
- Veroustraete, F., Sabbe, H., & Eerens, H. (2002). Estimation of carbon mass fluxes over Europe using the C-Fix model and Euroflux data. *Remote Sensing of Environment*, 83, 376–399.
- Wang, Y., Woodcock, C. E., Buermann, W., Stenberg, P., Voipio, P., Smolander, H., et al. (2004). Evaluation of the MODIS LAI algorithm at a coniferous forest site in Finland. *Remote Sensing of Environment*, 91, 114–127.
- Weiss, M., Baret, F., Garrigues, S., & Lacaze, R. (2007). LAI and fAPAR CYCLOPES global products derived from VEGETATION. Part 2: Validation and comparison with MODIS collection 4 products. *Remote Sensing of Environment*, 110, 317–331.
- Yang, W., Huang, D., Tan, B., Stroeve, J., Shabanov, N., Knyazikhin, Y., et al. (2006). Analysis of leaf area index and fraction of PAR absorbed by vegetation products from the Terra MODIS sensor: 2000–2005. *IEEE Transactions on Geoscience and Remote Sensing*, 44(7), 1829–1842.



Improved light and temperature responses for light-use-efficiency-based GPP models

I. McCallum¹, O. Franklin¹, E. Moltchanova², L. Merbold³, C. Schmullius⁴, A. Shvidenko¹, D. Schepaschenko¹, and S. Fritz¹

¹International Institute for Applied Systems Analysis, Laxenburg, Austria

²Department of Mathematics and Statistics, University of Canterbury, Christchurch, New Zealand

³ETH Zurich, Institute of Agricultural Sciences, Zurich, Switzerland

⁴Department of Geography, Friedrich-Schiller-University Jena, Jena, Germany

Correspondence to: I. McCallum (mccallum@iiasa.ac.at)

Received: 12 March 2013 – Published in Biogeosciences Discuss.: 29 May 2013

Revised: 2 September 2013 – Accepted: 9 September 2013 – Published: 17 October 2013

Abstract. Gross primary production (GPP) is the process by which carbon enters ecosystems. Models based on the theory of light use efficiency (LUE) have emerged as an efficient method to estimate ecosystem GPP. However, problems have been noted when applying global parameterizations to biome-level applications. In particular, model–data comparisons of GPP have shown that models (including LUE models) have difficulty matching estimated GPP. This is significant as errors in simulated GPP may propagate through models (e.g. Earth system models). Clearly, unique biome-level characteristics must be accounted for if model accuracy is to be improved. We hypothesize that in boreal regions (which are strongly temperature controlled), accounting for temperature acclimation and non-linear light response of daily GPP will improve model performance.

To test this hypothesis, we have chosen four diagnostic models for comparison, namely an LUE model (linear in its light response) both with and without temperature acclimation and an LUE model and a big leaf model both with temperature acclimation and non-linear in their light response. All models include environmental modifiers for temperature and vapour pressure deficit (VPD). Initially, all models were calibrated against five eddy covariance (EC) sites within Russia for the years 2002–2005, for a total of 17 site years. Model evaluation was performed via 10-out cross-validation.

Cross-validation clearly demonstrates the improvement in model performance that temperature acclimation makes in modelling GPP at strongly temperature-controlled sites in Russia. These results would indicate that inclusion of

temperature acclimation in models on sites experiencing cold temperatures is imperative. Additionally, the inclusion of a non-linear light response function is shown to further improve performance, particularly in less temperature-controlled sites.

1 Introduction

Terrestrial plants fix carbon dioxide (CO₂) as organic compounds through photosynthesis, a carbon flux also known at the ecosystem level as gross primary production (GPP) (Beer et al., 2010). A variety of methods have been developed to estimate ecosystem carbon fluxes. These include flux towers (e.g. Friend et al., 2007), carbon accounting techniques (e.g. Shvidenko and Nilsson, 2003), process-based vegetation models (e.g. Sitch et al., 2003), atmospheric measurements (e.g. Stephens et al., 2007) and diagnostic satellite-based techniques (e.g. Running et al., 2004), with each methodology having advantages and shortcomings. Satellite-based models in particular have been developed to monitor gross primary production – with the advantage that they can model the globe at high temporal frequency using remotely sensed products of fine resolution and may be calibrated against flux tower data. These models are generally based on the theory of light use efficiency (LUE), which states that a relatively constant relationship exists between photosynthetic carbon uptake (GPP) and absorbed photosynthetically

active radiation (APAR) at the canopy level (Anderson et al., 2000; Sjoestroem et al., 2011).

Problems have however been noted with the LUE approach, particularly when applying global parameterizations to local applications (Pan et al., 2006; Turner et al., 2006; Shvidenko et al., 2010; McCallum et al., 2009). This is not surprising as temperature, radiation, and water interact to impose complex and varying limitations on vegetation activity and LUE in different parts of the world (Churkina and Running, 1998). A recent model–data comparison of GPP from 26 models (including LUE models) noted that none of the models matched estimated GPP within observed uncertainty (Schaefer et al., 2012). On average, models over-predicted GPP under dry conditions and for temperatures below 0 °C. This occurs for many reasons, including the following: (1) the majority of models have not been calibrated with flux tower data and hence can not replicate the detailed in situ estimates; (2) models generally operate at much coarser spatial resolution than flux tower measurements; and (3) models are designed to be generally applicable at the continental or global level, and thus often do not include certain biome-level specificities which may be captured in flux tower estimates.

The recent increasing availability of empirical canopy-level estimates of GPP from eddy covariance (EC) measuring stations (FLUXNET) is however making the calibration process more feasible (Mäkelä et al., 2008), potentially leading to improved models. We now have the ability both to create statistically fitted models (e.g. van Dijk et al., 2005; Jung et al., 2008) and to parameterize more general summary-type photosynthesis models. Several recent studies have demonstrated model calibration of summary-type LUE models at continental (Mäkelä et al., 2008; King et al., 2011) and global (Beer et al., 2010) scales.

The objective of this paper is to calibrate four GPP models (of increasing complexity) simultaneously across five Russian boreal EC stations and evaluate their performance. As Russia represents a large land mass that is strongly climate controlled with relatively few in situ measurements, such analysis can improve our ability to model GPP across the Eurasian continent. We hypothesize that accounting for temperature acclimation and to a lesser extent non-linear light response of daily GPP will largely improve model performance.

2 Methods

2.1 Study region

Russia comprises almost one fourth of the world's forest cover, making these boreal forests a unique natural phenomenon at the global scale. In addition vast areas are characterized by tundra ecosystems, dominated by shrubs, grasses and sedges, mostly above permafrost. Furthermore,

significant agricultural and grassland areas occur outside of permafrost regions. This large land area undergoes great annual changes in albedo and productivity as seasonal temperatures swing well above and below 0 °C. Large regions lie in various stages of permafrost and the area is prone to catastrophic disturbance in the form of fire (Goldammer, 1996; Kajii et al., 2002; Balzter et al., 2005). Furthermore, the climate of both the boreal forests and the tundra ecosystems in eastern Siberia can resemble that of a boreal/arctic desert during long periods of the growing season (Vygodskaya et al., 1997).

2.2 Model description

Four diagnostic models were chosen for comparison in this study, namely (1) the LUE approach parameterized according to Running (2000), (2) the LUE approach parameterized according to Mäkelä et al. (2008) but without a light modifier, (3) the LUE approach parameterized according to Mäkelä et al. (2008) with a light modifier and (4) a non-rectangular hyperbola (big leaf) model (e.g. Hirose and Werger, 1987; Hirose et al., 1997). All parameters are listed in Table 1. The LUE models follow the standard approach, each including two environmental modifiers for temperature and vapour pressure deficit (VPD), and in the third instance a non-linear light modifier. The big leaf (BL) model also includes two environmental modifiers for temperature and VPD, and is inherently non-linear in its light response. Initially, all models are calibrated against five EC sites within Russia for the years 2002–2005. Model evaluation is performed via 10-out cross-validation.

2.2.1 Light use efficiency (LUE)

The basic LUE approach is as follows:

$$\text{GPP} = \text{PAR} f_{\text{APAR}} \text{LUE} f_1(T) f_2(\text{VPD}), \quad (1)$$

where GPP represents daily gross primary productivity (g C m^{-2}), PAR is photosynthetic active radiation (MJ m^{-2}), f_{APAR} is the fraction of absorbed PAR and LUE is the potential LUE in terms of GPP (g C MJ^{-1}). Potential LUE is the maximum LUE attainable on a site without environmental constraints. Potential LUE is reduced to actual LUE via the environmental scalars for daily minimum temperature $f_1(T)$ and daily vapour pressure deficit $f_2(\text{VPD})$, both of which are defined as linear ramp functions [0,1] as per Running (2000). $f_1(T)$ is 0 when daily minimum temperature (°C) is less than or equal to $T_{\text{min}_{\text{min}}}$ (°C) and increases linearly to 1 at temperature $T_{\text{min}_{\text{max}}}$ (°C). As a global generalization, the algorithm truncates GPP on days when the minimum temperature is below -8 °C (Running et al., 2004); however in our study, this value was optimized for each site year. $f_2(\text{VPD})$ has a value of 1 when VPD is less than or equal to VPD_{min} (Pa) and declines linearly to 0 as VPD increases to VPD_{max} (Pa) (Running, 2000).

Table 1. Parameters required for LUE, LUE-TA, LUE-TAL and BL models.

Symbol	Description	Unit	Model	Parameter Values		Increment	Reference
				Min	Max		
$T_{\min_{\min}}$	Minimum temperature: minimum	°C	LUE	-11	-2	2	King et al. (2011)
$T_{\min_{\max}}$	Minimum temperature: maximum	°C	LUE	4	13	2	King et al. (2011)
V_{\min}	Minimum VPD	Pa	LUE	0	2500	500	King et al. (2011)
V_{\max}	Maximum VPD	Pa	LUE	1500	4500	500	King et al. (2011)
LUE	Light use efficiency (Maximum)	g C MJ ⁻¹	LUE, LUE-TA, LUE-TAL	0.5	4	0.1	King et al. (2011)
S_{\max}	Saturating level	°C	LUE-TA, LUE-TAL, BL	15	30	3	Mäkelä et al. (2008)
t	Time constant	days	LUE-TA, LUE-TAL, BL	1	22	3	Mäkelä et al. (2008)
X_0	Threshold value	°C	LUE-TA, LUE-TAL, BL	-10	5	3	Mäkelä et al. (2008)
K	VPD	kPa ⁻¹	LUE-TA, LUE-TAL, BL	-0.1	-0.9	-0.2	Landsberg and Waring (1997)
γ	Light	m ² mol ⁻¹	LUE-TAL	0	0.12	0.03	Mäkelä et al. (2008)
A_{\max}	Light saturated photosynthesis	umol CO ₂ m ⁻² s ⁻¹	BL	0	40	2	Ruimy et al. (1996)
θ	Convexity of leaf photosynthesis	-	BL		0.8	-	Hirose et al. (1997)
ϕ	Photosynthetic quantum efficiency	ug C J ⁻¹	BL		2.73	-	Wong et al. (1979)
h	Day length	h d ⁻¹	BL		12	-	Estimated

2.2.2 Light use efficiency – temperature acclimation (LUE-TA)

The basic LUE approach (Eq. 1) was again employed; however both $f_1(T)$ and $f_2(\text{VPD})$ were parameterized differently. The effect of temperature on daily GPP was modelled using the concept of acclimation S_k (°C), a piecewise linear function of X_k (°C) calculated from the mean daily ambient temperature T_k (°C), using a first-order dynamic delay model:

$$X_k = X_{k-1} + \frac{1}{t}(T_k - X_{k-1}), \quad X_1 = T_1, \quad (2)$$

$$S_k = \max\{X_k - X_0, 0\}, \quad (3)$$

where t (days) is the time constant of the delay process and X_0 (°C) is a threshold value of the delayed temperature (Mäkelä et al., 2008). The modifying function $f_1(T)$ is defined here as (Mäkelä et al., 2008)

$$f_1(T) = \min\left\{\frac{S_k}{S_{\max}}, 1\right\}, \quad (4)$$

where the empirical parameter S_{\max} (°C) determines the value of S_k (°C) at which the temperature modifier attains its saturating level. The effect of VPD $f_2(\text{VPD})$ was estimated according to Landsberg and Waring (1997):

$$f_2(\text{VPD}) = e^{KD}, \quad (5)$$

where K is an empirical parameter (see Table 1) assuming typically negative values and D (kPa) is vapour pressure deficit.

2.2.3 Light use efficiency – temperature acclimation and light (LUE-TAL)

Again the basic LUE approach (Eq. 1) was used, parameterized according to LUE-TA. In addition, to account for

non-linearity in the photosynthetic response to APAR, a light modifier $f_3(L)$ was defined to yield the rectangular hyperbola light response function when multiplied with the linear response included in the LUE-TA model (Mäkelä et al., 2008):

$$f_3(L) = \frac{1}{\gamma \text{APAR} + 1}, \quad (6)$$

where γ (m² mol⁻¹) is an empirical parameter (see Table 1) defined according to Mäkelä et al. (2008). Because this light response function does not vary with environmental modifiers, it differs from the non-rectangular BL model (described below), in which the light response interacts (changes shape) with the environmental modifiers.

2.2.4 Non-rectangular hyperbola/big leaf (BL)

Leaf photosynthesis is described with the non-rectangular hyperbola model (Hirose and Werger, 1987; Hirose et al., 1997). Leaf level photosynthesis is up-scaled to daily canopy photosynthesis by integration over the canopy (Franklin, 2007) using canopy f_{APAR} to determine the amount of absorbed incoming radiation. Daily gross primary production GPP is thus defined here according to

$$\text{GPP} = \frac{h}{2\theta} \left[\phi I_a + E_a A_{\max} - \sqrt{(\phi I_a + E_a A_{\max})^2 - 4\phi I_a E_a A_{\max} \theta} \right], \quad (7)$$

where

$$E_a = f_1(T) f_2(\text{VPD}), \quad (8)$$

h is day length; θ convexity of leaf photosynthesis; ϕ quantum efficiency; I_a absorbed photosynthetically active radiation; E_a environmental modifier for temperature $f_1(T)$ and

VPD $f_2(\text{VPD})$; and A_{max} light-saturated canopy photosynthesis. The effect of temperature $f_1(T)$ on daily A_{max} was modelled using the concept of state of acclimation (Mäkelä et al., 2008); i.e. it acclimates dynamically to temperature with a time delay. The effect of VPD $f_2(D)$ on A_{max} was estimated according to Landsberg and Waring (1997).

2.3 Eddy covariance, meteorological and satellite data

Eddy covariance data for model calibration was obtained from <http://www.fluxdata.org> for five sites (Table 2, Fig. 1). The eddy covariance method, a micrometeorological technique, provides a direct measure of the net exchange of carbon and water between vegetated canopies and the atmosphere (Baldocchi et al., 2001). Although flux tower data represent point measurements with a maximum footprint of 1 km^2 (dependent upon whether sensor height was selected to observe such a dimension), they can be used to validate models and to spatialize biospheric fluxes at regional and continental scales (Papale and Valentini, 2003). In reality however, the footprint is highly dynamic in space and time depending on friction velocity, sensible heat flux, temperature, and wind direction.

The Cherskii (RU-Che) tower was situated in an arctic wet tundra ecosystem in the far east of Russia. The site was characterized by late thawing of permafrost soils in June and periodic spring floods with a stagnant water table below the grass canopy (Merbold et al., 2009). The climate is continental with average daily temperature in the warmest months of 13°C (maximum temperature at midday: 28°C by the end of July), dry air (maximum VPD at midday: 28 hPa) and low rainfall of 50 mm during summer (July–September) (Corradi et al., 2005). The Chokurdakh (RU-Cho) tower is located on a tundra ecosystem in the far east of Russia, underlain by continuous permafrost. It is characterized by a continental climate, which is reflected in low winter soil temperatures (-14°C) and short, relatively warm summers, stimulating high photosynthesis rates (van der Molen et al., 2007). The Fyoderovskoe (RU-Fyo) tower is located in a 150 yr old European Russia spruce forest, with no permafrost. In general, air temperatures increase from March until June, remaining relatively warm up until late September, after which a rapid decline occurs. Air temperatures is typically below 0°C between November and March (Milyukova et al., 2002). The Hakasia (RU-Ha1) tower is located in a natural steppe ecosystem in southern Siberia (Marchesini et al., 2007). The climate at the site is semi-arid cool, continental, with an annual mean temperature of 0.4°C and annual precipitation of 304 mm. The steppe was managed as a pasture until 2001, but with low grazing pressure. The Zotino (RU-Zot) tower is located in a 200 yr old pine forest in central Siberia, without permafrost though experiencing heavy snowfall in winter ($> 1 \text{ m}$). The long-term average length of the growing season is 132 days, lasting from approximately early May to late

September (Tchebakova et al., 2002). Permission was not obtained to include further sites in this study.

GPP data are commonly derived by flux-partitioning methods due to the fact that eddy covariance fluxes are only capable of measuring the net ecosystem exchange (NEE) of carbon dioxide and water vapour amongst other trace gases. NEE, a combination of the two counteracting processes, ecosystem respiration (R_{eco}) and GPP, is commonly separated by applying statistical flux-partitioning methods (e.g. Falge et al., 2001; Reichstein et al., 2005; Moffat et al., 2007; Stoy et al., 2006) in order to fill data gaps in NEE. A study comparing 23 gap-filling methods for a ten-year record of NEE data revealed a good agreement among the different methods with a variation of about 10 % when comparing annual flux values (Desai et al., 2008). Furthermore, the choice of the driving variables to model R_{eco} , e.g. air temperature or soil temperature, may be of importance (Lasslop et al., 2012). To date there has been no agreement on a general method to partition CO_2 fluxes. Therefore we chose the available data products from the FLUXNET synthesis database including gap-filled and flux-partitioned daily data for all sites used in this study. Gap filling and flux partitioning are based on the procedures given by Papale et al. (2006) and Reichstein et al. (2005).

Daily GPP ($\text{g C m}^{-2} \text{ d}^{-1}$) from each site was selected with a quality flag = 1 (i.e. highest quality). This resulted in variable amounts of data being available for calibration for each site year. Additionally, the following meteorological data recorded at each site were used: mean air temperature ($^\circ\text{C}$), minimum air temperature ($^\circ\text{C}$), vapour pressure deficit (kPa) and global radiation ($\text{MJ m}^{-2} \text{ d}^{-1}$). PAR was set to half of global radiation (Stanhill and Fuchs, 1977). Finally, f_{APAR} was retrieved from <http://fapar.jrc.ec.europa.eu/> (Gobron et al., 2006).

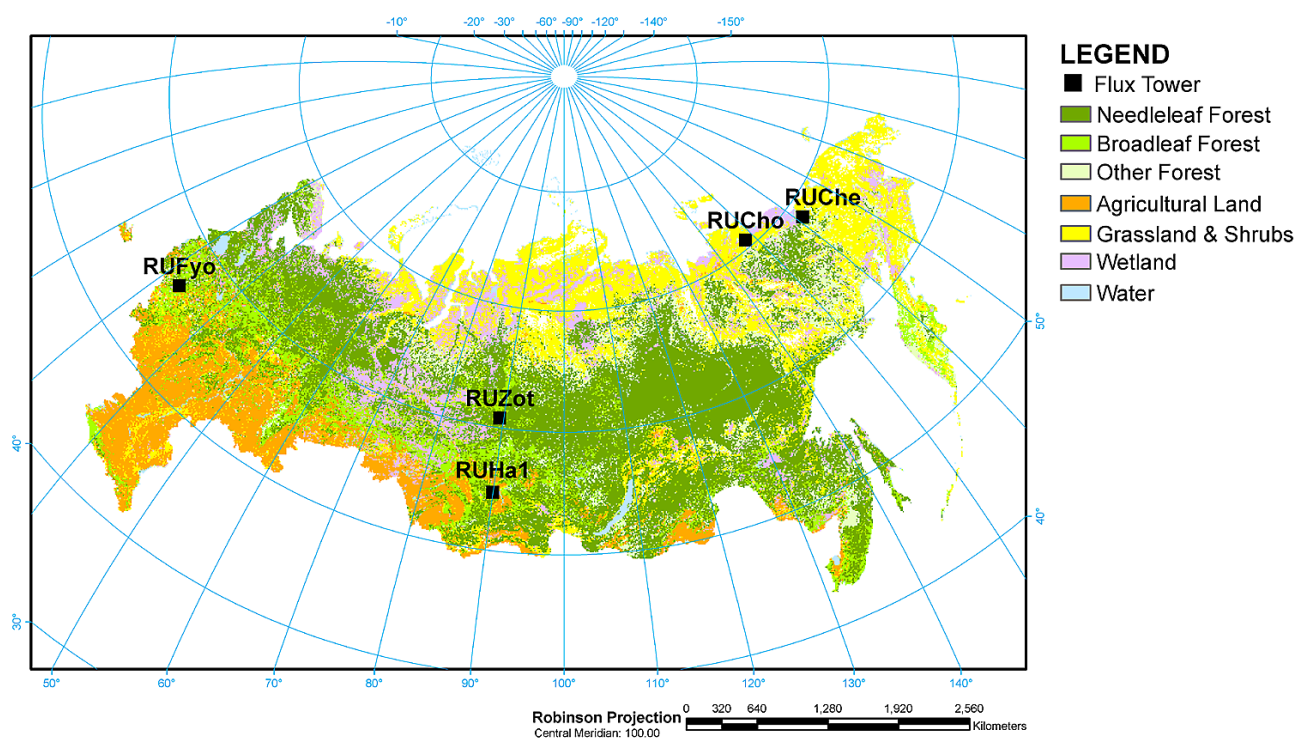
2.4 Parameter optimization

Each model was estimated separately for each site and year. Parameters were optimized by means of a search on a coarse grid (see Table 1 for parameter ranges and increments). Model diagnostics were based on the regression of EC tower based GPP against modelled GPP. The minimum residual sum of squares (RSS) has been used as the calibration criteria. Fit was further appraised using both the coefficient of determination (r^2) and root mean square error (RMSE).

All possible combinations of parameters were tested. The initial parameter range and increment was conceived by consulting the existing literature (see Table 1 for references). The step width is the increment listed in Table 1. We generally applied a rather coarse increment as RMSE has been found to be generally insensitive to the parameters close to the optimum (King et al., 2011) and use of a finer increment greatly increased computing time.

Table 2. A description of the five flux towers used in this study.

Site Name	Location (°)	Tower Height (m)	Data Years Used	Dominant Land Cover	Mean Annual Temperature (°C)	Mean Annual Precipitation (mm)	Tower References
Cherskii (RU-Che)	68.61° N 161.34° E	5.3	2002–2004	Tundra-grass	−12.5	200–215	Merbold et al. (2009), Corradi et al. (2005)
Chokurdakh (RU-Cho)	70.61° N 147.89° E	4.7	2003–2004	Tundra-grass	−10.5	212	van der Molen et al. (2007)
Fyodorovskoe (RU-Fyo)	56.46° N 32.92° E	31.0	2003–2004	Evergreen needle-leaf spruce forest	3.7	584.3	Milyukova et al. (2002)
Hakasia (RU-Ha1)	54.72° N 90.00° E	4.5	2002–2004	Steppe	0.4	304	Marchesini et al. (2007)
Zotino (RU-Zot)	60.80° N 89.35° E	27.0	2002–2004	Evergreen needle-leaf pine forest	−1.5	593	Tchebakova et al. (2002), Arneith et al. (2002)

**Fig. 1.** Map of dominant Russian land cover (Schepaschenko et al., 2011), along with locations of the flux towers used in this study.

2.5 Cross-validation

Evaluation of the performance of the models used in this study utilized 10-out cross-validation. Cross-validation is a widely used method for estimating prediction error. It allows comparison of completely different models and is independent of the number of parameters and possible correlation between them as well as of the distributional assumptions (Hastie et al., 2001). Furthermore cross-validation was selected as we are actually interested in predictive power more than explanatory power. Cross-validation implicitly takes parsimony into consideration: although a higher number of

parameters might mean a better fit, it does not necessarily mean better prediction due to resulting volatility of the estimates. Various methods exist for model selection (Forster, 2000), with cross-validation and AIC being noted as asymptotically equivalent (Stone, 1977).

For each site, measured GPP values were dropped (consecutively) ten at a time, while the remaining values were used to estimate the parameters. The estimated parameter values were then used to predict GPP of the dropped data points (i.e. those not used in the parameter estimation). The differences between these predictions (of the dropped data points) and the measured data were used to calculate the mean square

Table 3. Resulting optimized model parameters and regression diagnostics for the LUE model by site and year.

Site	Year	Optimized Parameters					Diagnostics		
		LUE (g C MJ ⁻¹)	$T_{\min_{\min}}$ (°C)	$T_{\min_{\max}}$ (°C)	V_{\min} (Pa)	V_{\max} (Pa)	r^2	RMSE (g C m ⁻² d ⁻¹)	n
RU-Che	2002	2	-10	4	0	3500	0.91	0.44	53
	2003	1.7	-6	12	0	3000	0.42	1.2	82
	2004	1.4	-2	4	0	2000	0.55	0.91	105
	2005	1.7	-2	10	0	2500	0.37	0.91	21
RU-Cho	2003	0.9	-6	4	1000	1500	0.48	1.2	117
	2004	1.2	-10	4	1000	1500	0.62	0.61	64
	2005	1	-10	4	1000	1500	0.4	0.48	58
RU-Fyo	2002	1.9	-10	12	0	3000	0.72	1.6	125
	2003	2.8	-8	6	0	2000	0.76	1.6	183
	2004	2.3	-10	8	0	2000	0.82	1.4	217
	2005	3.1	-10	10	0	1500	0.88	1.5	196
RU-Ha1	2002	1.3	-10	4	0	2000	0.81	0.59	106
	2003	1.3	-10	6	0	2500	0.73	0.65	148
	2004	1.5	-10	12	0	3000	0.91	0.69	182
RU-Zot	2002	1.7	-6	12	0	3500	0.79	1	98
	2003	2.1	-10	4	0	2500	0.64	0.87	62
	2004	1.9	-6	8	0	4000	0.83	0.95	91

error (MSE), which was used to evaluate the model's ability to predict GPP, averaged for all data. The leave-10-out cross-validation was performed a similar amount of times for each model for every site year.

3 Results and discussion

Model calibration resulted in a set of optimized parameters for the four approaches compared in this study, namely LUE, LUE-TA, LUE-TAL and BL (Tables 3, 4, 5 and 6, respectively). The LUE model (Table 3) showed clear discrepancies in obtaining a good fit, obtaining generally low coefficients of determination and high RMSE values at both the Cherskii (except in 2002) and Chokurdakh sites. This is in part due to the low values of $T_{\min_{\min}}$ selected during optimization, which allowed the model to record positive values of the temperature scalar early in the season. For the more southern sites, however, the LUE model generally performed as well as the other models, with similar RMSE values. The LUE-TA model (accounting for temperature acclimation) clearly outperformed the LUE model at the two northern sites (RU-Che and RU-Cho) (Table 4), demonstrating the importance of accounting for temperature acclimation in the northern regions. At the remaining sites the models performed equally well. Both the LUE-TAL and BL models (Tables 5 and 6) generally achieved higher r^2 across all sites and years than the LUE and LUE-TA models, suggesting that the inclusion of a non-linear light response improved model performance.

In addition, scatterplots, annual flux and environmental scalars are presented for three sites, namely tundra (Cherskii), forest (Fyodorovskoe) and grassland (Hakasia), in Fig. 2–4, respectively, for the year 2003. For the Cherskii site, situated in the tundra, the LUE model performs poorly, in comparison with the LUE-TA, LUE-TAL and BL models (Fig. 2), as noted previously. Both the scatterplot and annual flux indicate that the LUE approach is not able to capture the daily measurements, while the LUE-TA, LUE-TAL and BL approaches are more successful. The environmental scalars used in the four approaches are notably different, with the LUE model scalars for temperature and VPD showing large variation over the year. In contrast, the scalars for the LUE-TA and in particular the BL approaches are smoother, with VPD showing negligible effect and temperature having a very strong effect. This is in contradiction to the clear response to VPD (but not to temperature) of half-hourly photosynthesis at the Cherskii site as noted by Merbold et al. (2009). In the case of the LUE-TAL model, the light scalar allows the temperature scalar to increase, while the VPD scalar remains largely non-limiting. Furthermore, the scatterplots in Fig. 2 (top row) imply that the LUE and BL models are the least biased. The LUE-TA and LUE-TAL models seem to have a clear problem with overestimation of low values of GPP.

For the Fyodorovskoe site (Fig. 3), situated in evergreen needleleaf forest, all models generally capture the seasonal GPP flux, with the LUE-TAL model performing marginally better. Here again, the environmental scalars are different

Table 4. Resulting optimized model parameters and regression diagnostics for the LUE-TA model by site and year.

Site	Year	Optimized Parameters					Diagnostics	
		S_{\max} (°C)	t (days)	X_0 (°C)	K (kPa ⁻¹)	LUE (g C MJ ⁻¹)	r^2	RMSE (g C m ⁻² d ⁻¹)
RU-Che	2002	24	7	-10	-0.5	2.4	0.9	0.47
	2003	15	22	2	-0.3	2.4	0.87	0.57
	2004	15	22	-1	-0.5	2.5	0.87	0.5
	2005	15	1	2	-0.9	2.3	0.41	0.88
RU-Cho	2003	27	22	-1	-0.1	3.6	0.85	0.62
	2004	15	13	-10	-0.1	1.2	0.61	0.61
	2005	15	22	2	-0.1	3	0.56	0.41
RU-Fyo	2002	30	1	-7	-0.9	3.2	0.74	1.6
	2003	18	1	-7	-0.9	3.2	0.76	1.6
	2004	24	13	-10	-0.7	2.5	0.83	1.4
	2005	24	22	-10	-0.9	3.5	0.89	1.4
RU-Ha1	2002	15	16	-4	-0.9	1.5	0.8	0.6
	2003	15	16	-1	-0.9	1.8	0.78	0.59
	2004	15	10	-1	-0.5	1.5	0.92	0.64
RU-Zot	2002	15	19	-4	-0.5	2	0.86	0.82
	2003	15	1	-10	-0.7	2.3	0.62	0.89
	2004	15	10	-4	-0.3	1.9	0.84	0.92

Table 5. Resulting optimized model parameters and regression diagnostics for the LUE-TAL model by site and year.

Site	Year	Optimized Parameters						Diagnostics	
		S_{\max} (°C)	t (days)	X_0 (°C)	K (kPa ⁻¹)	LUE (g C MJ ⁻¹)	γ (m ² mol ⁻¹)	r^2	RMSE (g C m ⁻² d ⁻¹)
RU-Che	2002	21	4	-10	-0.3	3.1	0.09	0.93	0.39
	2003	15	19	2	-0.1	3.6	0.12	0.91	0.47
	2004	15	16	2	-0.5	3.7	0.06	0.88	0.47
	2005	15	1	2	-0.7	3.2	0.12	0.4	0.89
RU-Cho	2003	15	19	-1	-0.1	3.5	0.12	0.91	0.49
	2004	15	22	-7	-0.1	2.1	0.12	0.72	0.52
	2005	15	22	-1	-0.1	3.8	0.12	0.61	0.39
RU-Fyo	2002	30	1	-7	-0.7	3.7	0.03	0.73	1.6
	2003	18	22	-7	-0.5	4	0.06	0.79	1.5
	2004	21	22	-10	-0.1	4	0.12	0.87	1.2
	2005	24	10	-10	-0.3	4	0.06	0.92	1.2
RU-Ha1	2002	15	13	-4	-0.3	2.1	0.12	0.89	0.44
	2003	15	19	-1	-0.3	2.4	0.12	0.84	0.51
	2004	18	7	-1	-0.3	2.6	0.09	0.94	0.55
RU-Zot	2002	15	10	-1	-0.3	3.4	0.12	0.89	0.72
	2003	15	7	-4	-0.5	3.7	0.12	0.73	0.75
	2004	15	10	-4	-0.1	3.2	0.12	0.89	0.77

between the models. The temperature scalar for the LUE, LUE-TA and LUE-TAL models rapidly reach a non-limiting value, while in the BL model temperature is only briefly non-limiting late in the growing season. VPD has a similar but

slightly stronger effect in the LUE and LUE-TA models as compared to the LUE-TAL and BL models. Additionally in Fig. 3, there appears to be consistent underestimation all over and for all models, which is also evidenced by fairly similar

Table 6. Resulting optimized model parameters and regression diagnostics for the BL model by site and year.

Site	Year	Optimized Parameters					Diagnostics	
		S_{\max} (°C)	t (days)	X_0 (°C)	K (kPa ⁻¹)	A_{\max} ($\mu\text{mol CO}_2$ $\text{m}^{-2}\text{s}^{-1}$)	r^2	RMSE ($\text{g C m}^{-2} \text{d}^{-1}$)
RU-Che	2002	18	1	-4	-0.5	18	0.91	0.46
	2003	18	10	5	-0.1	20	0.92	0.44
	2004	15	13	5	-0.3	20	0.8	0.6
	2005	21	1	5	-0.7	16	0.41	0.88
RU-Cho	2003	21	10	2	-0.1	22	0.93	0.42
	2004	15	1	-10	-0.1	8	0.8	0.44
	2005	30	19	-10	-0.1	14	0.57	0.41
RU-Fyo	2002	30	1	-4	-0.7	38	0.68	1.8
	2003	18	22	-4	-0.5	38	0.76	1.6
	2004	15	10	-1	-0.3	28	0.88	1.2
	2005	15	4	-1	-0.5	40	0.91	1.2
RU-Ha1	2002	27	1	-7	-0.1	8	0.87	0.48
	2003	21	10	5	-0.1	16	0.78	0.6
	2004	27	4	5	-0.1	26	0.9	0.69
RU-Zot	2002	15	7	2	-0.3	16	0.9	0.69
	2003	15	10	-1	-0.3	14	0.74	0.73
	2004	15	7	-1	-0.1	16	0.89	0.77

r^2 and RMSE values. In particular, it seems that all models underestimate the latter half of the growing season.

At the Hakasia site (Fig. 4), situated on the southern steppe, the LUE-TAL model appears to best capture the seasonal GPP flux. The environmental scalars again display large discrepancies among models. There appears a consistent overestimation for all models in the early stages of the growing season, most apparent in the LUE-TA, LUT-TAL and BL models. This is the only site among the five sites studied which is potentially water-limited. As none of the models account for possible water constraints (aside from VPD), it may be that results at this site would benefit from the addition of a water-related environmental scalar.

3.1 Model evaluation

Mean square error was used as an indicator of performance resulting from cross-validation where the smaller of the MSE values is preferred (Table 7). For the majority of site year combinations (with the exception of RU-Che 2004/2005 and RU-Fyo 2002), the MSE values for the LUE and LUE-TA models are larger than those of the LUE-TAL and BL models. Hence, based on the 10-out cross-validation performed here, the LUE-TAL and BL models, accounting for temperature acclimation and a non-linear light response, generally outperform the LUE and LUE-TA approaches. In particular, the LUE-TAL records a lower MSE in 8 of the 17 site year combinations, along with the lowest overall mean MSE. The

Table 7. Cross-validation results (MSE) from the LUE, LUE-TA, LUE-TAL and BL models for all site years, and mean results for each model. Bold indicates lowest recorded MSE values per site year and model.

Site	Year	LUE	LUE-TA	LUE-TAL	BL
RU-Che	2002	0.451	0.43	0.24	0.309
	2003	2.152	0.377	0.269	0.211
	2004	1.269	0.43	0.452	0.672
	2005	1.646	1.62	1.806	1.804
RU-Cho	2003	1.873	0.743	0.573	0.493
	2004	0.907	0.844	0.381	0.295
	2005	3.522	1.86	1.069	0.903
RU-Fyo	2002	5.393	5.544	6.944	5.869
	2003	4.013	4.506	3.116	3.827
	2004	2.87	2.44	1.543	1.796
	2005	3.207	2.491	1.534	1.886
RU-Ha1	2002	0.505	0.458	0.223	0.289
	2003	0.732	0.557	0.313	0.492
	2004	0.589	0.477	0.462	0.576
RU-Zot	2002	1.783	0.879	0.785	0.782
	2003	1.591	1.431	0.96	0.836
	2004	1.422	1.281	0.802	1.03
Mean		1.996	1.551	1.263	1.298

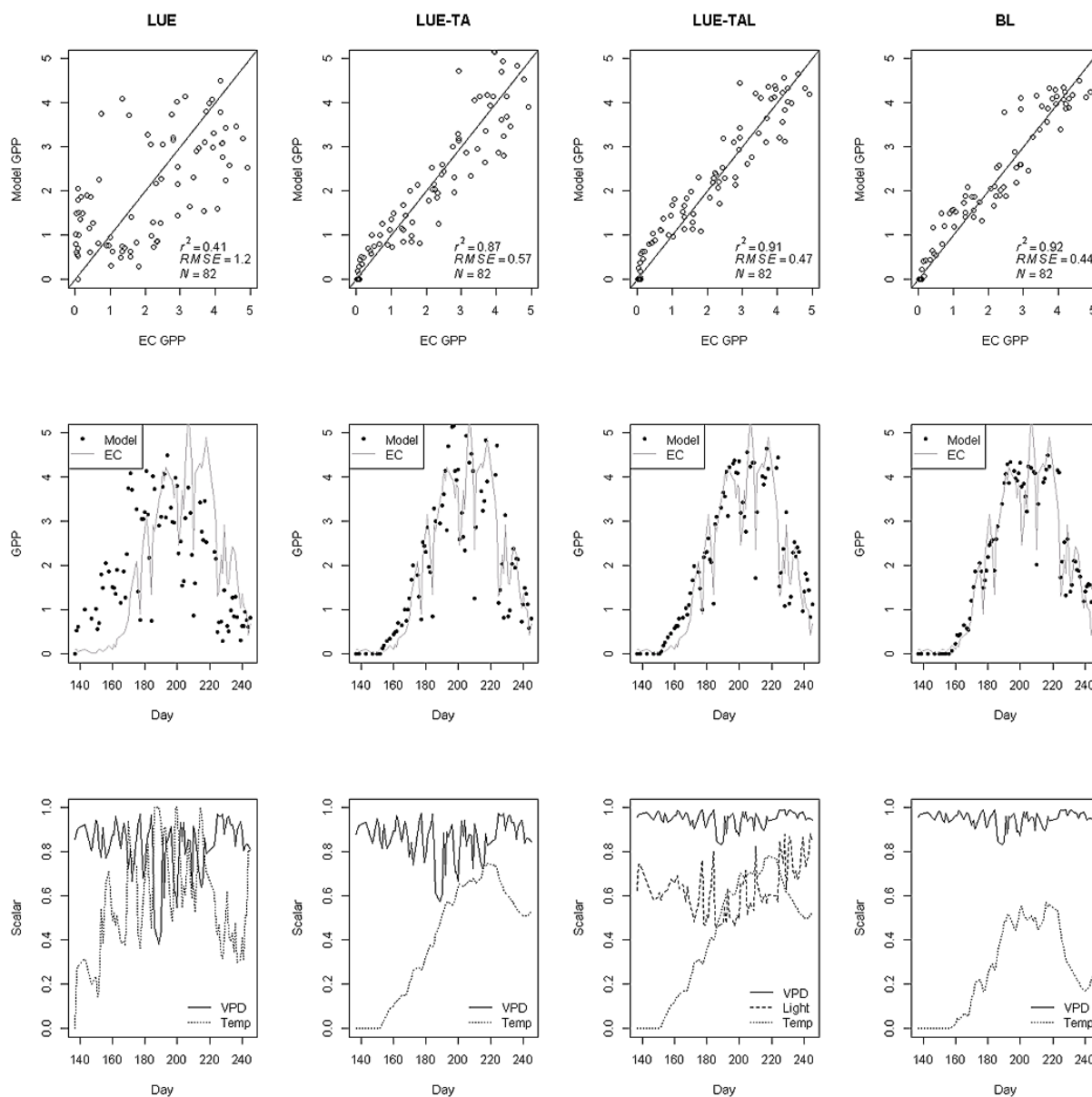


Fig. 2. Results for Cherskii, 2003, from the LUE (1st column), LUE-TA (2nd column), LUE-TAL (3rd column) and BL (4th column) models where the top row depicts scatterplots of eddy covariance (EC) GPP vs. model GPP, the middle row depicts the daily course of GPP (EC and model) and the bottom row depicts the environmental scalars for temperature and VPD. GPP in units of $\text{g C m}^{-2} \text{d}^{-1}$.

BL model records the lowest MSE in 6 of the 17 site year combinations.

Based on this assessment, the LUE-TAL model appears to perform better in less environmentally stressful sites, while the BL model generally outperforms in more climate-controlled sites. On two occasions at the Cherskii site, the LUE-TA model outperforms the models with a non-linear light response, underscoring the effect of temperature at these locations.

The results of this study are novel in terms of the following:

1. The results compare the response of four diagnostic GPP models over Russia, clearly demonstrating the improvement that temperature acclimation makes when included in the models at strongly temperature-controlled high latitudes. Owing to the paucity of available flux tower data over Russia and its enormous size and unique biome characteristics, such a comparison is warranted.
2. The first of the non-linear models is actually the MODIS GPP algorithm. To our knowledge this is the first study to point to potential difficulties in

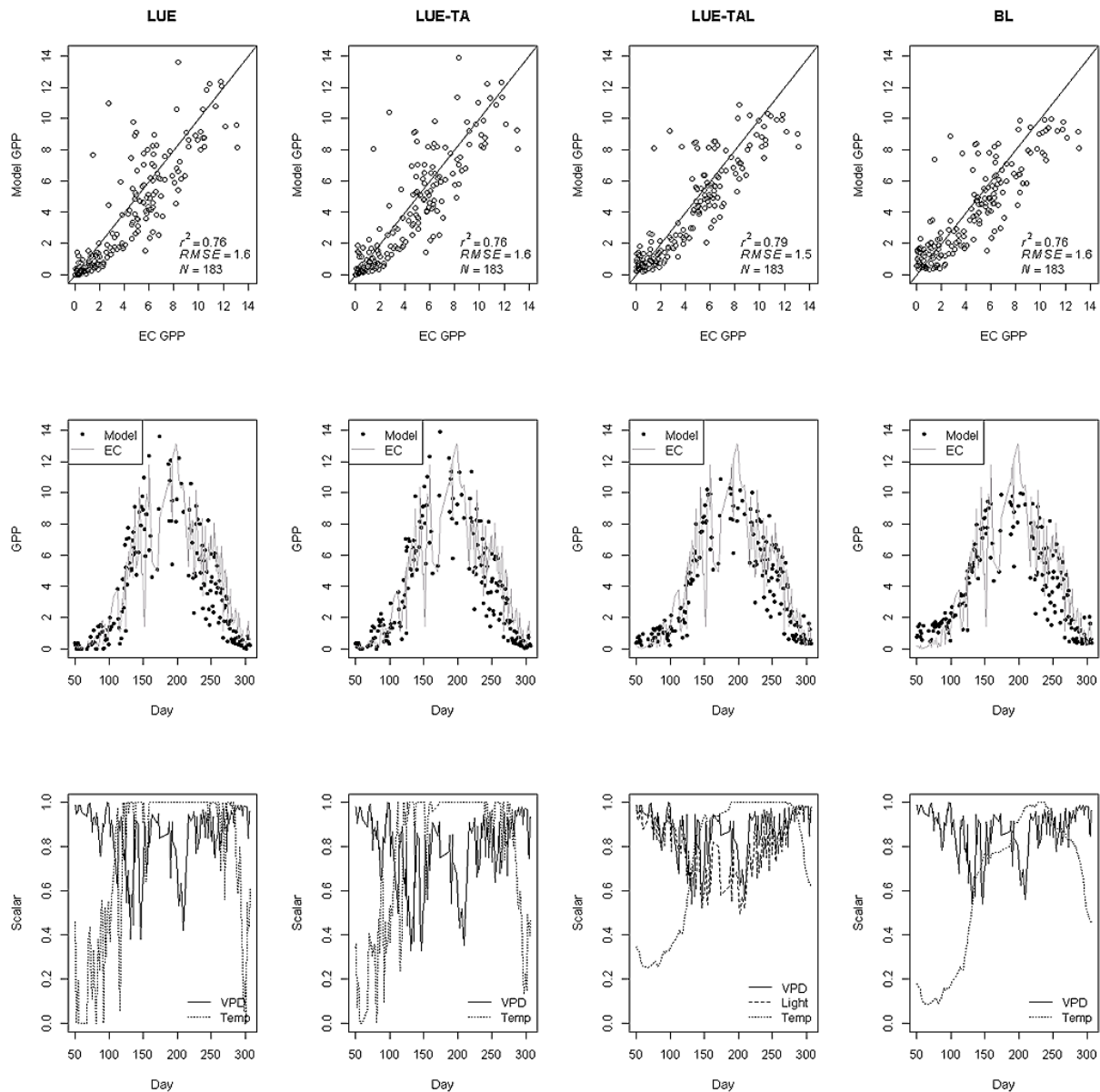


Fig. 3. Results for Fyodorovskoe, 2003, from the LUE (1st column), LUE-TA (2nd column), LUE-TAL (3rd column) and BL (4th column) models where the top row depicts scatter plots of EC GPP vs. model GPP, the middle row depicts the daily course of GPP (EC and model) and the bottom row depicts the environmental scalars for temperature and VPD. GPP in units of $\text{g C m}^{-2} \text{d}^{-1}$.

the MODIS approach at flux tower sites in the far north, which could potentially be resolved by applying temperature acclimation. To date many studies have pointed to difficulties in comparing MODIS results with flux tower estimates; however they have largely identified problems with input data (f_{APAR} , meteo, etc) or a lack of a soil water modifier (Pan et al., 2006; Turner et al., 2006).

3. The model comparison includes the big leaf model, parameterized with modifiers for temperature acclimation and VPD. To our knowledge, our use of environ-

mental modifiers in a big-leaf light absorption model is new.

4 Conclusions

In this study we present a comparison of four LUE-based GPP modelling approaches parameterized over five EC sites across Russia. This study focused on Russia, a vast country with large carbon pools and fluxes, properties unique to the northern hemisphere (i.e. permafrost which holds vast quantities of soil carbon; Tarnocai et al., 2009), and one predicted

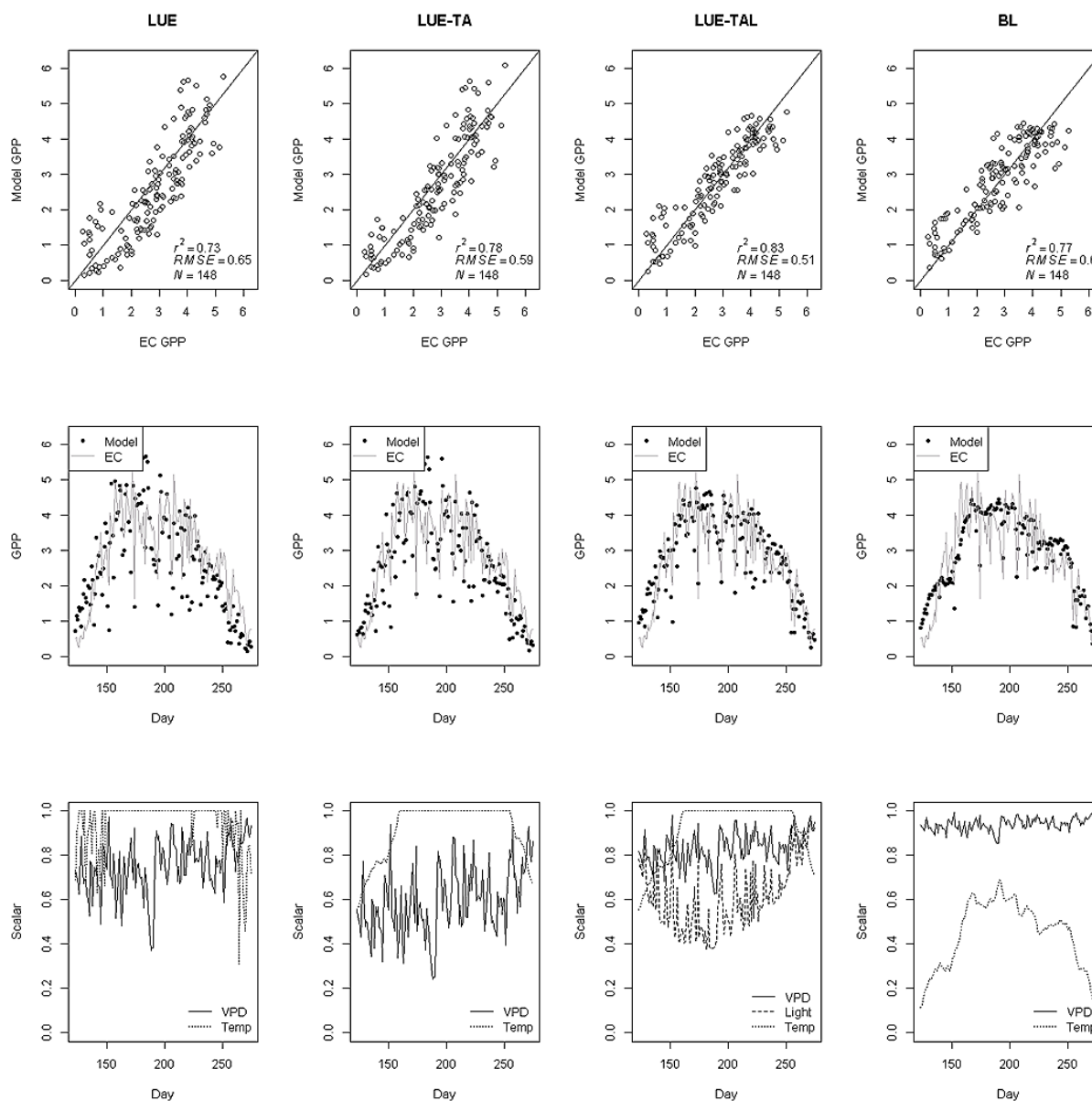


Fig. 4. Results for Hakasia, 2003, from the LUE (1st column), LUE-TA (2nd column), LUE-TAL (3rd column) and BL (4th column) models where the top row depicts scatter plots of EC GPP vs. model GPP, the middle row depicts the daily course of GPP (EC and model) and the bottom row depicts the environmental scalars for temperature and VPD. GPP in units of $\text{g C m}^{-2} \text{d}^{-1}$.

to experience significant forms of environmental change. Various studies have pointed to difficulties when examining results from global diagnostic LUE models at the biome level (Pan et al., 2006; Turner et al., 2006; Shvidenko et al., 2010). The results presented here (using cross-validation) clearly demonstrate that accounting for temperature acclimation particularly at northern (temperature-controlled) sites significantly improves fit of modelled versus eddy-covariance-derived daily GPP values. These results indicate that inclusion of temperature acclimation on sites experiencing cold temperatures is imperative. Furthermore, models with a non-

linear light response generally outperform models with a linear light response, increasingly so at the southern less temperature-controlled sites. Thus, developing models that address unique biome-level properties calibrated with EC data may help to improve the accuracy of global LUE-based models.

Findings from this study are important as vegetation productivity is a key input variable in many ecosystem models. These models require, among other datasets, an accurate depiction of vegetation productivity in order to address a variety of global land use issues. Hence, reducing uncertainty

in gross primary productivity estimates is a key goal within the scientific community. Future efforts should focus on up-scaling the results presented here and in similar studies. In order to facilitate this, there is a need for a substantial expansion (by several orders of magnitude) of the ground-based observation network (Ciais et al., 2013). Finally, we think the findings from our study are useful for the modelling community in general, who are perhaps not entirely aware of the impacts that including (in particular) temperature acclimation may have on model results.

Acknowledgements. N. Khabarov (IIASA), A. Smirnov (IIASA), N. Gobron (JRC) and C. Beer (MPI) provided assistance and data. FLUXNET (<http://www.fluxdata.org>) provided access to the TCOS eddy covariance data (special thanks to D. Papale and the tower Principle Investigators). The IIASA Library provided valuable resources. The EnerGEO (FP7 226364) and GEOCARBON (FP7 283080) projects partially supported this study. R statistical software is also acknowledged. M. van der Molen provided comments on an earlier draft.

Edited by: P. Stoy

References

- Anderson, M. C., Norman, J. M., Meyers, T. P., and Diak, G. R.: An analytical model for estimating canopy transpiration and carbon assimilation fluxes based on canopy light-use efficiency, *Agr. Forest Meteorol.*, 101, 265–289, 2000.
- Arneth, A., Kurbatova, J., Kolle, O., Shibistova, O. B., Lloyd, J., Vygodskaya, N. N., and Schulze, E. D.: Comparative ecosystem-atmosphere exchange of energy and mass in a european russian and a central siberian bog ii. Interseasonal and interannual variability of CO₂ fluxes, *Tellus B*, 54, 514–530, 2002.
- Baldocchi, D., Falge, E., Gu, L., Olson, R., Hollinger, D., Running, S., Anthoni, P., Bernhofer, C., Davis, K., Evans, R., Fuentes, J., Goldstein, A., Katul, G., Law, B., Lee, X., Malhi, Y., Meyers, T., Munger, W., Oechel, W., Paw, U. K. T., Pilegaard, K., Schmid, H. P., Valentini, R., Verma, S., Vesala, T., Wilson, K., and Wofsy, S.: Fluxnet: A new tool to study the temporal and spatial variability of ecosystem-scale carbon dioxide, water vapor, and energy flux densities, *B. Am. Meteorol. Soc.*, 82, 2415–2434, 2001.
- Balzer, H., Gerard, F. F., George, C. T., Rowland, C. S., Jupp, T. E., McCallum, I., Shvidenko, A., Nilsson, S., Sukhinin, A., Onuchin, A., and Schmullius, C.: Impact of the arctic oscillation pattern on interannual forest fire variability in central siberia, *Geophys. Res. Lett.*, 32, 1–4, 2005.
- Beer, C., Reichstein, M., Tomelleri, E., Ciais, P., Jung, M., Carvalhais, N., Roedenbeck, C., Arain, M. A., Baldocchi, D., Bonan, G. B., Bondeau, A., Cescatti, A., Lasslop, G., Lindroth, A., Lomas, M., Luysaert, S., Margolis, H., Oleson, K. W., Rouspard, O., Veenendaal, E., Viovy, N., Williams, C., Woodward, F. I., and Papale, D.: Terrestrial gross carbon dioxide uptake: Global distribution and covariation with climate, *Science*, 329, 834–838, 2010.
- Churkina, G. and Running, S. W.: Contrasting climatic controls on the estimated productivity of global terrestrial biomes, *Ecosystems*, 1, 206–215, 1998.
- Ciais, P., Dolman, A. J., Bombelli, A., Duren, R., Pregon, A., Rayner, P. J., Miller, C., Gobron, N., Kinderman, G., Marland, G., Gruber, N., Chevallier, F., Andres, R. J., Balsamo, G., Bopp, L., Bréon, F.-M., Broquet, G., Dargaville, R., Battin, T. J., Borges, A., Bovensmann, H., Buchwitz, M., Butler, J., Canadell, J. G., Cook, R. B., DeFries, R., Engelen, R., Gurney, K. R., Heinze, C., Heimann, M., Held, A., Henry, M., Law, B., Luysaert, S., Miller, J., Moriyama, T., Moulin, C., Myneni, R. B., Nussli, C., Obersteiner, M., Ojima, D., Pan, Y., Paris, J.-D., Piao, S. L., Poulter, B., Plummer, S., Quegan, S., Raymond, P., Reichstein, M., Rivier, L., Sabine, C., Schimel, D., Tarasova, O., Valentini, R., van der Werf, G., Wickland, D., Williams, M., and Zehner, C.: Current systematic carbon cycle observations and needs for implementing a policy-relevant carbon observing system, *Biogeosciences Discuss.*, 10, 11447–11581, doi:10.5194/bgd-10-11447-2013, 2013.
- Corradi, C., Kolle, O., Walter, K., Zimov, S. A., and Schulze, E. D.: Carbon dioxide and methane exchange of a north-east siberian tussock tundra, *Glob. Change Biol.*, 11, 1910–1925, doi:10.1111/j.1365-2486.2005.01023.x, 2005.
- Desai, A. R., Richardson, A. D., Moffat, A. M., Kattge, J., Hollinger, D. Y., Barr, A., Falge, E., Noormets, A., Papale, D., Reichstein, M., and Stauch, V. J.: Cross-site evaluation of eddy covariance gpp and re decomposition techniques, *Agr. Forest Meteorol.*, 148, 821–838, 2008.
- Falge, E., Baldocchi, D., Olson, R., Anthoni, P., Aubinet, M., Bernhofer, C., Burba, G., Ceulemans, R., Clement, R., Dolman, H., Granier, A., Gross, P., Grünwald, T., Hollinger, D., Jensen, N. O., Katul, G., Keronen, P., Kowalski, A., Lai, C. T., Law, B. E., Meyers, T., Moncrieff, J., Moors, E., Munger, J. W., Pilegaard, K., Rannik, Ü., Rebmann, C., Suyker, A., Tenhunen, J., Tu, K., Verma, S., Vesala, T., Wilson, K., and Wofsy, S.: Gap filling strategies for defensible annual sums of net ecosystem exchange, *Agr. Forest Meteorol.*, 107, 43–69, 2001.
- Forster, M. R.: Key concepts in model selection: Performance and generalizability, *J. Math. Psychol.*, 44, 205–231, doi:10.1006/jmps.1999.1284, 2000.
- Franklin, O.: Optimal nitrogen allocation controls tree responses to elevated CO₂, *New Phytol.*, 174, 811–822, 2007.
- Friend, A. D., Arneth, A., Kiang, N. Y., Lomas, M., Ogee, J., Roedenbeck, C., Running, S. W., Santaren, J. D., Sitch, S., Viovy, N., Ian Woodward, F., and Zaehle, S.: Fluxnet and modelling the global carbon cycle, *Glob. Change Biol.*, 13, 610–633, 2007.
- Gobron, N., Pinty, B., Aussenat, O., Chen, J. M., Cohen, W. B., Fensholt, R., Gond, V., Huemmrich, K. F., Lavergne, T., Mélin, F., Privette, J. L., Sandholt, I., Taberner, M., Turner, D. P., Verstraete, M. M., and Widlowski, J.-L.: Evaluation of fraction of absorbed photosynthetically active radiation products for different canopy radiation transfer regimes: Methodology and results using joint research center products derived from seawifs against ground-based estimations, *J. Geophys. Res.-Atmos.*, 111, D13110, doi:10.1029/2005jd006511, 2006.
- Goldammer, J. G.: The boreal forest, fire, and the global climate system: Achievements and needs in joint east-west boreal fire research and policy development, *Combust. Explo. Shock+*, 32, 544–557, 1996.

- Hastie, T., Tibshirani, R., and Friedman, J.: The elements of statistical learning, "Data mining, inference, and prediction", Springer, New York, NY, USA, 2001.
- Hirose, T. and Werger, M. J. A.: Nitrogen use efficiency in instantaneous and daily photosynthesis of leaves in the canopy of a *solidago altissima* stand, *Physiol. Plant.*, 70, 215–222, 1987.
- Hirose, T., Ackerly, D. D., Traw, M. B., Ramseier, D., and Bazzaz, F. A.: CO₂ elevation, canopy photosynthesis, and optimal leaf area index, *Ecology*, 78, 2339–2350, 1997.
- Jung, M., Verstraete, M., Gobron, N., Reichstein, M., Papale, D., Bondeau, A., Robustelli, M., and Pinty, B.: Diagnostic assessment of european gross primary production, *Glob. Change Biol.*, 14, 2349–2364, 2008.
- Kajii, Y., Kato, S., Streets, D. G., Tsai, N. Y., Shvidenko, A., Nilsson, S., McCallum, I., Minko, N. P., Abushenko, N., Altyntsev, D., and Khodzer, T. V.: Boreal forest fires in siberia in 1998: Estimation of area burned and emissions of pollutants by advanced very high resolution radiometer satellite data, *J. Geophys. Res.-Atmos.*, 107, 4745, doi:10.1029/2001JD001078, 2002.
- King, D. A., Turner, D. P., and Ritts, W. D.: Parameterization of a diagnostic carbon cycle model for continental scale application, *Remote Sens. Environ.*, 115, 1653–1664, 2011.
- Landsberg, J. J. and Waring, R. H.: A generalised model of forest productivity using simplified concepts of radiation-use efficiency, carbon balance and partitioning, *Forest Ecol. Manag.*, 95, 209–228, 1997.
- Lasslop, G., Migliavacca, M., Bohrer, G., Reichstein, M., Bahn, M., Ibrom, A., Jacobs, C., Kolari, P., Papale, D., Vesala, T., Wohlfahrt, G., and Cescatti, A.: On the choice of the driving temperature for eddy-covariance carbon dioxide flux partitioning, *Biogeosciences*, 9, 5243–5259, doi:10.5194/bg-9-5243-2012, 2012.
- Mäkelä, A., Pulkkinen, M., Kolari, P., Lagergren, F., Berbigier, P., Lindroth, A., Loustau, D., Nikinmaa, E., Vesala, T., and Hari, P.: Developing an empirical model of stand gpp with the lue approach: Analysis of eddy covariance data at five contrasting conifer sites in europe, *Glob. Change Biol.*, 14, 92–108, 2008.
- Belelli Marchesini, L., Papale, D., Reichstein, M., Vuichard, N., Tchebakova, N., and Valentini, R.: Carbon balance assessment of a natural steppe of southern Siberia by multiple constraint approach, *Biogeosciences*, 4, 581–595, doi:10.5194/bg-4-581-2007, 2007.
- McCallum, I., Wagner, W., Schmulilius, C., Shvidenko, A., Obersteiner, M., Fritz, S., and Nilsson, S.: Satellite-based terrestrial production efficiency modeling, *Carbon Balance and Management*, 4, 8, doi:10.1186/1750-0680-4-8, 2009.
- Merbold, L., Kutsch, W. L., Corradi, C., Kolle, O., Rebmann, C., Stoy, P. C., Zimov, S. A., and Schulze, E. D.: Artificial drainage and associated carbon fluxes (CO₂/CH₄) in a tundra ecosystem, *Glob. Change Biol.*, 15, 2599–2614, 2009.
- Milyukova, I. M., Kolle, O., Varlagin, A. V., Vygodskaya, N. N., Schulze, E. D., and Lloyd, J.: Carbon balance of a southern taiga spruce stand in european russia, *Tellus B*, 54, 429–442, 2002.
- Moffat, A. M., Papale, D., Reichstein, M., Hollinger, D. Y., Richardson, A. D., Barr, A. G., Beckstein, C., Braswell, B. H., Churkina, G., Desai, A. R., Falge, E., Gove, J. H., Heimann, M., Hui, D., Jarvis, A. J., Kattge, J., Noormets, A., and Stauch, V. J.: Comprehensive comparison of gap-filling techniques for eddy covariance net carbon fluxes, *Agr. Forest Meteorol.*, 147, 209–232, 2007.
- Pan, Y., Birdsey, R., Hom, J., McCullough, K., and Clark, K.: Improved estimates of net primary productivity from modis satellite data at regional and local scales, *Ecol. Appl.*, 16, 125–132, 2006.
- Papale, D. and Valentini, R.: A new assessment of european forests carbon exchanges by eddy fluxes and artificial neural network spatialization, *Glob. Change Biol.*, 9, 525–535, 2003.
- Papale, D., Reichstein, M., Aubinet, M., Canfora, E., Bernhofer, C., Kutsch, W., Longdoz, B., Rambal, S., Valentini, R., Vesala, T., and Yakir, D.: Towards a standardized processing of Net Ecosystem Exchange measured with eddy covariance technique: algorithms and uncertainty estimation, *Biogeosciences*, 3, 571–583, doi:10.5194/bg-3-571-2006, 2006.
- Reichstein, M., Falge, E., Baldocchi, D., Papale, D., Aubinet, M., Berbigier, P., Bernhofer, C., Buchmann, N., Gilmanov, T., Granier, A., Grünwald, T., Havránková, K., Ilvesniemi, H., Janous, D., Knohl, A., Laurila, T., Lohila, A., Loustau, D., Matteucci, G., Meyers, T., Miglietta, F., Ourcival, J.-M., Pumpanen, J., Rambal, S., Rotenberg, E., Sanz, M., Tenhunen, J., Seufert, G., Vaccari, F., Vesala, T., Yakir, D., and Valentini, R.: On the separation of net ecosystem exchange into assimilation and ecosystem respiration: Review and improved algorithm, *Glob. Change Biol.*, 11, 1424–1439, doi:10.1111/j.1365-2486.2005.001002.x, 2005.
- Ruimy, A., Dedieu, G., and Saugier, B.: Turc: A diagnostic model of continental gross primary productivity and net primary productivity, *Global Biogeochem. Cy.*, 10, 269–285, 1996.
- Running, S. W., Thornton, P. E., Nemani, R., and Glassy, J. M.: Global terrestrial gross and net primary productivity from the earth observing system., in: *Methods in ecosystem science*, edited by: Sala, O. E., Jackson, R. B., Mooney, H. A., and Howarth, R. W., Springer-Verlag, New York, 44–57, 2000.
- Running, S. W., Nemani, R. R., Heinsch, F. A., Zhao, M., Reeves, M., and Hashimoto, H.: A continuous satellite-derived measure of global terrestrial primary production, *BioScience*, 54, 547–560, 2004.
- Schaefer, K., Schwalm, C. R., Williams, C., Arain, M. A., Barr, A., Chen, J. M., Davis, K. J., Dimitrov, D., Hilton, T. W., Hollinger, D. Y., Humphreys, E., Poulter, B., Raczka, B. M., Richardson, A. D., Sahoo, A., Thornton, P., Vargas, R., Verbeeck, H., Anderson, R., Baker, I., Black, T. A., Bolstad, P., Chen, J., Curtis, P. S., Desai, A. R., Dietze, M., Dragoni, D., Gough, C., Grant, R. F., Gu, L., Jain, A., Kucharik, C., Law, B., Liu, S., Lokipitiya, E., Margolis, H. A., Matamala, R., McCaughey, J. H., Monson, R., Munger, J. W., Oechel, W., Peng, C., Price, D. T., Ricciuto, D., Riley, W. J., Roulet, N., Tian, H., Tonitto, C., Torn, M., Weng, E., and Zhou, X.: A model-data comparison of gross primary productivity: Results from the north american carbon program site synthesis, *J. Geophys. Res.-Biogeo.*, 117, G03010, doi:10.1029/2012JG001960, 2012.
- Schepaschenko, D., McCallum, I., Shvidenko, A., Fritz, S., Kraxner, F., and Obersteiner, M.: A new hybrid land cover dataset for russia: A methodology for integrating statistics, remote sensing and in situ information, *J. Land Use Sci.*, 6, 245–259, doi:10.1080/1747423x.2010.511681, 2011.
- Shvidenko, A. and Nilsson, S.: A synthesis of the impact of russian forests on the global carbon budget for 1961–1998, *Tellus B*, 55, 391–415, 2003.
- Shvidenko, A., Schepaschenko, D., McCallum, I., and Nilsson, S.: Can the uncertainty of full carbon accounting of forest ecosys-

- tems be made acceptable to policymakers?, *Climatic Change*, 103, 137–157, 2010.
- Sitch, S., Smith, B., Prentice, I. C., Arneth, A., Bondeau, A., Cramer, W., Kaplan, J. O., Levis, S., Lucht, W., Sykes, M. T., Thonicke, K., and Venevsky, S.: Evaluation of ecosystem dynamics, plant geography and terrestrial carbon cycling in the Isp dynamic global vegetation model, *Glob. Change Biol.*, 9, 161–185, 2003.
- Sjoestrom, M., Ardoe, J., Arneth, A., Boulain, N., Cappelaere, B., Eklundh, L., de Grandcourt, A., Kutsch, W. L., Merbold, L., Nouvellon, Y., Scholes, R. J., Schubert, P., Seaquist, J., and Veenendaal, E. M.: Exploring the potential of modis evi for modeling gross primary production across african ecosystems, *Remote Sens. Environ.*, 115, 1081–1089, doi:10.1016/j.rse.2010.12.013, 2011.
- Stanhill, G. and Fuchs, M.: The relative flux density of photosynthetically active radiation, *J. Appl. Ecol.*, 14, 317–322 1977.
- Stephens, B. B., Gurney, K. R., Tans, P. P., Sweeney, C., Peters, W., Bruhwiler, L., Ciais, P., Ramonet, M., Bousquet, P., Nakazawa, T., Aoki, S., Machida, T., Inoue, G., Vinnichenko, N., Lloyd, J., Jordan, A., Heimann, M., Shibistova, O., Langenfelds, R. L., Steele, L. P., Francey, R. J., and Denning, A. S.: Weak northern and strong tropical land carbon uptake from vertical profiles of atmospheric CO₂, *Science*, 316, 1732–1735, 2007.
- Stone, M.: An asymptotic equivalence of choice of model by cross-validation and akaike's criterion, *J. R. Stat. Soc. B Meth.*, 39, 44–47, <http://www.jstor.org/stable/2984877>, 1977.
- Stoy, P. C., Katul, G. G., Siqueira, M. B. S., Juang, J. Y., Novick, K. A., Uebelherr, J. M., and Oren, R.: An evaluation of models for partitioning eddy covariance-measured net ecosystem exchange into photosynthesis and respiration, *Agr. Forest Meteorol.*, 141, 2–18, 2006.
- Tarnocai, C., Canadell, J. G., Schuur, E. A. G., Kuhry, P., Mazhitova, G., and Zimov, S.: Soil organic carbon pools in the northern circumpolar permafrost region, *Global Biogeochem. Cy.*, 23, GB2023, doi:10.1029/2008gb003327, 2009.
- Tchebakova, N. M., Kolle, O., Zolotoukhine, D., Arneth, A., Styles, J. M., Vygodskaya, N. N., Schulze, E. D., Shibistova, O., and Llyod, J.: Inter-annual and seasonal variations of energy and water vapour fluxes above a pinus sylvestris forest in the siberian middle taiga, *Tellus B*, 54, 537–551, 2002.
- Turner, D. P., Ritts, W. D., Cohen, W. B., Gower, S. T., Running, S. W., Zhao, M., Costa, M. H., Kirschbaum, A. A., Ham, J. M., Saleska, S. R., and Ahl, D. E.: Evaluation of modis npp and gpp products across multiple biomes, *Remote Sens. Environ.*, 102, 282–292, 2006.
- van der Molen, M. K., van Huissteden, J., Parmentier, F. J. W., Petrescu, A. M. R., Dolman, A. J., Maximov, T. C., Kononov, A. V., Karsanaev, S. V., and Suzdalov, D. A.: The growing season greenhouse gas balance of a continental tundra site in the Indigirka lowlands, NE Siberia, *Biogeosciences*, 4, 985–1003, doi:10.5194/bg-4-985-2007, 2007.
- van Dijk, A. I. J. M., Dolman, A. J., and Schulze, E. D.: Radiation, temperature, and leaf area explain ecosystem carbon fluxes in boreal and temperate european forests, *Global Biogeochem. Cy.*, 19, 1–15, 2005.
- Vygodskaya, N. N., Milyukova, I., Varlagin, A., Tatarinov, F., Sogachev, A., Kobak, K. I., Desyatkin, R., Bauer, G., Hollinger, D. Y., Kelliher, F. M., and Schulze, E. D.: Leaf conductance and CO₂ assimilation of larix gmelinii growing in an eastern siberian boreal forest, *Tree Physiol.*, 17, 607–615, 1997.
- Wong, S. C., Cowan, I. R., and Farquhar, D. G.: Stomatal conductance correlates with photosynthetic capacity, *Nature*, 282, 424–426, 1979.

Continental GPP mapping: use of a diagnostic model parameterized with FLUXNET data

I. McCallum¹, O. Franklin¹, E. Moltchanova², A. Shvidenko¹, D. Schepaschenko¹

[1] International Institute for Applied Systems Analysis, Laxenburg, Austria

[2] Department of Mathematics and Statistics, University of Canterbury, Christchurch, New Zealand

Abstract

In recent decades, a number of methodologies have been developed to map regional to global Gross Primary Productivity (GPP). With the advent of the global FLUXNET network, an in-situ dataset is now available to aid in this task. The FLUXNET network has varying density dependent upon location, with Northern Eurasia (in particular Russia) being a particularly sparsely sampled region. Hence different approaches may need to be applied where coverage is sparse, as opposed to parts of the globe which are densely sampled. The method presented here relies on a diagnostic GPP model parameterized with available FLUXNET data. In particular it explicitly models long term mean values for growing season temperature, deemed to be the most limiting environmental factor over northern Eurasia. Additionally, satellite derived fAPAR and meteorological data are used. Evaluation of model performance is made by comparing the resulting map against a global satellite-based GPP model and a carbon accounting approach. Results indicate that this method provides a potentially valuable approach in regions such as Russia where in-situ data are sparse and such a strong temperature control exists.

Introduction

Continental mapping of Gross Primary Productivity (GPP) has traditionally been performed with process-based vegetation models e.g. ([Quegan, Beer et al. 2011](#)), atmospheric measurements e.g. ([Stephens, Gurney et al. 2007](#)), diagnostic satellite-based techniques e.g. ([Running, Nemani et al. 2004](#)) or carbon accounting e.g. ([Shvidenko and Nilsson 2003](#)). Recent efforts however have focused on exploiting the increasing amount of flux towers via various forms of upscaling ([Beer, Reichstein et al. 2010](#); [Xiao, Chen et al. 2012](#)). Upscaling methods can be generally defined as data-driven or data-assimilation approaches. Data-assimilation approaches as employed in this study are typically based on simple ecosystem models and parameter estimation techniques ([Xiao, Chen et al. 2012](#)). The challenge is implementing these techniques over large areas where few FLUXNET measurements exist (i.e. Russia). Obviously, the representativeness of flux networks will influence the accuracy of the gridded flux estimates derived from tower fluxes through upscaling ([Xiao, Chen et al. 2012](#)).

This study presents a method of continental GPP mapping using a diagnostic model parameterized with limited FLUXNET data over Russia ([McCallum, Franklin et al. 2013](#)). It employs an fAPAR dataset that was deemed applicable over this region ([McCallum, Wagner et al. 2010](#)). Additionally it accounts for temperature acclimation, a phenomenon known to affect photosynthesis in boreal regions ([Mäkelä, Pulkkinen et al. 2008](#)). The model parameters for temperature, Vapour Pressure Deficit (VPD) and A_{max} were found to vary geographically and to have a linear association with long-term mean values of temperature. This finding was used to extrapolate GPP beyond the initial flux tower sites to the whole of Russia. Evaluation of the methodology presented here was made by comparison against results obtained from carbon accounting ([Shvidenko and Nilsson 2003](#)) and a diagnostic satellite-based model ([Running, Nemani et al. 2004](#)). Previous results obtained from carbon accounting over Siberia ([Quegan, Beer et al. 2011](#)), demonstrate that the carbon accounting method acts as a good benchmark for primary productivity.

Methods

Study Region

The study region was chosen to approximate the extent of boreal Russia, with coordinates 50°N, 30°E; and 70°N, 150°E. The boreal forests of Russia comprise almost one fourth of the worlds forest cover, making these forests a unique natural phenomenon at the global scale ([Shvidenko, Schepaschenko et al. 2007](#)). In addition, vast areas are characterized by tundra ecosystems, dominated by shrubs, grasses and sedges, mostly above permafrost. This large land area undergoes great annual changes in albedo and productivity as seasonal temperatures swing well above and below 0° C. Large regions lie in various stages of permafrost and the area is prone to catastrophic disturbances including fire ([Goldammer 1996](#); [Kajii, Kato et al. 2002](#); [Balzter, Gerard et al. 2005](#)).

Data

The various datasets required for this study appear in Table 1. The datasets represent a mixture of meteorological reanalysis data and satellite-based datasets. All datasets were resampled to 0.25°. fAPAR (the fraction of absorbed photosynthetically active radiation) was resampled to daily resolution. All data spans the years 2002 - 2005. Additionally, a long term growing season (May to September) mean annual dataset was produced spanning years 1975 – 2000 for temperature.

Table 1. Required input datasets.

Description	Time	Orig. Size	Units	Source
Photosynthetically Active Radiation (PAR)	2002-2005	1.5°	W m ⁻² s ⁻¹	ecmwf.int (ERA-Interim)
Temperature	2002-2005	1.5°	K	ecmwf.int (ERA-Interim)
Dew Point Temperature	2002-2005	1.5°	K	ecmwf.int (ERA-Interim)
Fraction of Absorbed PAR	2002-2005	0.25°	%	fAPAR.jrc.ec.europa.eu
Mean Temperature (May to September)	1975 - 2000	1.0°	K	http://mars.jrc.ec.europa.eu/

This study employs reanalysis data from the European Centre for Medium Range Weather Forecast (ECMWF) – specifically the ERA-Interim and ERA40 datasets. ERA-Interim makes use of data from the increasing number of new instruments on satellites from 2003 onwards. A major problem with the use of observations for climate analysis is the presence of biases ([Dee, Uppala et al. 2011](#)). In spite of best efforts to remove all systematic errors at the source, some residual biases inevitably remain. It is, however, assumed that the coarse resolution meteorological data represent ground conditions and are homogeneous within each cell. VPD was estimated from dew point temperature T_d (°K) and

air temperature T_a (°K) according to ([Monteith and Unsworth 1990](#)). Among several existing meteorological reanalysis datasets, ECMWF was found to have the highest accuracy([Zhao, Running et al. 2006](#)).

fAPAR is defined as the fraction of Photosynthetically Active Radiation (PAR) absorbed by vegetation, where PAR is the solar radiation reaching the vegetation in the wavelength region 0.4 – 0.7 micrometers. Various fAPAR datasets were compared over Northern Eurasia ([McCallum, Wagner et al. 2010](#)). Results suggested that the JRC fAPAR ([Gobron, Pinty et al. 2006](#)) performed well for this region, and hence that dataset was used in this study.

Flux Towers

Data for model calibration were obtained from www.fluxdata.org for five sites with eddy covariance flux measurements in Russia: Cherskii, Chokurdakh, Fyodorovskoe, Zotino, and Yakutia (Table 2). The eddy covariance method, a micrometeorological technique, provides a direct measure of the net exchange of carbon and water between vegetated canopies and the atmosphere ([Baldocchi, Falge et al. 2001](#)). For all sites, gap-filled and flux-partitioned daily data was obtained, having been treated according to standard procedures ([Reichstein, Falge et al. 2005](#); [Papale, Reichstein et al. 2006](#)). In particular, the partitioning of net ecosystem exchange into GPP and terrestrial ecosystem respiration was done according to ([Reichstein, Falge et al. 2005](#)). See individual tower references for a description of the methodology applied at each tower (Table 2). In addition to the data used in([McCallum, Franklin et al. 2013](#)), we used the Yakutia Larch site ([Dolman, Maximov et al. 2004](#)). This data was partitioned into GPP using an online flux partitioning tool (<http://www.bgc-jena.mpg.de/~MDIwork/eddyproc/>). Figure 1 demonstrates the correlation between the daily GPP, biophysical variable fAPAR and meteorological data (temperature, VPD and radiation) at the tower sites.

Table 2. Description of the five FLUXNET tower sites used in this study.

Site	Location (°)	Data Years	Land Cover	References
Cherskii (RU-Che)	68.61N 161.34 E	2002 – 2005	Tundra - Grass	(Corradi, Kolle et al. 2005 ; Merbold, Kutsch et al. 2009)
Chokurdakh (RU-Cho)	70.61N 147.89E	2003 – 2005	Tundra - Grass	(van der Molen, van Huissteden et al. 2007)
Fyodorovskoe	56.46 N	2003	Evergreen	(Milyukova, Kolle et al. 2002)

(RU-Fyo)	32.92 E	2005	Needleleaf Spruce Forest	
Zotino (RU-Zot)	60.80 N 89.35 E	2002 2005	- Evergreen Needleleaf Pine Forest	(Tchebakova, Kolle et al. 2002)
Yakutia (RU-Ylr)	62.255N 129.619E	2002 2005	- Larch Forest	(Dolman, Maximov et al. 2004)

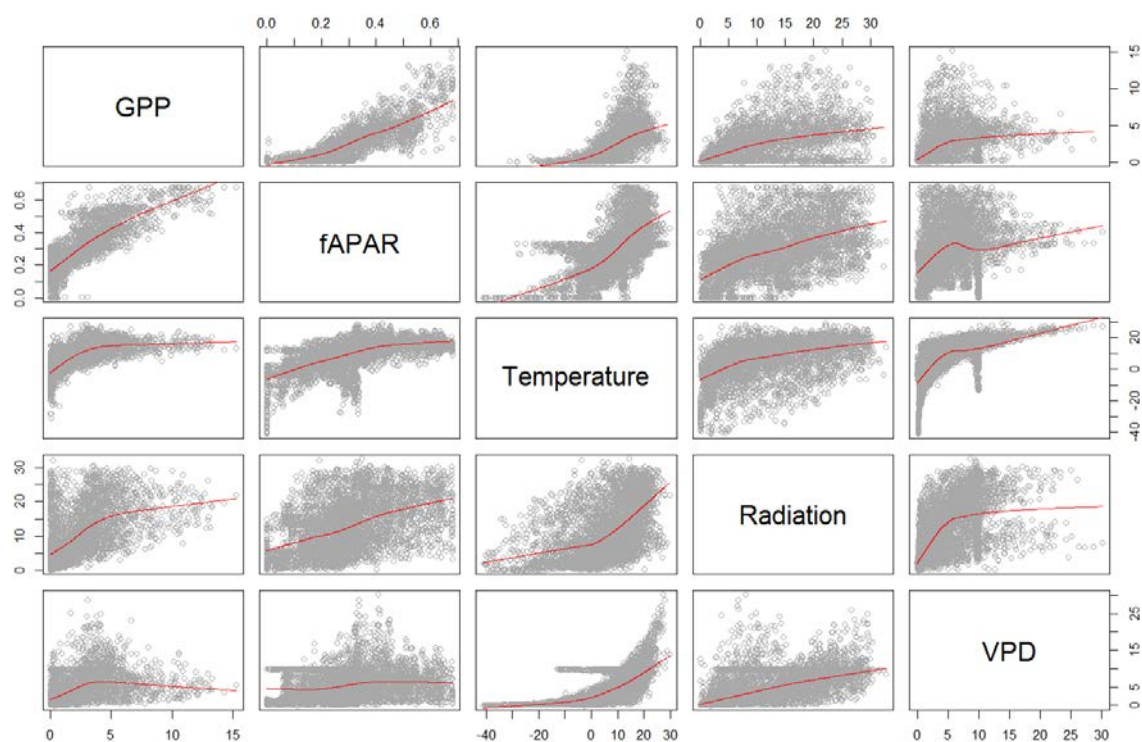


Figure 1. Scatterplots of GPP ($\text{g C m}^{-2} \text{ day}^{-1}$) against fAPAR, Temperature ($^{\circ}\text{C}$), Radiation ($\text{MJ m}^{-2} \text{ day}^{-1}$) and VPD (hPa) at the flux tower sites for the years 2002-2005. Red line shows locally weighted regression.

Model Description

The model applied in this study was parameterized for northern Eurasia ([McCallum, Franklin et al. 2013](#)) and is explained below. Leaf photosynthesis is described with the non-rectangular hyperbola big leaf (BL) model ([Hirose and Werger 1987](#); [Hirose, Ackerly et al. 1997](#)). Leaf level photosynthesis is up-scaled to daily canopy photosynthesis by integration over the canopy ([Franklin 2007](#)) and using

daily canopy f_{APAR} to determine the amount of absorbed incoming radiation. Daily gross primary production P_g is thus defined here according to

$$P_d = \frac{h}{2\theta} \left[\phi I_a + E_a A_{max} - \sqrt{(\phi I_a + E_a A_{max})^2 - 4\phi I_a E_a A_{max} \theta} \right] \quad (1a)$$

where

$$E_a = f_1(T) f_2(D) \quad (1b)$$

defined as h day length; ϑ convexity of leaf photosynthesis; ϕ quantum efficiency; I_a absorbed photosynthetically active radiation; E_a environmental modifier for temperature $f_1(T)$ and VPD $f_2(D)$; and A_{max} light saturated canopy-photosynthesis. The effect of temperature $f_1(T)$ on daily A_{max} was modelled using the concept of state of acclimation ([Mäkelä, Pulkkinen et al. 2008](#)). The effect of VPD $f_2(D)$ on A_{max} was estimated according to ([Landsberg and Waring 1997](#)). All parameters are described in Table 3.

Table 3. Model parameter description and values.

Symbol	Description	Unit	Parameter Values		Increment	Reference
			Min	Max		
S_{max}	Saturating level	° C	15	30	3	(Mäkelä, Pulkkinen et al. 2008)
t	Time constant	days	1	22	3	(Mäkelä, Pulkkinen et al. 2008)
X_0	Threshold value	° C	-10	5	3	(Mäkelä, Pulkkinen et al. 2008)
K	VPD	kPa ⁻¹	-0.1	-0.9	-0.2	(Landsberg and Waring 1997)
A_{max}	Light saturated photosynthesis	umol CO ₂ m ⁻² s ⁻¹	0	40	2	(Ruimy, Dedieu et al. 1996)
θ	Convexity of leaf photosynthesis	-	0.8	-	-	(Hirose, Ackerly et al. 1997)
ϕ	Photosynthetic quantum efficiency	ug C J ⁻¹	2.73	-	-	(Wong, Cowan et al. 1979)

<i>h</i>	Day length	hours d ⁻¹	12	-	Estimated
-----------------	------------	-----------------------	----	---	-----------

Temperature $f_1(T)$

The springtime recovery of photosynthetic capacity has been attributed to a delayed effect of rising air temperatures ([Mäkelä, Hari et al. 2004](#)). The effect of temperature on daily GPP was modelled using the concept of state of acclimation, calculated from the mean daily ambient temperature, using a first-order dynamic delay model where t (days) is the time constant of the delay process and X_0 (°C) is a threshold value of the delayed temperature ([Mäkelä, Pulkkinen et al. 2008](#)). The modifying function $f_1(T)$ is defined here as ([Mäkelä, Pulkkinen et al. 2008](#))

$$f_1(T) = \min \left\{ \frac{S_k}{S_{max}}, 1 \right\}, \quad (2)$$

where the empirical parameter S_{max} (°C) determines the value of S_k (°C) at which the temperature modifier attains its saturating level. The model was parameterized with flux tower data as per ([McCallum, Franklin et al. 2013](#)).

Vapour Pressure Deficit $f_2(D)$

Water stress is one of the primary limiting functions controlling photosynthesis by terrestrial ecosystems ([Mu, Zhao et al. 2007](#)). Under-estimation of VPD contributes greatly to overestimation of GPP ([Heinsch, Zhao et al. 2006](#)). In summer in Siberia, daytime air temperatures regularly exceed 30 °C and VPDs reach more than 3 KPa ([Vygodskaya, Milyukova et al. 1997](#)). In particular, the climate of boreal forests in eastern Siberia resembles that of a boreal desert during long periods of the growing season ([Vygodskaya, Milyukova et al. 1997](#)). $f_2(D)$ accounts for reduced stomatal conductance caused by high atmospheric water vapour pressure deficits (KPa). This allows for stomatal closure even in the presence of significant soil moisture ([Prince and Goward 1995](#)). The effect of VPD $f_2(D)$ was estimated according to ([Landsberg and Waring 1997](#)) as:

$$f_2(D) = e^{KD} \quad (3)$$

where K is an empirical parameter assuming typically negative values and D (KPa) is vapour pressure deficit. The model was parameterized with flux tower data as per ([McCallum, Franklin et al. 2013](#)).

A_{max}

Values for A_{max} were determined from parameterization against FLUXNET data over the region ([McCallum, Franklin et al. 2013](#)).

Parameter Optimization

Each model was initially estimated separately for each site and year, then at each site for all years. Parameters were optimized by means of a search on a coarse grid (see Table 3 for parameter ranges and increments). Model diagnostics were based on the regression of EC tower based GPP against modeled GPP. The minimum residual sum of squares (RSS) has been used as the calibration criteria. Fit was further appraised using both the coefficient of determination (r^2) and root mean square error (RMSE)([McCallum, Franklin et al. 2013](#)).

All possible combinations of parameters were tested. The initial parameter range and increment was conceived by consulting the existing literature (see Table 3 for references). The step width is the increment listed in Table 3. We generally applied a rather coarse increment as RMSE has been found to be generally insensitive to the parameters close to the optimum ([King, Turner et al. 2011](#)) and use of a finer increment greatly increased computing time.

Temperature-Parameter Relationship

In an effort to upscale the results obtained at the tower level to the country level, we investigated the relationship between the calibrated model parameters at each tower and the long-term mean growing season (May to September) temperature for the years 1975-2000 (Figure 2). A linear trend was found for each of the parameters, with the slope in agreement with previous studies([Mäkelä, Pulkkinen et al. 2008](#)). Due to the lack of unique tower locations, these linear models should be considered as guidelines for the trend. Using this regression, parameter values could now be obtained over Northern Eurasia with the long-term mean annual growing season temperature.

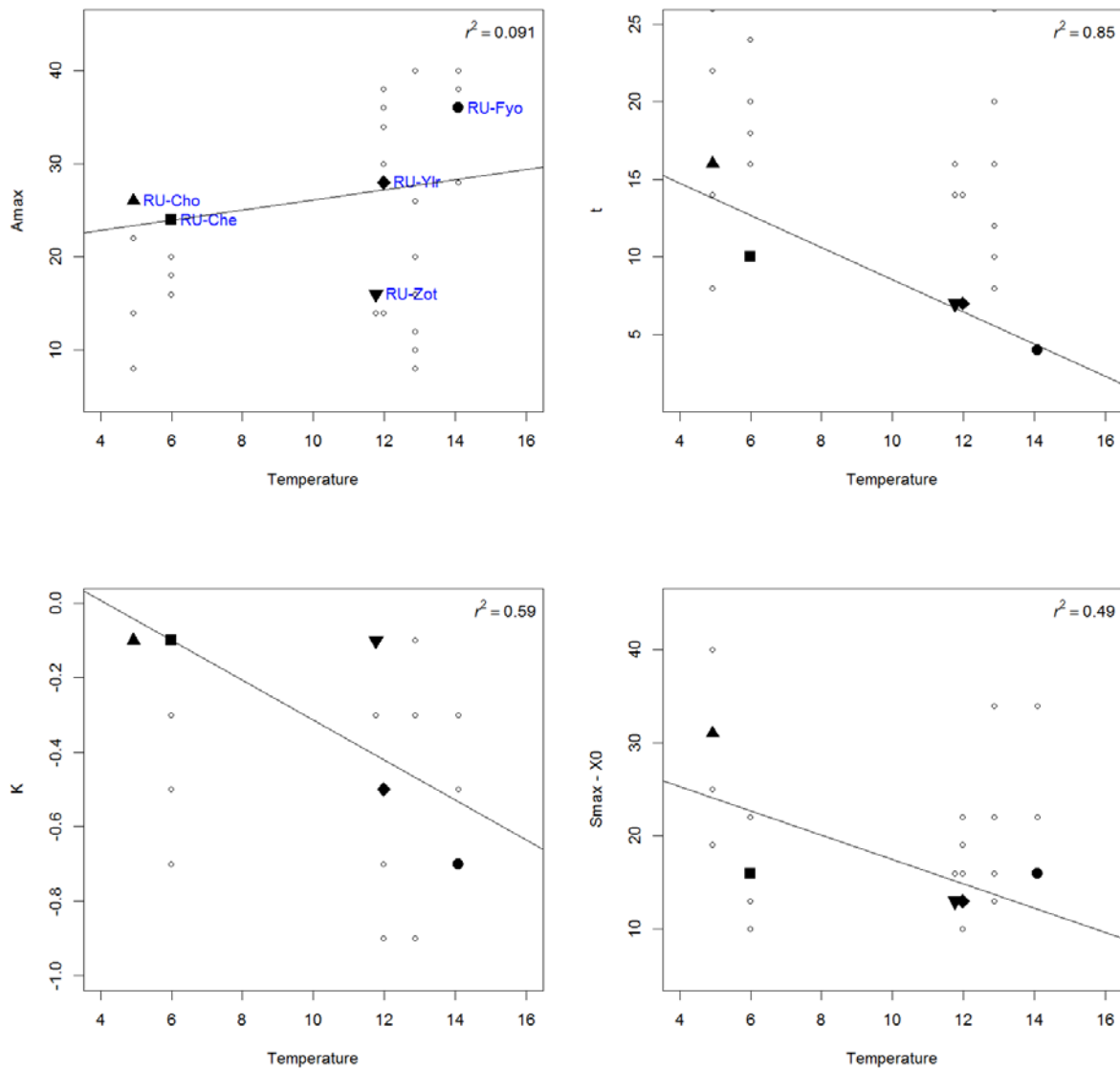


Figure 2. Relationship between calibrated model parameters and long-term (1975-2000) mean annual growing season temperature (May-September). Dark symbols represent the calibrated model parameters for each site (all years), while open circles represent the calibrated model parameters for each site-year individually. The solid line is the trendline.

Results & Discussion

The methodology described above has resulted in a spatial database mapping GPP across boreal Russia for the years 2002 - 2005. Figure 3 demonstrates a snapshot of the variables PAR, fAPAR, the environmental modifiers (temperature and VPD) and A_{\max} for day 200 in 2004. PAR shows large variation across the region resulting from cloud cover. fAPAR demonstrates generally moderate values correlated with vegetation productivity. The environmental modifiers for temperature and VPD both demonstrate favorable environmental growth conditions, with temperature still inhibiting in the far north and northeast and several pockets of limiting VPD in the warmer southeast. A_{\max} (as estimated by our model) is a relatively constant value across the region with lower values in the cooler regions of the far north and montane areas.

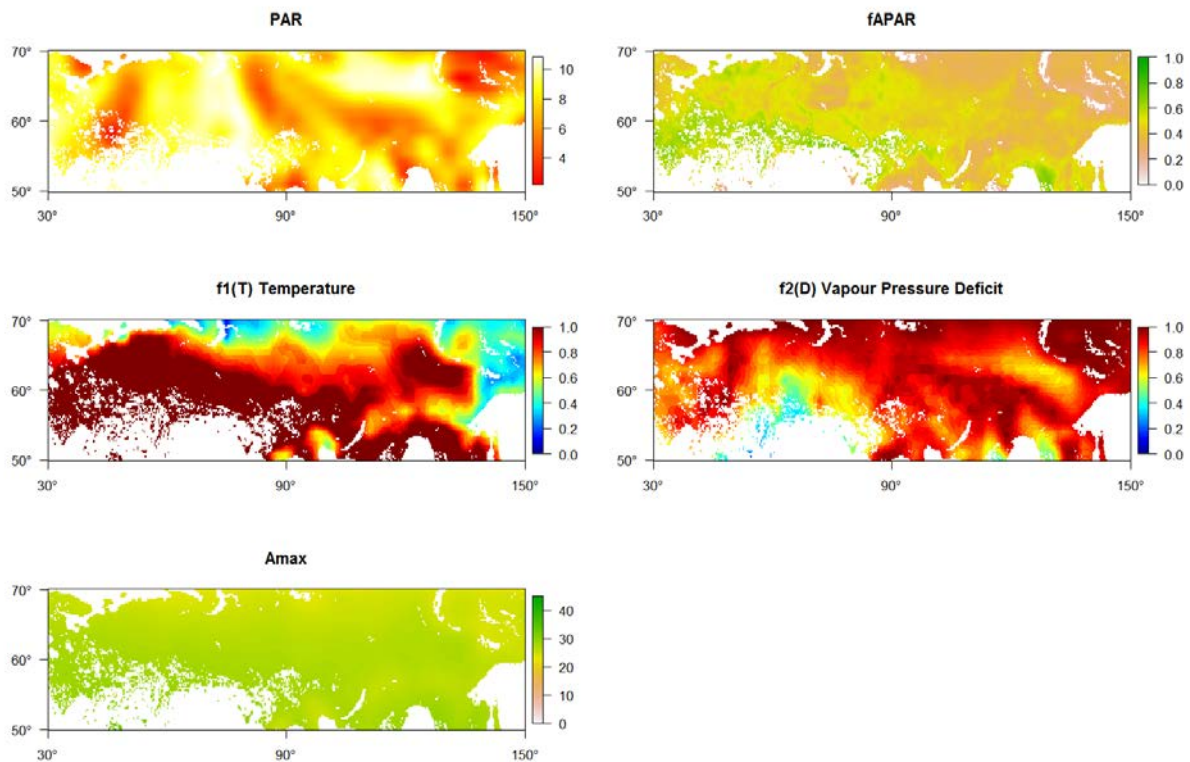


Figure 3. Maps of PAR ($W m^{-2} s^{-1}$) and environmental modifiers (temperature and VPD), fAPAR and A_{\max} ($umol CO_2 m^{-2} s^{-1}$) for day 200, year 2004.

Finally, after running the diagnostic model on a daily basis for GPP across the study area, we produce annual maps (2002-2005) of GPP ($g C m^{-2} y^{-1}$) (Figure 4). Subtle differences are apparent across the

years, although the general patterns remain similar. In all years, highest values appear west of the Ural mountains (60°E), with a general decrease in productivity moving from north to south and west to east.

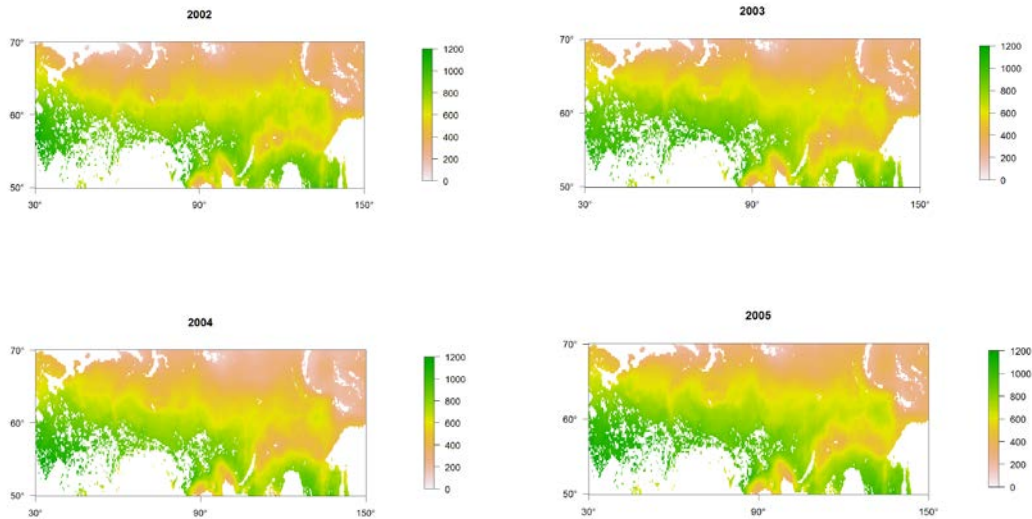


Figure 4. Annual summary for years 2002 - 2005 of GPP ($\text{g C m}^{-2} \text{y}^{-1}$) over entire study area derived from this study (BL approach).

Evaluation

Evaluation of the GPP maps produced from this study (BL approach) was made via comparison with the two existing products, namely MODIS GPP ([Zhao and Running 2010](#)) and IIASA Net Primary Productivity (NPP) ([Shvidenko, Schepashchenko et al. 2008](#)). The Moderate Resolution Spectroradiometer (MODIS) sensor has provided near real-time global estimates of GPP (MOD17A2) since March 2000, on an operational basis. Data was taken from the latest Collection 5.1 ([Zhao and Running 2010](#)). MOD17A2 employs a simple linear LUE algorithm, which assigned unique LUE values per biome. A minimum temperature scalar (i.e. a linear ramp function) reduces the conversion efficiency when cold temperatures limit plant function. Similarly, a linear ramp function is used to reduce the maximum conversion efficiency when the VPD is high enough to inhibit photosynthesis.

The IIASA NPP product is based on extensive experimental material, and multidimensional dynamic models of the phytomass (live biomass) of forest ecosystems, which allowed for transformation of growth models into models of biological productivity ([Shvidenko, Schepashchenko et al. 2008](#)). The latter models comprised the age dynamics of forest ecosystem biomass by major basic fractions (phytomass of stem wood, crown wood, leaves, needles, roots with separation of the fine root fraction, and phytomass of lower levels). The difference between two successive values of the total phytomass production of the ecosystem represents NPP; the dynamics of the latter parameter were obtained on the basis of an algorithm simulating the dynamics of total production with time ([Shvidenko, Schepashchenko et al. 2008](#)). This dataset can be considered as representing an average annual NPP for the years 1960-2000. Furthermore, this dataset was shown to be in close agreement with results from both DGVMs and atmospheric measurements over central Siberia and is hence deemed to accurately estimate baseline productivity ([Quegan, Beer et al. 2011](#)). GPP was assumed to be twice that of NPP ([Zhang, Xu et al. 2009](#)).

Figure 5 shows the three gridded GPP products for 2004, namely the BL approach (this study), IIASA and MODIS products. Both of the diagnostic approaches (i.e. the BL and MODIS datasets) appear smoother and more homogeneous in comparison to the IIASA dataset. The IIASA product is very heterogeneous as it contains the most detail in terms of its underlying land cover map and the hybrid approach taken to create it. Nonetheless, general patterns of GPP agree across the datasets, although absolute values differ. The associated histograms provide further insight into the distribution of GPP across the study area. The IIASA dataset appears unimodal, with a peak at 600 g C m⁻² although there is a hint of a second peak at 350 g C m⁻². Both the BL and MODIS show bimodality. The BL model obtains two peak distributions, one at 250 g C m⁻² and a second at 550 g C m⁻². The MODIS dataset in particular appears bimodal, with the first peak at 250 g C m⁻² and the second peak at 650 g C m⁻². The mixture of land classes across the region likely includes a mixture of distributions.

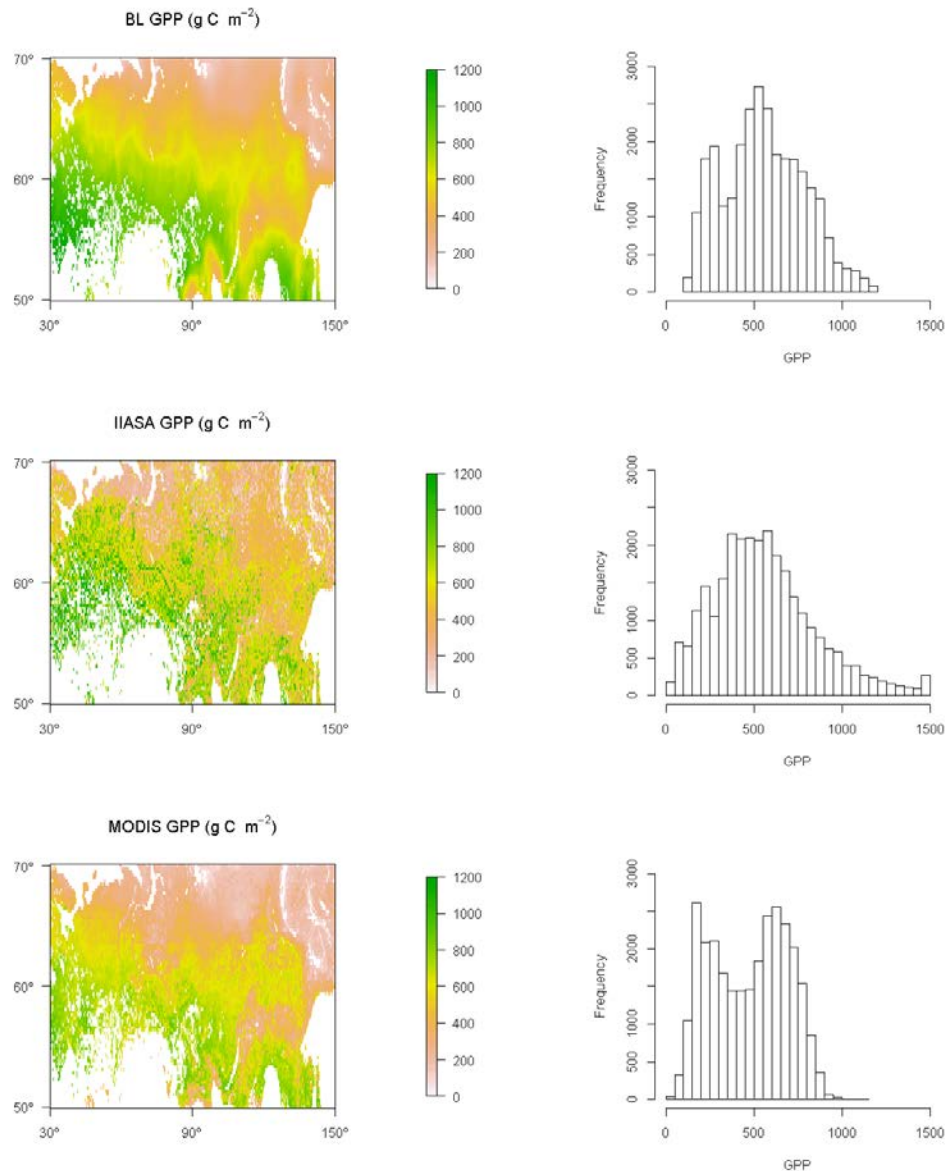
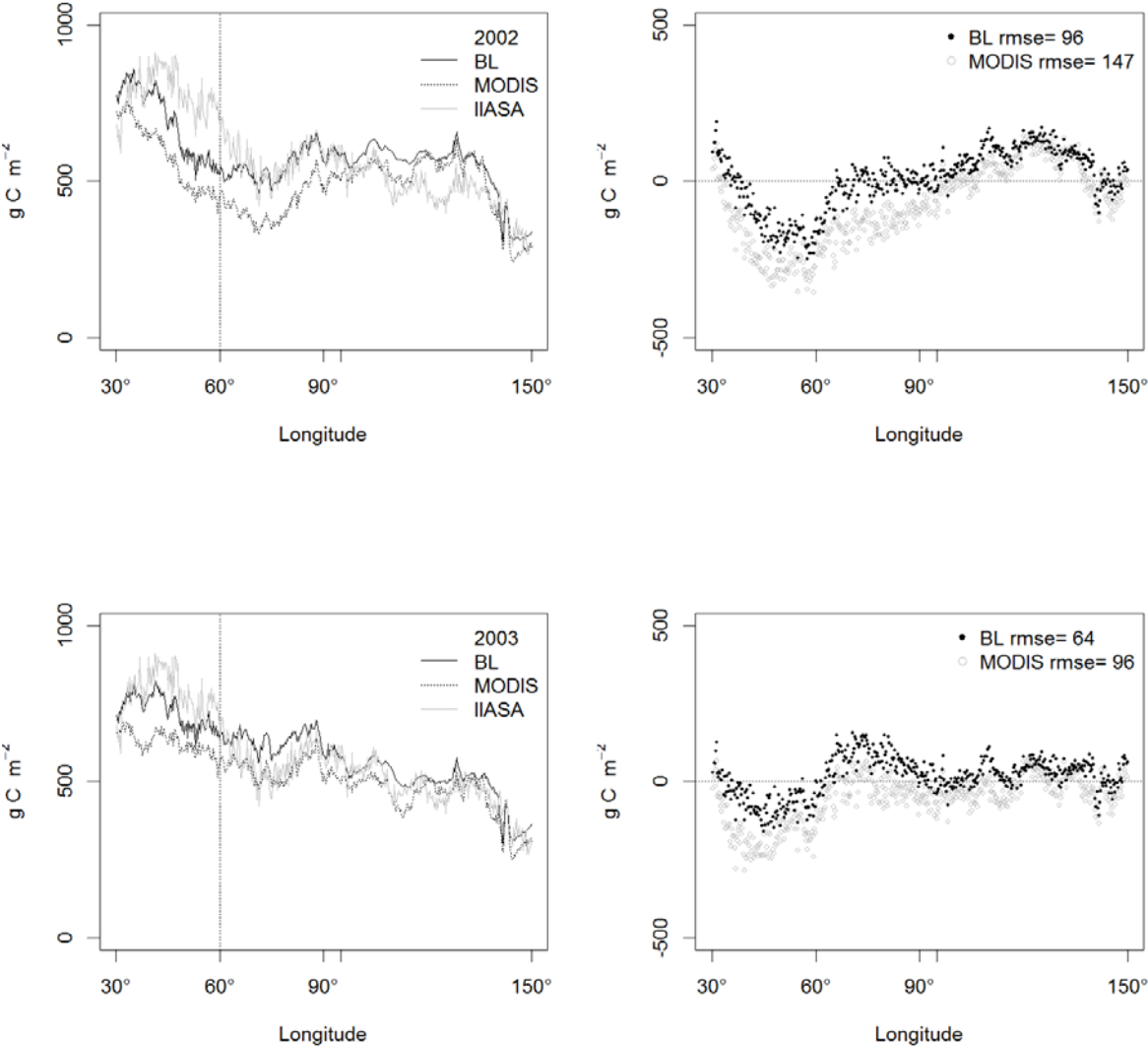


Figure 5. Annual summary for 2004 of GPP over entire study area from BL, MODIS and IIASA approaches. Scale bar set to limit of 1200 g C m⁻² for comparison. Histograms show respective distribution of GPP for each map.

Comparing the three datasets in broad 0.25° mean longitudinal bands provides further insight into observed patterns (Figure 6). Generally, disagreement among the three products is least, east of the Ural Mountains (denoted by the dashed vertical line at 60° E). However, to the west of the Urals, the diagnostic approach of MODIS records significantly lower values than the IIASA approach in all years except 2005. Both the BL and MODIS approaches record the worst agreement in year 2002. Agreement is highest among all three products in 2005, owing in part to a higher mean temperature (see Table 4).

The largest differences between the BL, MODIS and IIASA results were observed in the longitudes 30°-70° E, in particular for the year 2002. Both the BL and MODIS results underestimated the IIASA estimates, with MODIS recording twice the underestimation of BL, almost 300 g C m⁻². This large underestimation over the most productive region of Russia (namely west of the Ural Mountains) demonstrates the potential inaccuracy of the MODIS measurements over this region. This has large implications in terms of accurately depicting the carbon flux with this method over this region. These underestimations are somewhat balanced out by weaker overestimations to the east of the Urals. Overestimations to the east of the Urals are however less critical as the vegetation here is less productive, although the area is much larger.



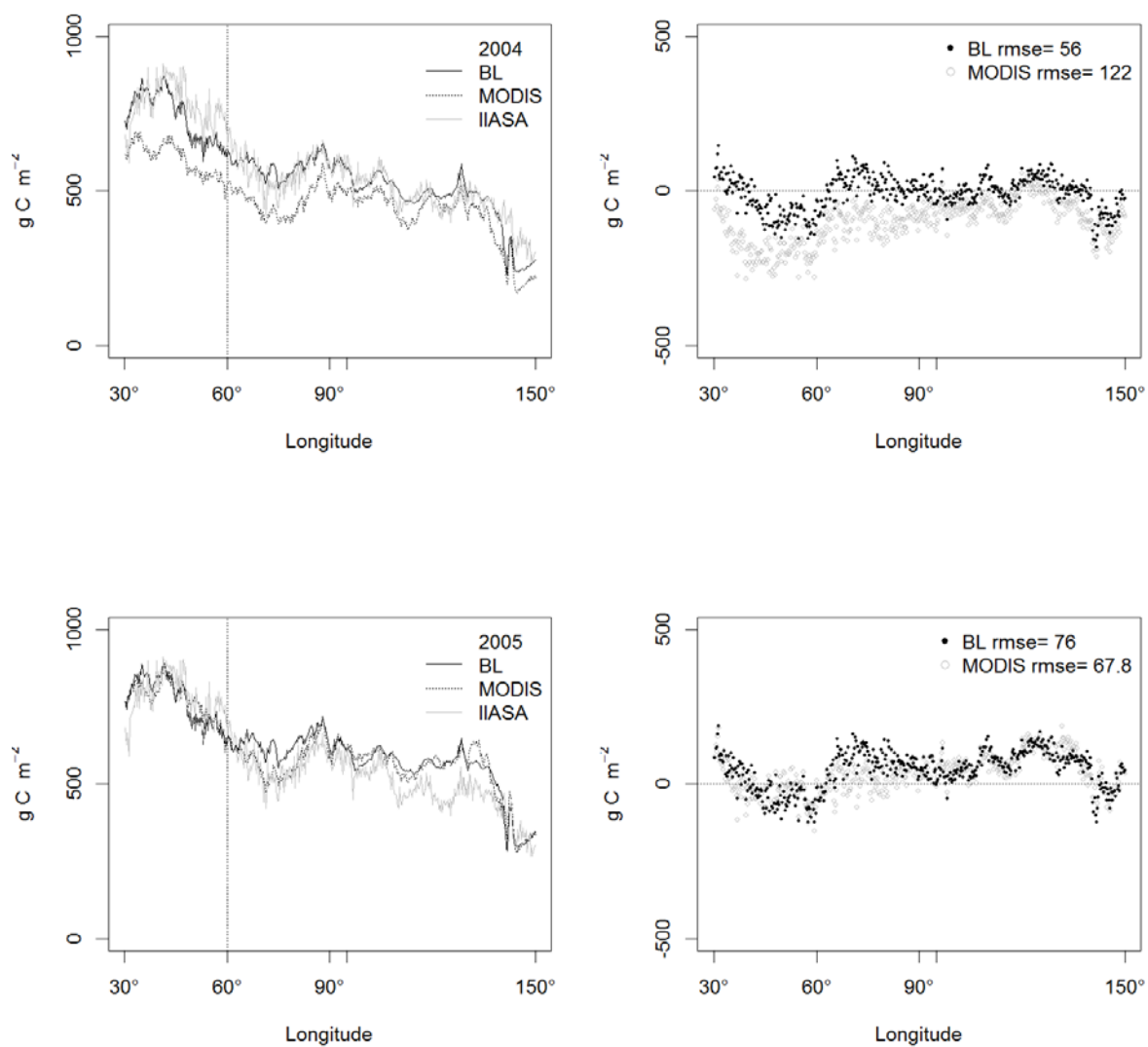


Figure 6. Mean annual longitudinal GPP in 2002 - 2005 for the BL, MODIS and IIASA datasets across the study region (0.25° bands) (left column) and difference plots where IIASA results were subtracted from the BL and MODIS results (right column). Vertical bar marks the approximate location of the Ural Mountain range at 60° E. Mean RMSE values are shown for the BL and MODIS approaches (where the IIASA approach is considered baseline).

Table 4. Mean RMSE and mean Temperature recorded over study area for years 2002-2005.

Year	RMSE		Mean Temperature ($^\circ\text{C}$)
	BL	MODIS	
2002	96	147	10.5

2003	64	96	10.8
2004	56	122	10.0
2005	76	68	11.3
Mean	73	108	10.7

Uncertainty

There are multiple sources of uncertainty associated with any estimate of carbon flux, including: uncertainties in eddy covariance flux measurements themselves, uncertainties arising from the representativeness of the flux network ([Xiao, Zhuang et al. 2011](#)), uncertainties in input data (e.g. fAPAR), model structural uncertainty, and others.

Regarding uncertainties in eddy flux measurements, we used only non-gap filled values in model parameterization. With respect to input data, we attempted to minimize this uncertainty by using the best available datasets (i.e. JRC fAPAR, ECMWF meteorological data). ([Xiao, Zhuang et al. 2011](#)) noted that land cover representation is particularly important. By not using land cover at all in this method, we have avoided the additional uncertainties that this layer can introduce. The JRC fAPAR dataset was chosen for this study after comparison with other available products ([McCallum, Wagner et al. 2010](#)). Additionally the ECMWF Interim Reanalysis Meteorological products were used. The ECMWF data has been shown to be the best of available reanalysis datasets available ([Zhao, Running et al. 2006](#)).

Model structural uncertainty was to some extent explored previously ([McCallum, Franklin et al. 2013](#)). Finally the representativeness of the flux network over the study region was not analyzed, but is deemed to be too few and is likely the greatest bottleneck in these efforts ([Ciais, Dolman et al. 2013](#)). Additional sites exist beyond those used in this study, but they either fall out of the area of interest (i.e. potentially water-limited southern grasslands), contain too few site years and no years within the timeframe of this study, contained errors after data partitioning, or were simply not available. In particular, parameter estimates from a single site are not representative of the parameter values of a given PFT; cross-site (or joint) optimization using observations from multiple sites encompassing a range of site and climate conditions considerably improves the representativeness and robustness of parameter estimates ([Xiao, Zhuang et al. 2011](#)).

Conclusion

This study has resulted in a technique for regional gridded GPP mapping utilizing eddy covariance estimates over a region sparsely covered with in-situ sites. The diagnostic model used in this study was previously validated over this region ([McCallum, Franklin et al. 2013](#)). Furthermore, it utilises satellite-derived fAPAR (i.e. not NDVI or an LAI correlation) and the fAPAR product used was previously analyzed over Russia ([McCallum, Wagner et al. 2010](#)). Finally, results were compared against MOD17A2/A3 C5.1 and an independent inventory based approach ([Shvidenko, Schepashchenko et al. 2008](#)) demonstrating that this new method yields plausible results. Our new predictions differ from the MODIS results and show the improvement that our methodology implies over a large region. Assuming that the carbon accounting approach is a viable baseline estimate, our results are consistently closer to the baseline than MODIS.

In particular, this study has demonstrated the parameterization of a diagnostic GPP model over Russia with estimates derived from a modest number of eddy covariance towers. This parameterization is based partly on the relationship between long term mean annual growing season temperature and calibrated model parameters. Results show that estimates derived from this approach compare well with both the in-situ based carbon accounting approach and the global MODIS diagnostic model, with results from this study most closely matching the carbon accounting approach. Furthermore, the model employed in this study applies the concept of temperature acclimation ([Mäkelä, Pulkkinen et al. 2008](#)) which is particularly important over such a temperature limited continental region as Russia.

The most obvious difficulty with the method presented here is the lack of flux tower locations. Additional tower locations do exist (approximately 14 eddy covariance sites exist in Russia), but as previously mentioned for a variety of reasons these could not be used. More tower locations would naturally increase the confidence in the results. All five eddy covariance locations used in the model parameterization were not water-limited, hence applied at water-limited sites, this model will likely over-estimate GPP. Thus this simple diagnostic model is most applicable over cold, non water-limited regions.

Acknowledgements

N. Gobron (JRC) and F. Venuti (ECMWF) provided assistance and data. FLUXNET (fluxdata.org) provided access to the TCOS eddy covariance data (special thanks to D. Papale, and the tower Principle Investigators). Additional thanks to Trofim Maximov at the IBPC in Yakutsk who provided the RU-Ylr larch tower data. The IIASA Library provided valuable resources. The GEOCARBON (FP7 283080) Project partially supported this study. R statistical software is also acknowledged. Special thanks to M. van der Molen (Wageningen UR) who assisted with flux data.

References

- Baldocchi, D., E. Falge, et al. (2001). "FLUXNET: A New Tool to Study the Temporal and Spatial Variability of Ecosystem-Scale Carbon Dioxide, Water Vapor, and Energy Flux Densities." Bulletin of the American Meteorological Society **82**(11): 2415-2434.
- Balzter, H., F. F. Gerard, et al. (2005). "Impact of the Arctic Oscillation pattern on interannual forest fire variability in Central Siberia." Geophysical Research Letters **32**(14): 1-4.
- Beer, C., M. Reichstein, et al. (2010). "Terrestrial gross carbon dioxide uptake: Global distribution and covariation with climate." Science **329**(5993): 834-838.
- Ciais, P., A. J. Dolman, et al. (2013). "Current systematic carbon cycle observations and needs for implementing a policy-relevant carbon observing system." Biogeosciences Discuss. **10**(7): 11447-11581.
- Corradi, C., O. Kolle, et al. (2005). "Carbon dioxide and methane exchange of a north-east Siberian tussock tundra." Global Change Biology **11**(11): 1910-1925.
- Dee, D. P., S. M. Uppala, et al. (2011). "The ERA-Interim reanalysis: configuration and performance of the data assimilation system." Quarterly Journal of the Royal Meteorological Society **137**(656): 553-597.
- Dolman, A., T. Maximov, et al. (2004). "Net ecosystem exchange of carbon dioxide and water of far eastern Siberian Larch (< /> Larix cajanderii< />) on permafrost." Biogeosciences **1**(2): 133-146.
- Franklin, O. (2007). "Optimal nitrogen allocation controls tree responses to elevated CO 2." New Phytologist **174**(4): 811-822.
- Gobron, N., B. Pinty, et al. (2006). "Evaluation of fraction of absorbed photosynthetically active radiation products for different canopy radiation transfer regimes: Methodology and results using Joint Research Center products derived from SeaWiFS against ground-based estimations." Journal of Geophysical Research: Atmospheres **111**(D13): (D13110).
- Goldammer, J. G. (1996). "The boreal forest, fire, and the global climate system: Achievements and needs in joint east-west boreal fire research and policy development." Combustion, Explosion and Shock Waves **32**(5): 544-557.
- Heinsch, F. A., M. Zhao, et al. (2006). "Evaluation of remote sensing based terrestrial productivity from MODIS using regional tower eddy flux network observations." IEEE Transactions on Geoscience and Remote Sensing **44**(7): 1908-1923.

- Hirose, T., D. D. Ackerly, et al. (1997). "CO₂ elevation, canopy photosynthesis, and optimal leaf area index." *Ecology* **78**(8): 2339-2350.
- Hirose, T. and M. J. A. Werger (1987). "Nitrogen use efficiency in instantaneous and daily photosynthesis of leaves in the canopy of a *Solidago altissima* stand." *Physiol. Plant.* **70**: 215-222.
- Kajii, Y., S. Kato, et al. (2002). "Boreal forest fires in Siberia in 1998: Estimation of area burned and emissions of pollutants by advanced very high resolution radiometer satellite data." *Journal of Geophysical Research D: Atmospheres* **107**(24).
- King, D. A., D. P. Turner, et al. (2011). "Parameterization of a diagnostic carbon cycle model for continental scale application." *Remote Sensing of Environment* **115**(7): 1653-1664.
- Landsberg, J. J. and R. H. Waring (1997). "A generalised model of forest productivity using simplified concepts of radiation-use efficiency, carbon balance and partitioning." *Forest Ecology and Management* **95**(3): 209-228.
- Mäkelä, A., P. Hari, et al. (2004). "Acclimation of photosynthetic capacity in Scots pine to the annual cycle of temperature." *Tree Physiology* **24**(4): 369-376.
- Mäkelä, A., M. Pulkkinen, et al. (2008). "Developing an empirical model of stand GPP with the LUE approach: Analysis of eddy covariance data at five contrasting conifer sites in Europe." *Global Change Biology* **14**(1): 92-108.
- McCallum, I., O. Franklin, et al. (2013). "Improved light and temperature responses for light-use-efficiency-based GPP models." *Biogeosciences* **10**(10): 6577-6590.
- McCallum, I., O. Franklin, et al. (2013). "Improved light and temperature responses for light use efficiency based GPP models." *Biogeosciences Discuss.* **10**(5): 8919-8947.
- McCallum, I., W. Wagner, et al. (2010). "Comparison of four global FAPAR datasets over Northern Eurasia for the year 2000." *Remote Sensing of Environment* **114**(5): 941-949.
- Merbold, L., W. L. Kutsch, et al. (2009). "Artificial drainage and associated carbon fluxes (CO₂/CH₄) in a tundra ecosystem." *Global Change Biology* **15**(11): 2599-2614.
- Milyukova, I. M., O. Kolle, et al. (2002). "Carbon balance of a southern taiga spruce stand in European Russia." *Tellus, Series B: Chemical and Physical Meteorology* **54**(5): 429-442.
- Monteith, J. L. and M. H. Unsworth (1990). *Principles of Environmental Physics*. New York, Edward Arnold.
- Mu, Q., M. Zhao, et al. (2007). "Evaluating water stress controls on primary production in biogeochemical and remote sensing based models." *Journal of Geophysical Research G: Biogeosciences* **112** (1): **G01012** (1).
- Papale, D., M. Reichstein, et al. (2006). "Towards a standardized processing of Net Ecosystem Exchange measured with eddy covariance technique: algorithms and uncertainty estimation." *Biogeosciences* **3**: 571-583.
- Prince, S. D. and S. N. Goward (1995). "Global primary production: a remote sensing approach." *Journal of Biogeography* **22**(4-5): 815-835.

- Quegan, S., C. Beer, et al. (2011). "Estimating the carbon balance of central Siberia using a landscape-ecosystem approach, atmospheric inversion and Dynamic Global Vegetation Models." Global Change Biology **17**(1): 351-365.
- Reichstein, M., E. Falge, et al. (2005). "On the separation of net ecosystem exchange into assimilation and ecosystem respiration: review and improved algorithm." Global Change Biology **11**(9): 1424-1439.
- Ruimy, A., G. Dedieu, et al. (1996). "TURC: A diagnostic model of continental gross primary productivity and net primary productivity." Global Biogeochemical Cycles **10**(2): 269-285.
- Running, S. W., R. R. Nemani, et al. (2004). "A continuous satellite-derived measure of global terrestrial primary production." BioScience **54**(6): 547-560.
- Shvidenko, A. and S. Nilsson (2003). "A synthesis of the impact of Russian forests on the global carbon budget for 1961-1998." Tellus, Series B: Chemical and Physical Meteorology **55**(2): 391-415.
- Shvidenko, A., D. Schepaschenko, et al. (2007). "Semi-empirical models for assessing biological productivity of Northern Eurasian forests." Ecological Modelling **204**(1-2): 163-179.
- Shvidenko, A. Z., D. G. Schepashchenko, et al. (2008). "Net primary production of forest ecosystems of Russia: A new estimate." Doklady Earth Sciences **421**(2): 1009-1012.
- Stephens, B. B., K. R. Gurney, et al. (2007). "Weak northern and strong tropical land carbon uptake from vertical profiles of atmospheric CO₂." Science **316**(5832): 1732-1735.
- Tchebakova, N. M., O. Kolle, et al. (2002). "Inter-annual and seasonal variations of energy and water vapour fluxes above a *Pinus sylvestris* forest in the Siberian middle taiga." Tellus, Series B: Chemical and Physical Meteorology **54**(5): 537-551.
- van der Molen, M. K., J. van Huissteden, et al. (2007). "The growing season greenhouse gas balance of a continental tundra site in the Indigirka lowlands, NE Siberia." Biogeosciences **4**(6): 985-1003.
- Vygodskaya, N. N., I. Milyukova, et al. (1997). "Leaf conductance and CO₂ assimilation of *Larix gmelinii* growing in an eastern Siberian boreal forest." Tree Physiology **17**(10): 607-615.
- Wong, S. C., I. R. Cowan, et al. (1979). "Stomatal conductance correlates with photosynthetic capacity." Nature **282**: 424-426.
- Xiao, J., J. Chen, et al. (2012). "Advances in upscaling of eddy covariance measurements of carbon and water fluxes." Journal of Geophysical Research G: Biogeosciences **117**(1).
- Xiao, J., Q. Zhuang, et al. (2011). "Assessing net ecosystem carbon exchange of U.S. terrestrial ecosystems by integrating eddy covariance flux measurements and satellite observations." Agricultural and Forest Meteorology **151**(1): 60-69.
- Zhang, Y., M. Xu, et al. (2009). "Global pattern of NPP to GPP ratio derived from MODIS data: Effects of ecosystem type, geographical location and climate." Global Ecology and Biogeography **18**(3): 280-290.

Zhao, M. and S. W. Running (2010). "Drought-induced reduction in global terrestrial net primary production from 2000 through 2009." Science **329**(5994): 940-943.

Zhao, M., S. W. Running, et al. (2006). "Sensitivity of Moderate Resolution Imaging Spectroradiometer (MODIS) terrestrial primary production to the accuracy of meteorological reanalyses." Journal of Geophysical Research G: Biogeosciences **111**(1).

Curriculum Vitae

Personal information

Surname(s) / First name(s)	McCallum, Ian
Address(es)	International Institute for Applied Systems Analysis (IIASA) Schlossplatz 1, A-2361 Laxenburg, Austria
Telephone(s)	+43-2236-807
E-mail	mccallum@iiasa.ac.at
Nationality	Canadian

Work experience

Dates	Since 2000
Occupation or position held	Researcher, Ecosystems Services & Management Program
Main activities and responsibilities	GIS, Remote Sensing, Terrestrial Carbon, GEOSS, Land Cover Science
Name and address of employer	International Institute for Applied Systems Analysis (IIASA) Schlossplatz 1, A-2361 Laxenburg, Austria

Education and training

Dates	1991 - 1993
Title of qualification awarded	M.Sc. in Forestry
Principal subjects/occupational skills covered	Forest science, Remote Sensing, GIS, Wildlife Habitat Suitability
Name and type of organisation providing education and training	Lakehead University, Thunder Bay, ON, Canada

Selected research activities

Selected activities and responsibilities	Numerous research projects e.g. for the European Commission, the Austrian Research Promotion Agency (FFG), the International Fund for Agricultural Development (IFAD), Zurich Insurance. Co-lead of the ID-03 GEO Task EuroGEOSS: a large scale integrated project in the 7 th Framework Program of the European Commission. It was part of the thematic area: "ENV.2008.4.1.1.1: European environment Earth observation system supporting INSPIRE and compatible with GEOSS". Responsible here in particular for GEO benefit assessment related work.
--	--

The EC 6th Framework Program sponsored project "Global Earth Observation – Benefit Estimation: Now, Next and Emerging" (GEOBENE): developing methodologies and analytical tools to assess societal benefits of GEO in the domains of: Disasters, Health, Energy, Climate, Water, Weather, Ecosystems, Agriculture and Biodiversity.

Participated in the Siberia-II Project: a shared-cost action financed through the 5th Framework Program of the European Commission, Generic Activity 7.2: Development of generic Earth Observation Technologies.

**Selected Peer-
Reviewed Scientific
Publications
(2013-2006)**

McCallum I, Franklin O, Moltchanova E, Merbold L, Schmullius C, Shvidenko A, Schepaschenko D, Fritz S (2013). Improved light and temperature responses for light-use-efficiency-based GPP models. *Biogeosciences*, 10(10):6577-6590

See L, Comber A, Salk CF, Fritz S, van der Velde M, Perger C, Schill C, McCallum I, Kraxner F, Obersteiner M (2013). Comparing the quality of crowdsourced data contributed by expert and non-experts. *PLoS ONE*, 8(7):e69958

Fritz S, McCallum I, Schill C, Perger C, See L, Schepaschenko D, van der Velde M, Kraxner F, Obersteiner M (2012). Geo-Wiki: An online platform for improving global land cover. *Environmental Modelling & Software*, 31:110-123

Schepaschenko D, McCallum I, Shvidenko A, Fritz S, Obersteiner M (2011). A new hybrid land cover dataset for Russia: A methodology for integrating statistics, remote sensing and in situ information. *Land Use Science*, 6(4):245-259

Fritz S, You L, Bun A, See L, McCallum I, Schill C, Perger C, Liu J, Hansen M, Obersteiner M (2011). Cropland for sub-Saharan Africa: A synergistic approach using five land cover data sets. *Geophysical Research Letters*, 38:L04404

Quegan S, Beer C, Shvidenko A, McCallum I, Handoh IC, Peylin P, Roedenbeck C, Lucht W, Schmullius C (2011). Estimating the carbon balance of central Siberia using a landscape-ecosystem approach, atmospheric inversion and Dynamic Global Vegetation Models. *Global Change Biology*, 17(1):351-365

Santoro M, Beer C, Cartus O, Schmullius C, Shvidenko A, McCallum I, Wegmueller U, Wiesmann A (2011). Retrieval of growing stock volume in boreal forest using hyper-temporal series of Envisat ASAR ScanSAR backscatter measurements. *Remote Sensing of Environment*, 115(2):490-507

Leduc S, Starfelt F, Dotzauer E, Kindermann G, McCallum I, Obersteiner M, Lundgren J (2010). Optimal location of lignocellulosic ethanol refineries with polygeneration in Sweden. *Energy*, 35(6):2709-2716

McCallum I, Wagner W, Schmullius C, Shvidenko A, Obersteiner M, Fritz S, Nilsson S (2010). Comparison of four global FAPAR datasets over Northern Eurasia for the year 2000. *Remote Sensing of Environment*, 114(5):941-949

McCallum I, Wagner W, Schmullius C, Shvidenko A, Obersteiner M, Fritz S, Nilsson S (2009). Satellite-based terrestrial production efficiency modeling. *Carbon Balance and Management*, 4:8

Kindermann G, McCallum I, Fritz S, Obersteiner M (2008). A global forest growing stock, biomass and carbon map based on FAO statistics. *Silva Fennica*, 42(3):387-396

Santoro M, Shvidenko A, McCallum I, Askne J, Schmullius C (2007). Properties of ERS-1/2 coherence in the Siberian boreal forest and implications for stem volume retrieval. *Remote Sensing of Environment*, 106(2):154-172

McCallum I, Obersteiner M, Nilsson S, Shvidenko A (2006). A spatial comparison of four satellite derived 1 km global land cover datasets. *International Journal of Applied Earth Observation and Geoinformation*, 8(4):246-255